A Novel Column Format for on-Chip Liquid Chromatography Fabricated in Cyclo Olefin Polymer

Xavier Illa Vila

Programa de Doctorat en Física

A Novel Column Format for on-Chip Liquid Chromatography Fabricated in Cyclo Olefin Polymer

Tesi que presenta Xavier Illa Vila

per optar al títol de Doctor per la Universitat de Barcelona

Directors de la Tesi:

Albert Romano Rodríguez
Professor Titular, Universitat de Barcelona

Wim De Malsche
Research Fellow, Vrije Universiteit Brussel

Departament d'Electrònica
Grup de Micro-nanotecnologies I Nanoscòpies per Dispositius electrònics i fotònics (MIND)
Institut de Nanociència i Nanotecnologia (IN^{2}UB)

UNIVERSITAT DE BARCELONA

A la Feli,

el Josep,

l'Albert

i la Jordina

AGRAÏMENTS / ACKNOWLEDGEMENTS

Ha estat molta gent la que d'una manera o altra ha contribuït a què aquesta tesi finalment vegi la llum. Per això vull aprofitar aquestes línies per donar les gràcies a tots aquells que han estat al meu costat durant aquest llarg periple.

Primer de tot m'agradaria donar les gràcies als meus directors de tesi. Primer a l'Albert Romano, que és el responsable directe que a hores d'ara em trobi aquí. Ell és qui em va obrir les portes d'aquest món i qui més m'ha animat a no defallir en els moments més difícils.

Secondly to Wim De Malsche who after our first meeting in Enschede, has guided me into this undiscovered (for a physicist) world of liquid chromatography. I really appreciate the time and the beers we have shared discussing about new wild experiments or trying to understand what was going on in our chips.

També voldria agrair al MICINN pel seu suport econòmic a través dels projectes CROMINA (ref. TEC2004-06854-C03-01/MIC) i ISIS (ref. TEC2007-67962-C04-04/MIC) i de la beca FPI de que he gaudit durant aquests anys i que, a més a més, m'ha permès realitzar estades en centres de recerca estrangers, sent aquestes unes de les millors experiències que he tingut durant el transcurs d'aquesta tesi.

During this time I have had the great opportunity to work in different groups. For that, I am more than thankful to Dr. Fredrik Nikolajeff of Uppsala Universiteit, prof. Jan Eijkel of Universiteit Twente, prof. Gert Desmet of the Vrije Universiteit Brussel and prof. Jörg P. Kutter of the Technical University of Denmark for the opportunity of working under their supervisions.

In all of those places I met a lot of people that make work and life easier. Thanks to Sara who introduced me into the PDMS world and guided me through the cleanroom in Uppsala; to Ruy, Jose, Nasser, Hanna and Marek for those coffees under the Swedish sun. In Enschede, I really appreciated those beers in the Faculty Club after working in the cleanroom where Wim and Johan showed everything I wanted to know about microfabrication.

I really enjoyed the summer in Brussels. At work it was Wim, Selm, Fredrik or Jeff who were always ready to help me with the setup or to prepare the samples. But out of work it wouldn't have been the same without the people we met each other in the *kot*. It was great to share with Manolo, Isma and Bety the crappiest dining-room ever!! Allà també vaig coincidir amb part de la família d'*Urgell* 57; primer la Cri i després en Marc van fer que em sentís com a casa. Finally, in Copenhagen I was really lucky to work with people like Olga (crec que mai oblidaré la primera litografia que vam fer junts a la sala blanca) and Detlef, who always had an idea to solve any problem. Massimo and Pedro help me in everything I asked for in the lab and out of work, I really appreciate that those guys were always ready for an easy beer or something more...

Una vegada a casa també hi hagut molta gent que m'ha ajudat. Gràcies al personal de la Plataforma de Nanotecnologia del Parc Científic de Barcelona, a en Xevi i la Liber per l'accés al laboratori de Nanotecnologia del CNM-IMB, a la Isabel i el Carles, també del CNM-IMB pels primers motlles de silici que vaig fer servir en aquesta tesi i per la contínua col·laboració, al personal dels Serveis Cientificotècnics, i més concretament a la gent del taller mecànic per tots els *holders* i *arreglos* varis, indispensables per a poder portar a terme els experiments, a la gent de l'IBEC, especialment a en Romén, l'Òscar, en Marc i en Toni per l'ajuda en aquests últims experiments que esperem que acabin de sortir algun dia. I com no, res hagués estat possible sense l'ajuda de tota la gent que forma part del Departament d'Electrònica de la UB, i en especial, dels meus companys de laboratori. Dels que hi havia quan vaig començar fins als que han anat entrant durant aquests anys: Cristian (per estar sempre al meu costat, mai més ben dit),

Dani (pel control del setup i per la simple disposició a ajudar en qualsevol moment), Elias (res hagués sigut el mateix sense els viatges a Berlin), Eva (merci per aquest últim *marrón*), Olga (per les inacabables mesures d'amines que al final mai han vist la llum), Alberto, Àlex, Anna, Jordi, Santi, Andrés, Cyrus, Erik, Luis, Marta, Román, Sara, Sergi, Sònia, Teresa... Tots m'heu ajudat en algun moment, ja sigui en alguna sessió de bricolatge com compartint un cafè. Moltes i moltes gràcies!!

Tampoc em puc oblidar de tota la gent amb qui he compartit tantes estones al pis d'Urgell, de tots els amics d'Artés i dels companys de bàsquet. I per acabar, només puc tenir paraules d'agraïment pels meus pares, que sempre m'han recolzat i animat a seguir endavant, per l'Albert, el meu germà, i per la Jordina, amb qui mai tindré prou paraules per agrair el seu suport incondicional durant aquests últims mesos.

Artés, juliol de 2010

INDEX

CHAPTER 1

Introduction & Objectives

1.1 Project Aim

Lab-on-a-chip (LOC) devices or micro-Total Analysis Systems (μ-TAS) have emerged during the last years taking advantage of the microfabrication techniques developed for the microelectronic industry as a way for integrating one or more laboratory functions into one single chip. A series of advantages are achieved when scaling down the traditional laboratory analytical systems, such as the decrease in time, analyte volume and cost of the analysis. Albeit many disciplines are taking advantage of these devices, separation systems have played a prominent role in the development of LOC systems for the last 20 years [1]. Among all the separation techniques, liquid chromatography (LC) is perhaps the most prevalent technique, being used in a wide range of different areas, such as environmental monitoring, biological and pharmaceutical research, clinical diagnosis, food quality and safety inspection...

In order to overcome the limitations that have been found for the traditional packed and coated columns, after the theoretical performance limits have seemed to be approached, a new column concept based on collocated monolithic support structures (COMOSS), was introduced by Fred Regnier's group [2-4]. With this idea, the packing homogeneity, a very important parameter responsible of the separation power of a

given chromatographic system [5], can be increased by the fabrication of support structures in an ordered manner using the microfabrication technology. In this field, Gert Desmet's group at the Vrije Universiteit Brussel (Belgium) has been denoted as one of the most active groups developing this idea. Theoretical analysis showing the advantages and limitations of this idea were first reported [6-8], and experimental work in collaboration with Han Gardeniers of the MESA+ Institute for Nanotechnology in the University of Twente (The Netherlands) has been presented lately [9,10].

The present PhD dissertation is focused on the study of this pillar array column structure using cyclo olefin polymer (COP) as a novel substrate material, and has been carried out in a collaboration between the Department of Electronics of the University of Barcelona and the Department of the Chemical Engineering of the Vrije Universiteit Brussel. A collaboration that started during one of the scientific stages included in the FPI grant that has supported the author of this thesis in the frame of the CROMINA project, financed by the Spanish Ministry Science and Innovation.

Furthermore, the use of an alternative detection technique (to the more conventional fluorescence detection) for this separation column structure has been also been started to study (as it is shown in chapter 6 of this dissertation) after a fruitful collaboration between our group and Jörg Kutter's group in the Department of Micro- and nanotechnologies of the Technical University of Denmark, where gold microelectrodes were successfully integrated in a COP microfluidic chip and their electrochemical characteristics were studied.

1.2 Objectives

The main objectives of this PhD dissertation can be summarized as follows:

1. To implement the protocols for (i) the optimal replication of microstructures in COP and (ii) the thermal-assisted pressure bonding between two COP sheets required for the fabrication of closed channels.
2. To assess the feasibility of using an ordered pillar array column fabricated in COP for pressure-driven reversed-phase liquid chromatography separations.
3. To develop a method for the fabrication of gold microelectrodes over COP along with the characterization of its response under aqueous and organic media.
4. To explore the possibility to use the above-mentioned gold microelectrodes fabricated in COP as a detection unit for the ordered pillar array column also mentioned above.

1.3 Dissertation Outline

With regards to the objectives that steered the course of this PhD work pointed out in the previous section, this dissertation is organized in six different chapters which are summarized below.

Chapter 2 presents a summary of the progress made in the LOC field during the last years, making special emphasis in the applications related to the on-chip liquid chromatography in polymer devices. For this reason, also some words on the fabrication methods of polymer-based LOC systems, along with some elementary theoretical background of liquid chromatography are presented.

The first polymer chip containing a pillar array column for pressure-driven reversed-phase liquid chromatography is described in *chapter 3*. The chip design and the fabrication, injection and separation procedure are reported. Analysis of the column efficiency are presented, along with the first chromatographic separations reported in a pillar array column fabricated in a polymer device

(which take advantage of the high hydrophobicity of the COP) to demonstrate the feasibility of this on-chip liquid chromatography device.

In the next chapter, *chapter 4*, an in-depth study of the efficiency of the pillar array column fabricated in COP presented in the previous chapter is given. For that, the band broadening in the column under non-retentive conditions is measured in COP chips with different pillar heights. The influence of the channel depth is assessed to study the extra band broadening contribution arising when taking into account the top and bottom plates. The differences between the experimental results and the theoretical 2D simulations are discussed and an explanation for the changes in the constant values of the van Deemter equation is given.

The experimental results of the measurements under retentive conditions performed in the same chips used in the previous chapter are presented in *chapter 5*. Relations between the retention factor and both the surface/volume ratio and the amount of organic modifier in the mobile phase, that are described theoretically for reversed-phase separations, are investigated. Moreover, the obtained retention factor values and the reduced plate heights obtained under retentive conditions are compared to the case of non-porous and porous silicon pillars, confirming the potential of this new column format that has been fabricated.

In the final experimental chapter, *chapter* 6, the fabrication of gold microelectrodes using COP as a substrate by standard lithography and lift-off techniques is described. To test the quality and the performance of the microelectrodes, they have been integrated into a COP microfluidic channel where electrochemical experiments in aqueous and organic media have been performed for the first time. Cyclic voltammetric measurements are described and the values achieved are compared to the theoretical steady state currents calculated theoretically for a band electrode. The small differences (less than 5%) between both experimental and calculated data validate both the fabrication

process and the behaviour of the fabricated device integrating the microelectrodes.

In the final chapter, *chapter* 7, a general conclusion including the feasibility and potential applications of the pillar array column fabricated in COP is given. Moreover, a discussion of the drawbacks of the fabricated device and the possible strategies to improve the performance of the column fabricated in COP are given. Finally, the integration of the gold microelectrodes described in chapter 6 as a detection system for the pillar array column format is shown. Preliminary results on the detection of proteins that indicate the feasibility of such integration are given, and the possibility to perform reversed-phase separations with simultaneous fluorescent and impedance detection is discussed.

It is worthy to mention that the fabrication of the silicon masters used to produce the COP chips in chapters 3, 4 and 5 have been done by Wim De Malsche at the MESA+ Institute for Nanotechnology in the University of Twente. Moreover, the chips used in chapter 6 were fabricated at the Technical University of Denmark with the help of Olga Ordeig.

1.4 References

[1] J.P. Kutter, Y. Fintschenko, Separation Methods In Microanalytical Systems, CRC Press, Boca Raton, 2006.

[2] B. He, N. Tait, F. Regnier, Analytical Chemistry 70 (1998) 3790.

[3] F.E. Regnier, HRC Journal of High Resolution Chromatography 23 (2000) 19.

[4] B.E. Slentz, N.A. Penner, E. Lugowska, F. Regnier, Electrophoresis 22 (2001) 3736.

[5] J.C. Giddings, Dynamics of Chromatography, Part I, Principles and Theory, Marcel Dekker, New York, 1965.

[6] P. Gzil, N. Vervoort, G.V. Baron, G. Desmet, Analytical Chemistry 75 (2003) 6244.

[7] J. De Smet, P. Gzil, M. Vervoort, H. Verelst, G.V. Baron, G. Desmet, Analytical Chemistry 76 (2004) 3716.

[8] N. Vervoort, J. Billen, P. Gzil, G.V. Baron, G. Desmet, Analytical Chemistry 76 (2004) 4501.

[9] M. De Pra, W.T. Kok, J.G.E. Gardeniers, G. Desmet, S. Eeltink, J.W. Van Nieuwkasteele, P.J. Schoenmakers, Analytical Chemistry 78 (2006) 6519.

[10] W. De Malsche, Ph.D Dissertation in Department of Chemical Engineering, Vrije Universiteit Brussel, Brussels, 2008.

CHAPTER 2

On-chip liquid chromatography: history, fabrication technology and theory

2.1 The lab-on-a-chip concept

Lab-on-a-chip is a more general idea derived from the miniaturized total chemical analysis system (μTAS) concept that was proposed by Manz *et al.* [1] for silicon chip analyzers incorporating injection, sample pre-treatment, separation and detection in the same micro-device. This concept was presented simultaneously to the first on-chip liquid chromatograph that consisted of a 5 × 5 mm silicon chip containing an open-tubular column and a conductometric detector [2], being an important benchmark study, even though the separation power of the chromatograph was never demonstrated. Despite this concept was presented in 1990, it was not the first work with the idea of integrating all the parts of a chemical analysis system in a single silicon wafer. That honour is credited to Stephen Terry and co-workers, who gave the first example of a microfabricated device for chemical analysis in 1979 [3]. They proposed a gas chromatograph integrated in a planar silicon wafer containing a sample injector system, a 1.5 m long column and a clamped thermal conductivity detector which was previously fabricated on a separate silicon wafer. Even if separations of complex mixtures were able to be performed in that chip, its resolving power was poor in comparison to the standard columns of those days. That poor resolution may be an explanation for the disinterest shown by the scientific

community as it took more than ten years to have other researchers exploring this track further.

The transition to miniaturized devices involve a lot of benefits which have been welcomed enthusiastically by a wide range of different areas including pharmaceutics, medicine, analytical science, synthetic chemistry, biotechnology, physics, materials science, (bio)engineering, etc. In addition to the initial idea that going smaller would enhance the analytical performance of the devices, its size reduction has also shown a lot of benefits. Some of the advantages achieved by the μTAS are the low volume consumption, the faster analysis and response times, which also lead to a better process control, the compactness of the system allowing parallel analysis which can be monitored in the same device, and also lower fabrication costs, which can be decreased even more if a base material different from silicon is used. More concretely, the use of polymers has been the trend followed by researchers during the last years, despite silicon and glass dominated the first years of the lab-on-a-chip revolution.

2.2 Fabrication technology

Different fabrication techniques have been employed during the work summarized in this PhD dissertation. An overview of the microfabrication techniques used to fabricate both silicon and polymer microstructures are given in the following pages.

2.2.1 Silicon micromachining

The typical processes involving silicon micromachining that have been used in this work mainly consist in the combination of photolithography and etching. The first consists in patterning the desired structures in a photosensitive polymer that has been previously deposited (typically by spinning) over a silicon wafer. For that, the polymer is illuminated through a photomask, where the structures are defined, making it soluble or non-soluble (depending on the negative or positive nature of the

photoresist) to the developing agent where the wafer is subsequently immersed. In this work, photomasks have been fabricated by laser lithography whereas mid-UV light was used to illuminate the photoresist, allowing minimal line widths of about 2 μm, which is enough to pattern the structures fabricated for this thesis work.

Etching consists in removing material of the previously exposed substrate surface. Different ways to etch silicon can be used, albeit they are basically divided in two process classes: wet etching and dry etching. In the former, the substrate material is dissolved when immersed in a chemical solution, while in the latter the material is sputtered or dissolved using reactive ions or a vapor phase etchant. An extensive overview of the different techniques involving these two process classes can be found in refs. [4,5], while here only a brief summary of the principles of the method employed in this work will be described.

In all the fabrication processes involving the production of silicon masters (like the one shown in Fig. 1), described in this PhD dissertation, reactive ion etching (RIE), which is also the most frequently used etching technique, has been employed. Reactive species in RIE are typically generated in a SF_6-based inductively coupled plasma process, which, depending on their nature, can etch the surface chemically (radicals), physically (ions, which are accelerated toward the surface by the electrical bias that this surface has in the plasma), or in a combined physical-chemical way [6]. In order to obtain perfect steep-sided structures, an specific deep reactive ion etching (DRIE) technique, the so-called Bosch® process, consisting in a cyclic process where the etching gas is alternated with a passivation gas (typically C_4F_8), can be implemented. This second gas is used to deposit a chemically inert passivation layer that protects the entire substrate from further chemical attack and prevents further etching. With this process, high-aspect ratio structures can be easily achieved although the sidewalls tend to present indentations with an amplitude of about 100–500 nm due to the two-phase process (in Fig. 12 indentation in etched pillars can be observed). However, the cycle time can be adjusted, yielding smoother walls for short cycles while long cycles lead to a higher etch rate.

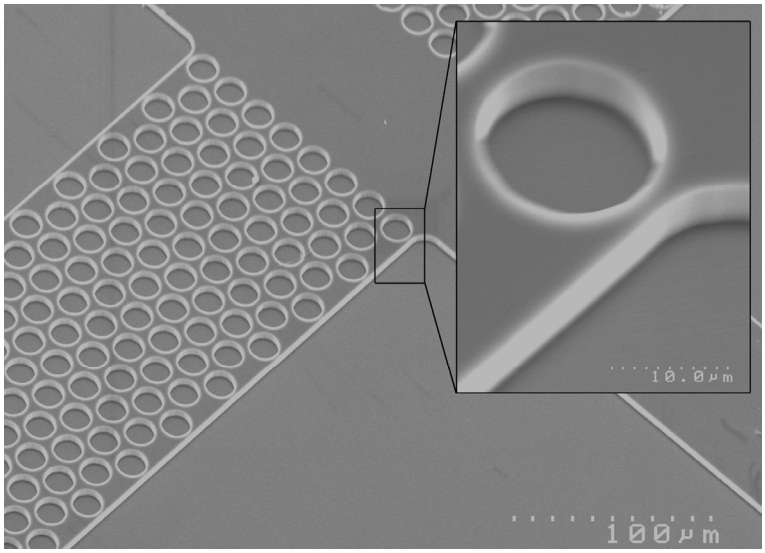

Fig. 1 SEM image of one of the silicon masters fabricated *via* DRIE. A detailed view of one of the master's holes to produce the pillars is shown in the embedded image.

2.2.2 Polymer microfabrication

The role of polymers as substrate materials for microfluidic devices is gaining importance in recent years as can be noted in Fig. 2 where the approximate numbers of annual publications referencing different materials used for microfluidics is depicted. Polymers offer a broad range of material parameters as well as material and surface chemical properties which enable microscopic design features that cannot be realised by any other class of materials [7]. Polymers can be divided in three different classes depending on the physical properties and the technological procedures for being micromachined. The main parameter to be considered for this classification is the glass transition temperature T_g, which can be described, in a simple way, as the critical temperature at which a non-crystalline material changes its behaviour from being 'glassy' to being 'rubbery'. 'Glassy' in this context means hard and brittle (and therefore relatively easy to break), while 'rubbery' means elastic and flexible. Thus, taking into account the T_g value and the behaviour of the polymer, polymers can be classified in thermosets, thermoplastics and elastomers.

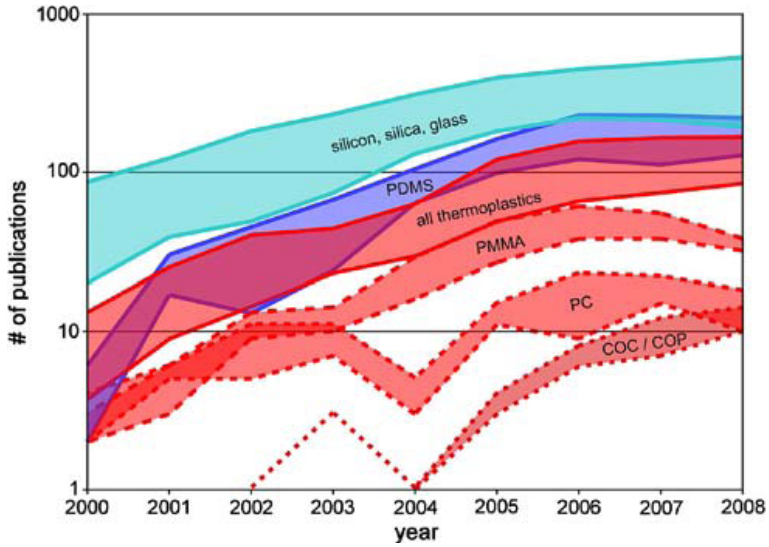

Fig. 2 Approximate numbers of annual publications referencing different materials for microfluidics. Maximum and minimum values defining the ranges were extracted from the Thomson Reuters ISI and NIH PubMed databases, respectively. Taken from ref. [8].

Thermosets, or often called resins, are materials that cannot be reshaped once cured, i.e., when the molecular polymer chains became cross-linked after being heated up or exposed to sufficient doses of radiation. If heated further, the polymer decomposes or burns instead of melting. Typical examples of thermoset polymers in microfabrication are the resist materials for lithography [5]. For microfluidic applications, specially the photoresist SU-8 [9,10], which can be micromolded by photolithography, and polyimide [11], which can be microstructured by photolithography or by dry etching techniques, are used.

Thermoplastics are materials that show a distinct softening at T_g, which makes them processable around this temperature, and a rather large temperature difference between T_g and the decomposition temperature, allowing a large process window. Thermoplastic materials include the technical polymers which can be structured using replication methods like injection moulding or hot embossing. The moulded parts of thermoplastics can be reshaped many times by reheating as no curing takes place at elevated temperatures. The most typical thermoplastics used in microfluidics are poly(methyl methacrylate) (PMMA) and

polycarbonate (PC), which were among the first materials used for polymer microfabrication [12]. Recently, cyclo olefin polymers (COPs) have attracted much attention due to their favourable properties like high organic solvent resistance, low water adsorption, glass-like optical clarity and low background fluorescence [13]. For these interesting properties, this material has been used for the fabrication of the different devices reported in this PhD dissertation.

Finally, elastomers or rubbers are materials which have the ability to undergo deformation under the influence of a force and regain its original shape once the force has been removed. This is possible because its molecular chains are longer than in the other two cases and typically do not show a chemical interaction but are physically entangled. Poly(dimethylsiloxane) (PDMS) is the most commonly used elastomer due its low cost and easy handling and, despite of its limitations, has become one of the most prevalent materials to manufacture microfluidic devices [14].

2.2.2.1 Replication methods

Different replication techniques to microfabricate polymers have been successfully developed during the last years, mainly encouraged by its low-cost manufacturing process. The underlying principle of all these methods is the replication of a master structure which has the geometrical inverse of the desired polymer structure. A wide range of technologies is available for the fabrication of the moulding tools, e.g. silicon micromachining, electroplating, laser ablation or mechanical micromachining. An overview of the processes involved in the silicon micromachining that have been performed to fabricate the silicon masters used in this work is given in the previous section, while for more information about the other techniques, the reader is encouraged to consult the extensive literature that covers this topic [15,16].

Among the different replication techniques that have been developed, this introduction will be focused on hot embossing, which has been the employed method for the fabrication of the COP devices that are described in this PhD dissertation.

Other common replication methods like injection moulding and casting are described below.

Injection moulding is a technique where the polymer material is fed as pre-dried granules into a heated barrel, mixed, and forced into a mould cavity where it cools and hardens to the configuration of the mould cavity [17,18]. Even though it is very well suited to produce three-dimensional structures and for mass-production due to the large variety of equipment suppliers and automation solutions available, the complexity of the process and the need for an often mechanically complicated and extremely expensive moulding tool, make this method rarely used in the academic world. Casting, which by far is the most reported fabrication method, is mainly limited to elastomeric materials. In this technique, also referred as soft lithography, the elastomer is poured over the master and cured in order to give time to the cross-linking reaction to take place [14,19-21]. This is a very fast, cheap and easy technique; however, the pros and cons of its use are strongly related to the properties of the casted material, typically PDMS. Other techniques like injection compression moulding [22] and microthermoforming [23,24] have also been employed although their use is very limited.

Hot embossing is an imprinting technique that was first described in the late 1990s [25-28]. Although in the early days different tools were used to replicate the structures, nowadays, a silicon stamp is the most common used imprinting tool for the fabrication of polymer microfluidic devices. The embossing process consists of different steps; first, the thermoplastic material is generally cleaned thoroughly, dried, and then placed on top of the silicon stamp. Then, the stamp and the plastic substrate are placed in the embossing system and heated up in vacuum to a temperature just above the T_g of the polymer. To end the process, pressure is applied for a certain time before being isothermally cooled to a temperature just below the T_g, where the two parts are separated (de-embossing or also called demoulding or detachment). This process may take around 20 min which for academic purposes is perfectly suited although it would be to slow for mass-production, unless larger imprinting areas or shorter times could be achieved. However, the accuracy that is accomplished with

this technique enables the reliable fabrication of structures in the few tens of nanometres range. In this size range, the process has been named nanoimprint [29] and is one of the potential methods for future lithography in the nanometer range.

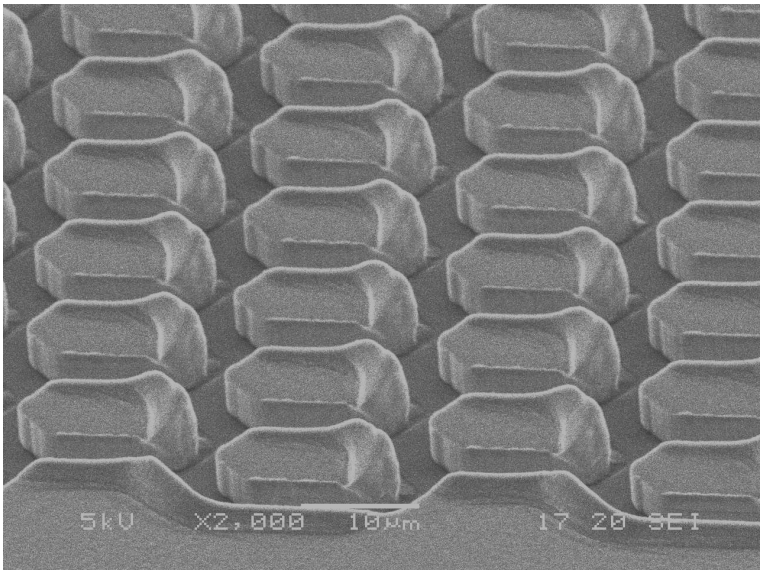

Fig. 3 SEM image of diamond-shaped pillars that have been demoulded at a sub-optimum de-embossing temperature, causing accumulation of material at the top parts of the pillars.

One should be aware of several critical issues to perform successful imprints. First of all, the choice of the optimal temperature and pressure conditions for a specific process is needed. As a general rule, the embossing should take place at 15 to 20 °C above the T_g and de-embossing at 10 °C below T_g [30]. It has been observed, that when embossing at sub-optimum temperatures the structures might not be completely transferred to the master while embossing at too high temperatures may affect to the substrate structure properties. Likewise, sub-optimum pressure will cause incomplete filling of the embossing master and therefore incompletely embossed channels, while embossing at too high pressures will facilitate a possible breaking of the master when demoulding. Another important parameter is the de-embossing temperature. As far as the thermal expansion coefficient of the master and the polymer substrate are not the same, their rates of expansion and shrinkage during temperature shifts are different. To minimize artefacts caused by the difference in thermal properties, separation must take place when the plastic is no longer soft and deformable, but has

not shrunk to a point where it mechanically interacts with the master due to contraction forces, causing accumulation of material at the top parts of the embossed structures, as it is shown in Fig. 3. Additionally, a good surface quality of the master along with the use of antisticking layers (typically fluorinated silane-based coatings are used [31-34]) in the master surface may be also required to avoid adhesion between the master and the polymer substrate. Finally, it is also necessary to have a uniform temperature distribution across the master structure and an optimal vacuum to prevent trapped air forming bubbles.

Fig. 4 Pictures of the Hot Embossing system (HEX01, Jenoptik AG, Germany) (left) and Nanoimprint Lithography system (Obducat, Sweden) (right) used to imprint and bond, respectively, the pillar array structures.

In the case of COP which is imprinted with a silicon mould, albeit the considerable difference between the thermal expansion coefficients of silicon and COP (2.6 ppm K^{-1} and 70 ppm K^{-1} respectively), optimal imprints can be achieved. The use of SU-8 as a master could facilitate the de-embossing step, since the interaction forces between the master and the substrate would be lower due to the similar thermal expansion coefficients (52 ppm K^{-1} for SU-8), but as reported previously, after few embossing experiments, the structures in the SU-8 start to show slight damage [30]. Optimal conditions to emboss the ZeonorFilm®, ZF 14–188 (T_g = 138 °C), the type of COP used to fabricate the pillar array columns, have been found to be 170 °C, 2000 N, 300 s and with a demoulding temperature of 120 °C in a HEX01 embossing system (Jenoptik AG, Germany), which is shown in Fig. 4. Moreover, and despite the use of antisticking coatings in the master, the use of smooth teflon films to protect the master and the substrate from the embossing plates has appeared to be excellent to assist the

embossing process. An image of the fabricated pillars using this procedure is shown in Fig. 5. For the fabrication of the microchannels described in chapter 6, a manual laboratory bonding press with hot/cooling plates (TEMPRESS, Paul-Otto Weber GmbH, Germany) was used, as the features to imprint did not require the precision of clean room equipment. With this laboratory press, optimal embossing of the COP was performed at 170 ◦C and 10 kN for 600 s. The demoulding of the system was done at 120 ◦C, following what it has been described in the previous paragraph.

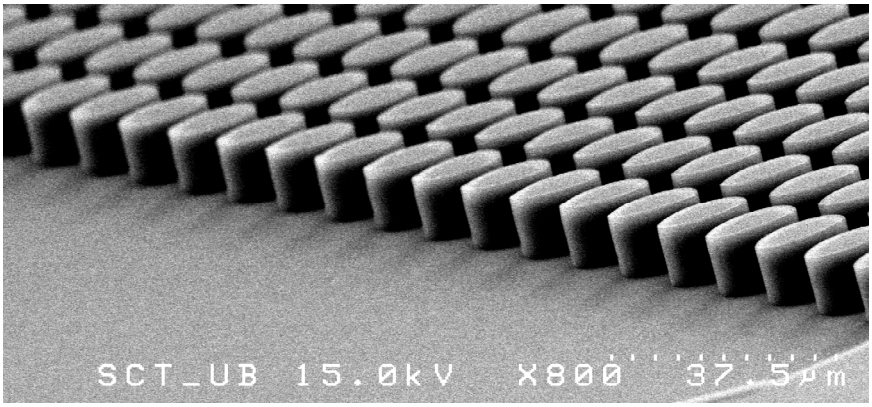

Fig. 5 SEM image of the pillars embossed in COP with a silicon master using optimum conditions: 170 ◦C and 10 kN for 600 s.

2.2.2.2 Electrode fabrication

The number of polymer microfluidic devices incorporating electrodes, which are mainly used for electrochemical detection, is increasing in recent days [35-39]. Microelectrodes have been fabricated using different techniques which can be roughly divided in thick-film and thin-film methods. Screen-printing is the most employed thick-film technique. It consists in the deposition of a paste containing metal particles over a screen containing the geometrical pattern of the electrodes [40]. More recently, an alternative to this technique using the same concept has been accomplished by spraying the paste through a patterned film, which is known as airbrushing [41]. Another thick-film method is the assembly [42], where the electrode material (typically being a carbon fiber or a platinum wire) is inserted into the device.

Meanwhile, the thin-film methods are based on the deposition of the electrode material (typically gold, aluminum, chromium or platinum) using microelectronic fabrication technologies like sputtering or evaporation. The deposition can be achieved directly, through a metal shadow mask [43], or *via* photolithography [44]. The resolution of the former is limited to few tens of micrometers, so if more precise microelectrodes are needed, photolithography has to be employed. Actually, that is the most widely and commonly used technique when the substrate is silicon or a glass-based material due to the near perfect control of the size, shape and interelectrode distance between two adjacent electrodes it affords [45]. However, the incompatibility of most of the thermoplastics to photolithographic techniques which involve the use of resins and organic solutions, make this method only available for thermosetting polymers [46]. The use of COPs has solved this issue as was first described by Nielssen *et al.* [47] and now, precise microelectrodes fabricated via photolithography can be easily integrated in a microfluidic polymer device as it is demonstrated in chapter 6.

2.2.2.3 Bonding methods

The inevitable requirement of having a closed channel configuration makes the sealing of thermoplastics a non-avoidable process, being another step in the polymer microfabrication process. The diverse material properties of thermoplastics open the door to an extensive array of substrate bonding options. In a recent review from Tsao *et al.* [8] the different microfluidic bonding techniques were categorized as either indirect or direct. Indirect bonding techniques involve the use of an adhesive layer to seal two substrates and encapsulate microchannels fabricated in one or both of the substrates. Common methods involve the use of liquid adhesives, which should have high viscosity to prevent blocking of the channel by adhesive overflow. Those adhesives may be activated by simple solvent evaporation or typically by UV-light irradiation [48-51]. Using the same idea, partially-cured PDMS has also been investigated as an adhesive layer for bonding PMMA microfluidic substrates instead of employing the above mentioned liquid adhesives [52]. Another common method for adhesive bonding is the use of lamination films, which can be either pressure or

thermally activated [53,54]. The simplicity of these methods makes this approach the most widely used for bonding thermoplastic polymers. However, the use of an intermediate adhesive layer may result in channel sidewalls with different chemical, optical, and mechanical properties than the bulk polymer which would be detrimental for the currently application described in this thesis.

On the contrary, direct bonding techniques do not use any additional material in the interface to seal the substrates. Four different methods are being used nowadays, depending on the polymer properties and future application of the microfabricated device. These methods are adhesion, thermal pressure bonding, solvent-assisted bonding and welding.

Adhesion is typically employed with elastomers (e.g. PDMS) and takes advantage of its surface adhesion which has to be activated by exposing them to oxygen plasma, UV light or corona discharges [14,55,56]. In thermal pressure bonding both substrates are heated up until a temperature slightly below its T_g and pressed together [57-59]. The combined temperature and pressure can generate sufficient flow of polymer at the interface to achieve intimate contact, with intense entanglement of polymer chains between the surfaces leading to a strong bond. Different or equal polymer substrates can be bonded with this technique by changing the values of both parameters if care in avoiding clogging or channel deformation is taken and hence, the process window is narrow. For that, to have an appropriate control of both parameters, thermal pressure bonding is usually performed in the same equipment as is used for embossing the substrates. To improve the bonding quality, surface treatment using plasma or UV-light has also been reported [60,61].

Solvent bonding of thermoplastics takes advantage of polymer solubility in different solvents. Polymers are softened by dipping or exposing them to the solvent solution. Then, both surfaces are attached while the material at the interface is still dissolved and, after subsequent evaporation of the solvent, solidifies again, combining the two parts by forming chemical bonds between them, leading to an exceptionally strong bond. This method has been typically used for sealing PMMA

structures using different solvents, e.g. ethanol, methanol, isopropanol, acetonitirile, dimethyl sulfoxide (DMSO) or mixtures of them [62-64]. The critical aspect in solvent bonding is the prevention of structural damage by "melting" the microstructures due to solvent excess. For that, this technique is partially restricted to small areas where the amount of solvent can be better controlled.

The last direct bonding method that has been described to fabricate polymer lab-on-a-chip systems is welding. There, energy to induce heating and softening at the interface of two polymer parts is deposited by either ultrasonically actuated relative mechanical movement [65] or laser radiation (typically a diode laser with IR-wavelength emission) [66]. While these bonding techniques provide interesting options for highly localized welding of thermoplastics, they have not been widely adopted for general microfluidic bonding applications. The need of special chip designs to focus the energy for ultrasonic welding and the constraints imposed on the substrate materials for laser welding have minimized its use.

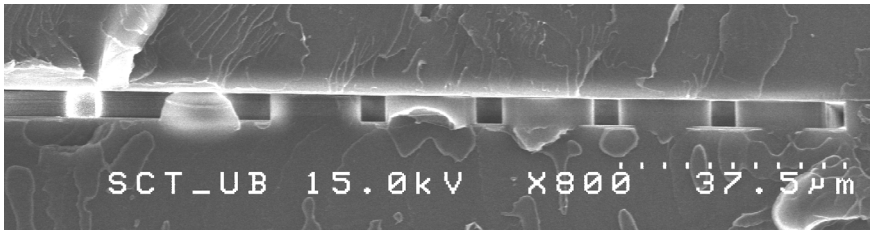

Fig. 6 Cross-section SEM image of one of the COP channels containing the pillar array column after the pressure-assisted thermal bonding. Conditions used were 123 °C and 40 bar for 600 s.

Bonding of COPs microstructures has been reported by using either lamination [67], thermal pressure bonding [57,58,68,69] or solvent bonding [70-72]. Higher bonding strengths have been reported for the solvent bonding method, e.g. Mair *et al.* [71] reported on COC chips bonded by 90 s cyclohexane vapour exposure and subsequent 15 min deep UV irradiation Maximum burst pressures which could withstand up to 34.6 MPa. As stated before, the difficulty to control solvent excess when working with higher and complex areas which could damage the structures make the thermal bonding more suitable for sealing the pillar structures reported in this PhD dissertation. In particular, the pillar arrays embossed in COP sheets have been

bonded to blank COP sheets in a NanoImprint Lithography apparatus (Obducat, Sweden) at 123 °C and 40 bar for 600 s. In Fig. 6 an image of a bonded microchannel containing the pillar structures is shown. Alternatively, the microchannels fabricated in chapter 6 were bonded in the same laboratory press as they were previously embossed at 120 °C and 8 kN for 900 s.

2.3 Chromatography

2.3.1 History & methods

The concept of chromatography, which is a transliteration from Greek *colour writing*, has its origin in the beginning of the 20th century, when the Russian botanist M. S. Tswett, who is generally credited with the discovery of chromatography, separated green leaf pigments using a column of powdered calcium carbonate [73]. The separation resulted yielded a series of coloured bands, by allowing a solvent to percolate through the column bed, hence the name of chromatography. But it was not until the 1930s that the true potential of the technique become widespread as an established laboratory method. Although many scientists made substantial contributions to the evolution of modern chromatography, not least among these is A.J.P. Martin who in 1941 (together with R.L.M. Synge) introduced the partition chromatography [74]. He also presented paper chromatography [75], which nowadays has been largely replaced by thin-layer chromatography. Lately, and together with A.T. James, he also developed gas chromatography [76], of which the development was extremely successful due to the simplicity of the open-tubular format, which for GC is highly efficient. Further milestones in the evolution of chromatographic separations can be found in the literature [77,78]. However, it is worthy to point out the pioneering work of C. Horvath, who was one of the responsible for the rebirth of liquid chromatography in its modern form, and also, for its enormously fast growth that has placed it as the dominant analytical technique in the twenty-first century [79]. For example, the high performance liquid chromatography

(HPLC) concept, the actual general name for all liquid chromatography techniques that require the use of elevated pressures to force the liquid through a packed bed, was first described in one of his papers [80].

Chromatography is essentially a physical method where a mixture is separated in its compounds. Basically, the different components to be separated are distributed between two phases: the stationary and the mobile phase. The former is typically immobile and can be a wax, solid or immobilized liquid, while the latter provides the analyte transport and can be any fluid having sufficient selective solubility for the analyte compounds in order to generate different migration velocities. In other words, separation results from differences in the distribution constants of the individual sample components between the two phases. These differences can be due to several selectivity mechanisms like charge, hydrophobicity, partitioning, size, adsorption, molecular recognition or a combination of them, therefore, chromatographic separations depend on a favourable contribution from these thermodynamic and kinetic properties of the compounds to be separated.

In general, chromatographic techniques can be classified according to the physical state of the mobile phase, as it can be either a gas, then we refer to gas chromatography (GC), or a liquid in the case of liquid chromatography (LC). Moreover, depending on the nature of the stationary phase, both techniques can be further divided. In gas chromatography it could be either a liquid or a solid; accordingly, we can distinguish between gas–liquid chromatography (stationary phases consisting in coatings of viscous liquids or liquid-like polymers), and gas–solid chromatography (coatings of thin porous layers or packings with porous particles). In liquid chromatography a similar distinction can be made. On the one hand, liquid-liquid chromatography, that was progressively abandoned because of their limited stability and experimental inconvenience, although it has recently resurfaced in the form of countercurrent chromatography with two immiscible liquid phases of different densities [81].

On the other hand, when the stationary phase is solid, liquid-solid chromatography (or just liquid chromatography) is described. LC can be further diversified according to the type of interactions between the analyte and the stationary phase surface and according to their relative polarity of the stationary and mobile phases. The different separation mechanisms used in HPLC are widely reviewed in the literature [82], while few lines of the more common used are given in the following.

The form of LC which was historically the first to be used [83], known as normal phase chromatography, employs a polar adsorbent and a non-polar mobile phase and it is based on the interaction of the polar functional groups of the analytes with polar sites on the surface of the packing. Reversed-phase chromatography, in contrast, works as the other way around, with a non-polar stationary phase in conjunction with a polar, largely aqueous mobile phase. This technique is by far the most used among all the HPLC applications being applicable to a wide range of neutral compounds of different polarity. There are two other techniques named hydrophilic and hydrophobic interaction chromatography that can be viewed as extensions of normal- and reversed-phase chromatography, respectively. In the former, very polar analytes and aqueous mobile phases are used, while in the latter, the analytes are typically adsorbed onto the packing in a buffer with a high salt concentration, and eluted with a buffer of low ionic strength. Another common liquid chromatography technique is the size-exclusion chromatography, where the packed stationary phase has a controlled pore size distribution and solutes are separated by size differences. Finally, in ion-exchange chromatography, retention is based on the electrostatic interactions between ions in the mobile phase and the ionic groups immobilized on the stationary phase.

2.3.2 Theory

The separation of a mixture in a chromatographic column can be thought as a result of two events that occur to the solution in its migration along the column.

The first is related to the interaction of the different specific compounds with the stationary phase, which can be assessed by the equilibrium distribution or partition coefficient, *K*:

$$K = \frac{C_s}{C_m} \tag{1}$$

where C_s and C_m are the concentration of a compound in the stationary phase and the mobile phase, respectively. The retention factor *k* of a component can be simply defined as a relation between the number of molecules in the stationary and the mobile phase which can be easily related to the partition coefficient:

$$k = \frac{N_s}{N_m} = \frac{C_s V_s}{C_m V_m} = \beta K \tag{2}$$

where β is the phase ratio, which is defined as the ratio between the volumes of the stationary and mobile phase, V_s and V_m, respectively. In the case of our study, the volume of the stationary phase can be substituted by just the surface due to the non-porous nature of the COP surface. Simultaneously, the retention factor can also be expressed as:

$$k = \frac{t_r - t_0}{t_0} \tag{3}$$

where t_r and t_0 are the respective residence times of the retained and a non-retained component.

The second event involved in solute migration is associated with the broadening of all component peaks. The effect is caused by all the kinetic processes associated with the adsorption-desorption and motion of the analytes through the column. The degree of this band broadening is related to the column efficiency. Among the different theories used for the description of the band broadening, Martin and Synge [74] introduced the plate theory for the evaluation of the column efficiency. They defined the height equivalent to a theoretical plate (HETP) as "the thickness of a layer in the column such that the eluting mobile phase is in equilibrium with

the solute concentration in the stationary phase". Therefore, the smaller the plate height or the greater the number of plates, the more efficient the analyte exchange is between two phases, and the better the separation. That is why column efficiency is expressed in number of theoretical plates. In particular, the plate height is a measure of the peak broadening on a certain distance:

$$H = \frac{\Delta\sigma_x^2}{\Delta x} \tag{4}$$

where σ_x is the standard deviation of the peak and Δx the travelled distance. Then, the total plate number, or in other words, the column efficiency in a column of length L is defined as:

$$N = \frac{L}{H} \tag{5}$$

The plate height is strongly dependant on the linear velocity u as it is denoted by the van Deemter equation [84]:

$$H = A + \frac{B}{u} + Cu \tag{6}$$

which, as it can be seen, is composed of three differentiated terms: the A-term, related to the heterogeneity of the system; the B-term, linked to the molecular diffusion in the axial direction; and the C-term, related to the mass-transfer resistance in (and between) the stationary and the mobile phase. The influence of the different terms on the Van Deemter curve is shown in Fig. 7.

A more approximate description of the band broadening process for a packed column at low mobile phase velocities was given by Giddings [85], including the definition of the different terms of the van Deemter equation:

$$H = 2\lambda d_p + \frac{2\gamma D_m}{u} + \left[\left(\frac{k}{k+1}\right)^2 \frac{d_p^2}{D_m} + \frac{k}{(k+1)^2}\frac{d_f^2}{D_s}\right]u \tag{7}$$

where λ and γ are a geometrical constant and an obstruction factor, respectively; d_p is the pillar diameter and D_m is the molecular diffusion coefficient. The last term is divided into a resistance from the interface towards the mobile phase and a resistance towards the mobile phase with d_f as the stationary film thickness and D_m as the stationary zone diffusivity. There it is clear to see the dependence of the plate height on the pillar diameter, so using small particles would increase the efficiency of the column.

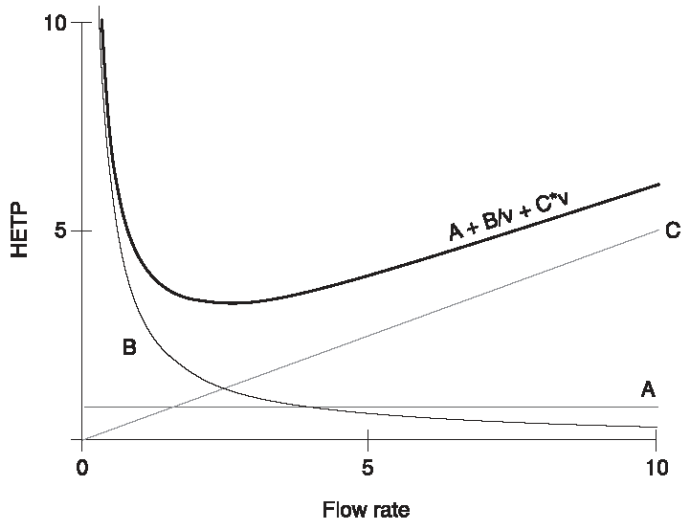

Fig. 7 Representation of the van Deemter curve and its different components.

Another interesting analysis of the efficiency of a packed column can be done by differentiating equation (6) with respect to the mobile phase velocity and setting the result equal to 0. Then, optimum values of the linear velocity (which can be associated as the mobile phase velocity) and the plate height can be obtained [78]:

$$u_{opt} = \left(B/C\right)^{1/2} \tag{8}$$

$$H_{\min} = A + 2\left(BC\right)^{1/2} \tag{9}$$

From equation (9) it is clear that the highest efficiency of a packed column would be never less than the contribution of the A-term. Consequently, the more homogeneous is the packing, the more efficient is the column.

In order to compare the efficiency of columns under a broad range of mobile phase conditions and different particle sizes, Knox and Parker defined the dimensionless forms of the plate height and the linear velocity, known as reduced plate height and reduced velocity [86]:

$$h = \frac{H}{d_p} \tag{10}$$

$$v = \frac{ud_p}{D_m} \tag{11}$$

Then the van Deemter equation can be re-written in the reduced form:

$$h = A + \frac{B}{v} + Cv \tag{12}$$

Other important parameters used to report characteristics of a chromatographic separation, besides the retention factor and the efficiency that have been already described, are the selectivity and the resolution. Selectivity (α) is the ability of a chromatographic system to discriminate two different analytes and it is described as the ratio of the corresponding retention factors:

$$\alpha = \frac{k_2}{k_1} \tag{13}$$

In Fig. 8 the importance of the selectivity and the efficiency in a separation is shown. As it can be seen, the optimization of both parameters is important to achieve satisfactory separations. While efficiency is essentially a property of the column, selectivity is the reflection at the nature of analytes and the surface chemistry of the packing material.

Finally, resolution (R_s) is used as an indicator of the quality of the separation. It is described as the ability of the column to resolve two analytes in two separate peaks. Its definition combines information of both the peak dispersion and the selectivity:

$$R_s = \frac{2\Delta t_r}{w_2 - w_1} \tag{14}$$

where w_i is the peak width. Achievement of good resolution between analytes in complex chromatograms is the main goal in HPLC method development. Optimal resolution could be achieved by optimization of system efficiency, or selectivity (or both). A fundamental relationship in LC that allows to control the resolution by varying selectivity, efficiency or retention is described with the assumption that the average of two peak widths is equal to the width of the second peak [88]:

$$R_s = \frac{\sqrt{N}}{4}\frac{k}{1+k}\frac{\alpha - 1}{\alpha} \tag{15}$$

The three terms of the equation (15) are roughly independent, so that we can optimize them separately. From there, it is also denoted that for achieving a separation, retention factor, selectivity and efficiency must be different from zero.

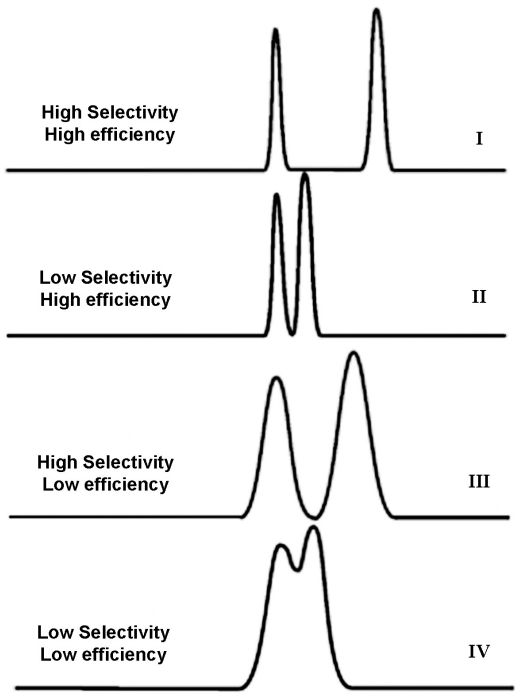

Fig. 8 Peaks are narrow and far from each other, simple decrease of the column length or flow rate can significantly shorten the runtime without the loss of separation quality. II: Acceptable separation, method may not be rugged. III: Acceptable separation, quantisation reproducibility could be low. IV: Bad separation. Reprinted from [87].

2.3.3 Column formats & on-chip LC

The more standard approach to liquid chromatography separations is through the use of columns packed with particles. The particles (which are normally porous) support the stationary phase, provide a large interfacial area for analyte partitioning and form a homogeneous medium for the transport of mobile phase. This format has been demonstrated to be more efficient than the open column format that is typically employed in gas chromatography. In particle-packed columns, decreasing the particle diameter leads to improved efficiency and speed; however the price paid in pressure will always be proportionally larger than the gain in column performance. Monolithic columns are a viable alternative to the packed bed format as a means to achieve efficient separations while overcoming the pressure limitation due to their lower flow resistances [89]. High efficiencies together with lower pressure drop make monolithic columns attractive options for fast HPLC. Monoliths are materials that have a continuous porous skeleton with relatively wide flow through pores, and are typically formed by *in situ* polymerization inside the column. The polymerization solution typically consists of a mixture of free monomers containing a free radical initiator and a so-called porogenic solvent. UV or thermally activation of the initiator causes the formation of the flow-through pore structure, which can be modified by adjusting the porogen solvent composition [89-92].

Nowadays, the miniaturisation of these conventional LC systems to the on-chip LC format is one of the prevalent demands in the lab on a chip field. Even though the first μTAS device was designed for pressure-driven LC, many drawbacks caused by mechanical problems have been encountered, making this transition more difficult than expected initially [93-95]. Limitations to achieve perfect bonding of the microchannels and concerning the interface with a pressure source have been difficult to solve. In particular, the latter has been hampered by the small scale of the microfluidic channels that require complete leak-free tubing connections. This can be partially solved using the idea presented by Tiggelaar *et al*. [96]. There, grooves were etched in a glass chip to couple the capillaries which were fixed by applying an epoxy

glue. The chips could withstand pressures up to 690 bar, however, when working with polymer materials this idea it is not applicable directly.

On the contrary, electrophoretically or electrokinetically driven separations have been successfully and easily developed in a microchip platform using different techniques such as capillary electrophoresis (CE) [97-99], isoelectric focusing (IEF) [100,101] micellar electrokinetic chromatography (MEKC) [102,103] and capillary electrochromatography (CEC) [104,105].

Besides the mechanical problems, much effort to develop the on-chip pressure-driven LC format has been made during the last years. Apart from the progress made in the traditional chromatography formats (packed beds and open tubular columns), the monolithic column format has become very popular for on-chip LC. Its fabrication process, which seems very suitable for microchannels, has attracted the attention of many researchers. Moreover, the pillar array concept, a new column format which takes advantage of the existing micromachining techniques, has been recently developed. This column structure specially designed for on-chip LC applications have shown very promising results, so further study in this direction may bring a bright future for on-chip [106]. In the following units, an evolution of the miniaturisation of the different column formats is given.

2.3.3.1 The packed-bed format

Many different particle materials have been employed for packing columns. Research in this area, since the big (from 30 to 100 μm) and irregular shaped particles of silica that were used in the early days of chromatography, has been continuously in development. The particle size of a packing is of utmost importance as it determines both the column efficiency and the pressure drop. Nowadays, the majority of packing materials are porous particles with average diameters between 3 and 10 μm, with particles down to 1.8 μm being commercially available. Introduction of small non-porous particles was an attempt to increase the column efficiency but their lower loading capacity has left it for only some specific applications (mainly protein and

nucleic acid separations) [107]. Recently, a novel column type marketed as Halo column has been introduced, based on the work made by Kirkland *et al.* [108]. These columns are packed with a new generation of particles composed of a solid silica core (1.7 μm in diameter) surrounded by a porous layer (0.5 μm thick), enabling fast separations with high sample loading and avoiding the ultra-high pressures required for the small porous particles.

When going to on-chip LC, Ocvirk *et al.* [109] were the first to present an experimental investigation and performance demonstration of an integrated liquid chromatography chip. The device integrated a split injector, a small-bore column packed with 5 μm C_8 particles, a retaining frit and an optical detector cell in a silicon chip where two fluorescent dyes were successfully separated. Nevertheless, the fabrication of frits, non-uniformity of packing at the walls and corners of the rectangular channels, and the difficulty of packing columns through the tortuous channel network on a wafer have been substantial problems difficult to overcome.

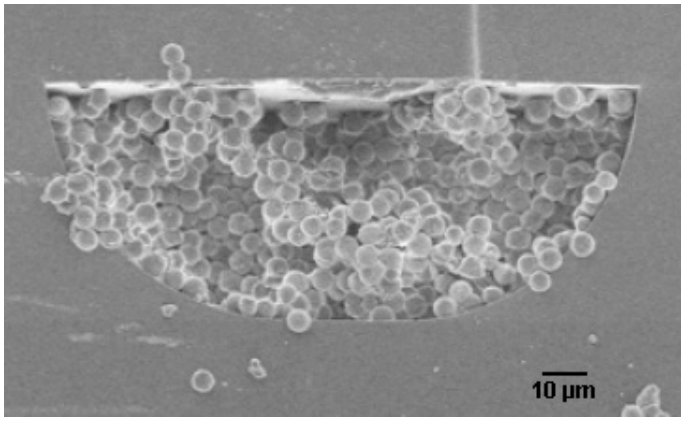

Fig. 9 SEM image of a cross section through a microfluidic LC channel fabricated in glass packed with 5-μm particles (taken from [111])

In spite of the difficulties encountered for packing the channels, the packed-bed column format has produced some interesting publications involving on-chip LC. Techniques using low-pressures to pack the columns have been employed, although their chromatographic performance, in terms of the number of theoretical plates, is relatively poor. Some examples of microchips fabricated in silicon or glass using

different injection and detection methods have been presented in this direction [110-112]. Focusing in devices fabricated in polymers, fritless chromatographic microchips fabricated in PDMS and packed with conventional reversed-phase silica particles [113,114] along with a PMMA microfluidic device, slurry-packed with C-18 octadecylsilane particles [115] have been reported, showing pressure-driven LC separations.

Herewith, packed separation channels of a reasonable length, with an efficiency comparable to that of standard packed columns, high-pressure packing methods are apparently still indispensable [116]. A successful application of high-pressure packing of microfluidic channels, with pressures up to 120 bar, has been described Yin *et al.* [117,118]. There, the different parts of the device were machined in three different polyimide films, which were joined together by hot lamination. Reversed-phase gradient separations of tryptic protein digests enabling subfemtomole detection sensitivity were reported with this chip which is now commercially available. Finally, a recent study from Ehlert *et al*. [119] using a similar polyimide HPLC microchip showed that microchips could be packed as densely as the cylindrical fused-silica capillaries used in nano-HPLC, achieving separation efficiencies comparable to those of nano-HPLC.

2.3.3.2 The open tubular approach

Open tubular columns, with the stationary phase supported on the tubing walls, are typically used in gas chromatography as they present a very high efficiency. Originally, its ease of fabrication stimulated their fabrication in a silicon chip [2] but their low efficiency, due to the limited rates of mobile-phase mass transfer, has made this format to be very unpopular in liquid chromatography [120]. Other attempts using the open tubular approach have been presented by McEnery *et al.* [121,122], who described the fabrication of a micro-LC device in a Si wafer integrating an on-chip injector, a coated microchannel and platinum electrodes (which were micromachined in the glass cover plate), Vahey *et al.* [123], who reported on a LC analyzer fabricated in PDMS, and recently by Benvenuto *et al.* [124], where a platinum

heater is included in a similar microdevice. In all this work no separations are reported, confirming the few advantages of using this column approach.

However, a renewed interest in the open tubular format has recently appeared as some authors have shown its potential in the proteomics field. An example of this trend was given by Fuentes *et al.* [125] who presented a microdevice fabricated in glass integrating electrochemical micropumps and where pressure-driven LC separations of three fluorescently labelled amino acids were achieved in a coated 5 μm deep microchannel.

2.3.3.3 Monoliths

The use of monoliths, besides the advantages described above, also solve the problems concerning the affixing of the packing particles inside the microchannels as no frits are required to hold the stationary material. Moreover, its ease of preparation makes it suitable for being integrated in microfluidic devices, although the batch-to-batch repeatability remains still an issue. The monolith can be chemically bonded and because they are more porous and more permeable than packed beds, lower pressures are required to perform chromatographic separations. For a microfluidic system this aspect is much more important than for instruments that use conventional columns and capillaries.

Successful attempts to obtain a continuous polymer bed in a microchannel were conducted by Ericsson *et al.* [126] who described both electroosmotic and pressure-driven chromatography separations of low-molecular weight compounds, as well as of proteins in planar quartz chips. Using a fused-silica chip, CEC separation of polyaromatic hydrocarbons on butylacrylate monoliths have been reported [127]. Also in CEC mode, separation of (derivatized) peptides with acrylate-based monoliths in a chip system can be comparable to or even better than capillaries, as was shown by Throckmorton *et al.* [104]. Lately, reversed-phase LC separations of fluorescently labeled peptide and protein mixtures were shown by Reichmuth *et al.* [128] in a 1.7-cm long microchannel filled with a stearyl-acrylate monolith. The

possibility to make microfluidic channels with silica-based monoliths has also been demonstrated. For example, Ishida *et al.* [110] presented a pressure-driven liquid chromatography microdevice fabricated in glass with an octadecylsilane (ODS)-monolithic silica separation channel providing the favourable chromatographic separation for catechins.

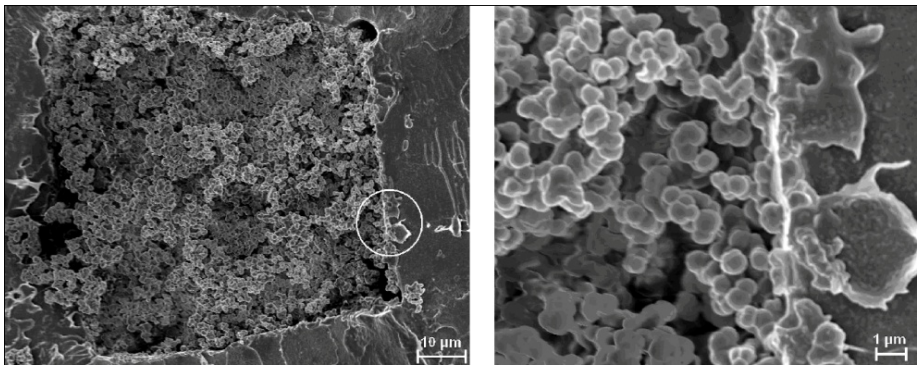

Fig. 10 SEM image of BMA-TMPTMA monolith (left). Magnification of the circular area in the left image revealing apparent covalent attachment of monolith to the COP channel surface (right). Images taken from [72].

Fabrication of monoliths in polymer microchips has been one of the latest achievements. As described before, polymers show many advantages for fabricating microfluidic devices, and particularly, cyclo olefin polymers (COPs) have been used for the fabrication of LC microchips due to its high chemical resistance to organic solvents. Stachowiak *et al.* [68] reported on the fabrication of porous polymer monoliths covalently attached to the walls of COC microchannels. Reproducible separations of tryptic digested proteins were reported by Ro *et al*. [70] using an off-line microchip LC-MALDI-MS system incorporating a poly-(ethylhexyl methacrylate-co-ethylene glycol dimethacrylate) (PEHMA/EDMA) column that was prepared by UV-initiated polymerization in a COC microfluidic channel. Recently, Liu *et al*. [72] described HPLC separations of peptides in COP microfluidic chips employing in situ photopolymerized polymethacrylate monoliths.

2.3.3.4 The pillar array concept

In 1998, Regnier and co-workers launched the concept of "collocated monolithic support structures" (COMOSS) taking advantage of the micromachining technology used in the microelectronics industry [129-132]. An image from the proposed structures is shown in Fig. 11. With this idea, they proposed that fabrication of liquid chromatography columns by microlithography would allow the creation of structures and channels in situ, which would circumvent the need for packing particles in a column. Moreover, objects could be positioned and arranged in columns by design, allowing simultaneous creation of all the structures and channels in a column and, finally, it should be possible to create multiple columns on a single wafer. Albeit they were working in electro-osmotic flow mode, the work from Regnier showed the potential of microfabrication also for on-chip pressure-driven chromatography.

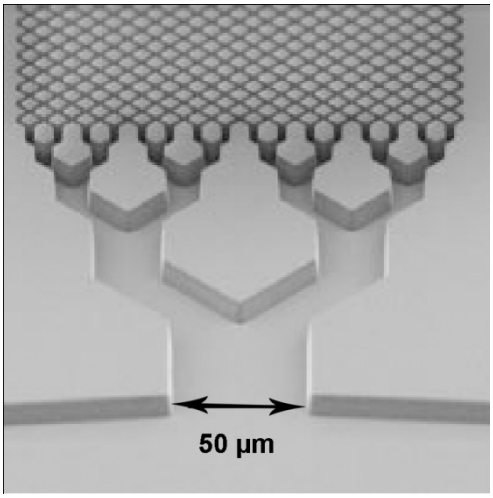

Fig. 11 SEM image of a microfabricated chromatography column and inlet proposed by Regnier and co-workers. Taken from ref. [129]

After the pillar array concept was introduced, some researchers have been working with this idea for different separation methods and applications [134,135]. But, it has been Desmet and his group in the Vrije Universiteit Brussel, who have carried out significant theoretical studies to investigate the ideal pillar structure and the practical limitations of this column format when working under pressure-driven liquid chromatography [136-138]. Specifically, computational fluid dynamics (CFD)

simulations were used to show the advantages of this column structure. Experimentally, de Pra *et al.* presented the first work where band broadening experiments on columns with non-porous silicon pillars under non-retentive conditions were performed [139], achieving a minimum plate height value very close to the predicted by Gzil *et al*. [136]. This paper was the precursor of subsequent work of De Malsche *et al.* where reversed-phase liquid chromatography separations have been performed in the pillar array format, either in non-porous or porous silicon [133,140-142]. These promising results combined with the recent work from Gustafsson *et al.* [69], where underivatized COC was used as the substrate material and the stationary phase for capillary and microchip electrochromatography (CEC), inspired the fabrication of the pillar array column fabricated in COP for pressure-driven reversed phase liquid chromatography separations that is described in this PhD dissertation.

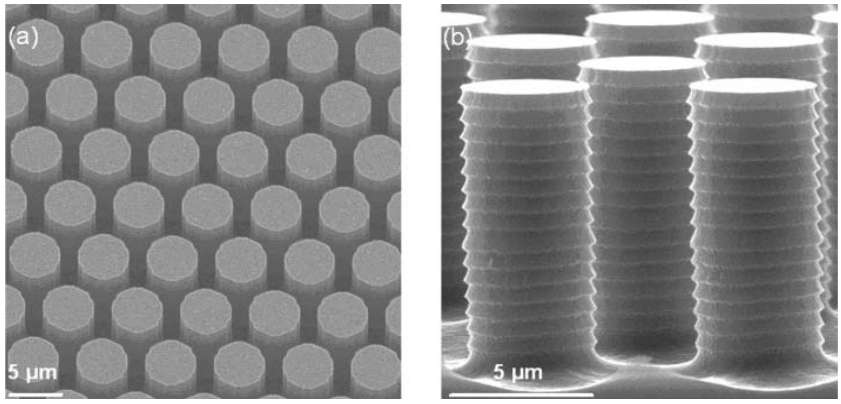

Fig. 12 (a) SEM image of the micromachined pillar array used by De Malsche and co-workers for on-chip reversed-phase LC; (b) SEM image of individual pillars with indentations caused by the Bosch® dry etching process. Images taken from [133].

2.4 References

[1] A. Manz, N. Graber, H.M. Widmer, Sensors and Actuators B: Chemical 1 (1990) 244.

[2] A. Manz, Y. Miyahara, J. Miura, Y. Watanabe, H. Miyagi, K. Sato, Sensors and Actuators B: Chemical 1 (1990) 249.

[3] S.C. Terry, J.H. Jerman, J.B. Angell, IEEE Transactions on Electron Devices 26 (1979) 1880.

[4] M. Elwenspoek, H.V. Jansen, Silicon Micromachining, Cambridge University Press, Cambridge, 1998.
[5] M.J. Madou, Fundamentals of microfabrication: the science of miniaturization, CRC Press, Boca Raton, 2002.
[6] J.P. Kutter, Y. Fintschenko, Separation Methods In Microanalytical Systems, CRC Press, Boca Raton, 2006.
[7] H. Becker, C. Gärtner, Analytical and Bioanalytical Chemistry 390 (2008) 89.
[8] C.-W. Tsao, D. DeVoe, Microfluidics and Nanofluidics 6 (2009) 1.
[9] K.Y. Lee, N. LaBianca, S.A. Rishton, S. Zolgharnain, J.D. Gelorme, J. Shaw, T.H.P. Chang, Journal of Vacuum Science and Technology B: Microelectronics and Nanometer Structures 13 (1995) 3012.
[10] H. Lorenz, M. Despont, N. Fahrni, N. LaBianca, P. Renaud, P. Vettiger, Journal of Micromechanics and Microengineering 7 (1997) 121.
[11] S. Metz, R. Holzer, P. Renaud, Lab on a Chip 1 (2001) 29.
[12] H. Becker, L.E. Locascio, Talanta 56 (2002) 267.
[13] P. Nunes, P. Ohlsson, O. Ordeig, J. Kutter, Microfluidics and Nanofluidics.
[14] D.C. Duffy, J.C. McDonald, O.J.A. Schueller, G.M. Whitesides, Analytical Chemistry 70 (1998) 4974.
[15] H. Becker, C. Gärtner, Electrophoresis 21 (2000) 12.
[16] M. Heckele, W.K. Schomburg, Journal of Micromechanics and Microengineering 14 (2004) R1.
[17] R.M. McCormick, R.J. Nelson, M.G. Alonso-Amigo, D.J. Benvegnu, H.H. Hooper, Analytical Chemistry 69 (1997) 2626.
[18] J. Giboz, T. Copponnex, P. Mélé, Journal of Micromechanics and Microengineering 17 (2007).
[19] B.D. Gates, Q. Xu, M. Stewart, D. Ryan, C.G. Willson, G.M. Whitesides, Chemical Reviews 105 (2005) 1171.
[20] S.K. Sia, G.M. Whitesides, Electrophoresis 24 (2003) 3563.
[21] G.M. Whitesides, E. Ostuni, S. Takayama, X. Jiang, D.E. Ingber, Annual Review of Biomedical Engineering 3 (2001) 335.
[22] M. Madou, J. Zoval, G. Jia, H. Kido, J. Kim, N. Kim, Annual Review of Biomedical Engineering 8 (2006) 601.
[23] S. Giselbrecht, T. Gietzelt, E. Gottwald, C. Trautmann, R. Truckenmüller, K.F. Weibezahn, A. Welle, Biomedical Microdevices 8 (2006) 191.
[24] E. Gottwald, S. Giselbrecht, C. Augspurger, B. Lahni, N. Dambrowsky, R. Truckenmüller, V. Piotter, T. Gietzelt, O. Wendt, W. Pfleging, A. Welle, A. Rolletschek, A.M. Wobus, K.F. Weibezahn, Lab on a Chip 7 (2007) 777.
[25] S.Y. Chou, P.R. Krauss, P.J. Renstrom, Science 272 (1996) 85.
[26] L. Martynova, L.E. Locascio, M. Gaitan, G.W. Kramer, R.G. Christensen, W.A. MacCrehan, Analytical Chemistry 69 (1997) 4783.
[27] M. Heckele, W. Bacher, K.D. Müller, Microsystem Technologies 4 (1998) 122.

[28] R.W. Jaszewski, H. Schift, J. Gobrecht, P. Smith, Microelectronic Engineering 41-42 (1998) 575.
[29] L.J. Guo, Advanced Materials 19 (2007) 495.
[30] M.B. Esch, S. Kapur, G. Irizarry, V. Genova, Lab on a Chip 3 (2003) 121.
[31] R.W. Jaszewski, H. Schift, B. Schnyder, A. Schneuwly, P. Gröning, Applied Surface Science 143 (1999) 301.
[32] C.A. Mills, E. Martinez, F. Bessueille, G. Villanueva, J. Bausells, J. Samitier, A. Errachid, Microelectronic Engineering 78-79 (2005) 695.
[33] H. Schift, Journal of Vacuum Science & Technology B: Microelectronics and Nanometer Structures 26 (2008) 458.
[34] H.C. Scheer, W. Hafner, A. Fidler, S. Mollenbeck, N. Bogdanski, Journal of Vacuum Science & Technology B: Microelectronics and Nanometer Structures 26 (2008) 2416.
[35] J.S. Rossier, M.A. Roberts, R. Ferrigno, H.H. Girault, Analytical Chemistry 71 (1999) 4294.
[36] M.L. Kovarik, N.J. Torrence, D.M. Spence, R.S. Martin, Analyst 129 (2004) 400.
[37] Y.N. Yang, C. Li, J. Kameoka, K.H. Lee, H.G. Craighead, Lab on a Chip 5 (2005) 869.
[38] Y. Kong, H.W. Chen, Y.R. Wang, S.A. Soper, Electrophoresis 27 (2006) 2940.
[39] M. Castano-Alvarez, M.T. Fernandez-Abedul, A. Costa-Garcia, Journal of Chromatography A 1109 (2006) 291.
[40] J. Wang, B. Tian, E. Sahlin, Analytical Chemistry 71 (1999) 5436.
[41] C.E. Walker, Z. Xia, Z.S. Foster, B.J. Lutz, Z.H. Fan, Electroanalysis 20 (2008) 663.
[42] J.G. Andrew, R.S. Martin, M.L. Susan, Electrophoresis 22 (2001) 242.
[43] N. Takano, L.M. Doeswijk, M.A.F. Van Den Boogaart, J. Auerswald, H.F. Knapp, O. Dubochet, T. Hessler, J. Brugger, Journal of Micromechanics and Microengineering 16 (2006) 1606.
[44] B. Graß, A. Neyer, M. Jöhnck, D. Siepe, F. Eisenbeiß, G. Weber, R. Hergenröder, Sensors and Actuators B: Chemical 72 (2001) 249.
[45] X.J. Huang, A.M. O'Mahony, R.G. Compton, Small 5 (2009) 776.
[46] S. Metz, R. Holzer, P. Renaud, Lab on a Chip 1 (2001) 29.
[47] T. Nielsen, D. Nilsson, F. Bundgaard, P. Shi, P. Szabo, O. Geschke, A. Kristensen, Journal of Vacuum Science and Technology B: Microelectronics and Nanometer Structures 22 (2004) 1770.
[48] O. Rötting, W. Röpke, H. Becker, C. Gärtner, Microsystem Technologies 8 (2002) 32.
[49] A.V. Pocius, Adhesion and Adhesives Technology: An Introduction, Hanser/Gardner Publications, 2002.

[50] J. Han, S.H. Lee, A. Puntambekar, S. Murugesan, J.W. Choi, G. Beaucage, C.H. Ahn, in Proc. 7th Int. Conf. Micro Total Analysis Systems (uTAS), 2003, p. 1113.
[51] F. Dang, S. Shinohara, O. Tabata, Y. Yamaoka, M. Kurokawa, Y. Shinohara, M. Ishikawa, Y. Baba, Lab on a Chip 5 (2005) 472.
[52] W.W.Y. Chow, K.F. Lei, G. Shi, W.J. Li, Q. Huang, Smart Materials and Structures 15 (2006).
[53] F.C. Huang, Y.F. Chen, G.B. Lee, Electrophoresis 28 (2007) 1130.
[54] M.A. Roberts, J.S. Rossier, P. Bercier, H. Girault, Analytical Chemistry 69 (1997) 2035.
[55] H. Makamba, J.H. Kim, K. Lim, N. Park, J.H. Hahn, Electrophoresis 24 (2003) 3607.
[56] K. Haubert, T. Drier, D. Beebe, Lab on a Chip 6 (2006) 1548.
[57] C.H. Ahn, J.W. Choi, G. Beaucage, J.H. Nevin, J.B. Lee, A. Puntambekar, J.Y. Lee, Proceedings of the IEEE 92 (2004) 154.
[58] A. Bhattacharyya, C.M. Klapperich, Analytical Chemistry 78 (2006) 788.
[59] R.T. Kelly, A.T. Woolley, Analytical Chemistry 75 (2003) 1941.
[60] A. Bhattacharyya, C.M. Klapperich, Lab on a Chip 7 (2007) 876.
[61] C.W. Tsao, L. Hromada, J. Liu, P. Kumar, D.L. DeVoe, Lab on a Chip 7 (2007) 499.
[62] H. Klank, J.P. Kutter, O. Geschke, Lab on a Chip 2 (2002) 242.
[63] Y.C. Hsu, T.Y. Chen, Biomedical Microdevices 9 (2007) 513.
[64] L. Brown, T. Koerner, J.H. Horton, R.D. Oleschuk, Lab on a Chip 6 (2006) 66.
[65] R. Truckenmüller, Y. Cheng, R. Ahrens, H. Bahrs, G. Fischer, J. Lehmann, Microsystem Technologies 12 (2006) 1027.
[66] J. Kim, X. Xu, Journal of Laser Applications 15 (2003) 255.
[67] D. Olivero, Z.H. Fan, Lab on a Chip (2008).
[68] T.B. Stachowiak, T. Rohr, E.F. Hilder, D.S. Peterson, M. Yi, F. Svec, J.M.J. Fréchet, Electrophoresis 24 (2003) 3689.
[69] O. Gustafsson, K.B. Mogensen, J.P. Kutter, Electrophoresis 29 (2008) 3145.
[70] K.W. Ro, J. Liu, D.R. Knapp, Journal of Chromatography A 1111 (2006) 40.
[71] D.A. Mair, M. Rolandi, M. Snauko, R. Noroski, F. Svec, J.M.J. Fréchet, Analytical Chemistry 79 (2007) 5097.
[72] J. Liu, C.-F. Chen, C.-W. Tsao, C.-C. Chang, C.-C. Chu, D.L. DeVoe, Analytical Chemistry 81 (2009) 2545.
[73] L. Ettre, K. Sakodynskii, Chromatographia 35 (1993) 223.
[74] A.J.P. Martin, R.L.M. Synge, Biochemical Journal 35 (1941) 1358.
[75] R. Consden, A.H. Gordon, A.J.P. Martin, Biochemical Journal 38 (1944) 224.
[76] A.T. James, A.J.P. Martin, Biochemical Journal 50 (1952) 679.
[77] A. Braithwaite, F.J. Smith, Chromatographic Methods, Blackie Academic & Professional, London, 1996.
[78] C.F. Poole, The Essence of Chromatography, Elsevier, Amsterdam, 2003.

[79] C.W. Gehrke, R.L. Wixom, E. Bayer, R.L.W. C.W. Gehrke, E. Bayer, in Journal of Chromatography Library, Elsevier, 2001, p. 237.
[80] C.G. Horvath, B.A. Preiss, S.R. Lipsky, Analytical Chemistry 39 (1967) 1422.
[81] W.D. Conway, R.J. Petroski, Modern Countercurrent Chromatography, ACS, Washington, D.C., 1995.
[82] U.D. Neue, HPLC Columns: Theory, Technology, and Practice, Wiley-VCH, New York, 1997.
[83] M.S. Tswett, Berichte der Deutschen Gesellschaft 24 (1906) 384.
[84] J.J. Van Deemter, F.J. Zuiderweg, A. Klinkenberg, Chemical Engineering Science 5 (1956) 271.
[85] J.C. Giddings, Dynamics of Chromatography, Part I, Principles and Theory, Marcel Dekker, New York, 1965.
[86] J.H. Knox, J.F. Parcher, Analytical Chemistry 41 (1969) 1599.
[87] Y. Kazakevich, R. LoBrutto, HPLC for pharmaceutical scientists John Wiley & Sons, Inc., Hoboken, 2007.
[88] L.R. Snyder, J.J. Kirkland, J.W. Dolan, Introduction to Modern Liquid Chromatography (Third Edition) John Wiley & Sons, Inc., Hoboken, 2010.
[89] F. Svec, J.M.J. Fréchet, Analytical Chemistry 64 (1992) 820.
[90] S. Hjertén, J.L. Liao, R. Zhang, Journal of Chromatography A 473 (1989) 273.
[91] S. Hjertén, Y.M. Li, J.L. Liao, J. Mohammad, K. Nakazato, G. Pettersson, Nature 356 (1992) 810.
[92] N. Tanaka, H. Nagayama, H. Kobayashi, T. Ikegami, K. Hosoya, N. Ishizuka, H. Minakuchi, K. Nakanishi, K. Cabrera, D. Lubda, HRC Journal of High Resolution Chromatography 23 (2000) 111.
[93] C.S. Effenhauser, Topics in Current Chemistry 194 (1998) 51.
[94] F.E. Regnier, B. He, S. Lin, J. Busse, Trends in Biotechnology 17 (1999) 101.
[95] A. De Mello, Lab on a Chip 2 (2002).
[96] R.M. Tiggelaar, F. Benito-López, D.C. Hermes, H. Rathgen, R.J.M. Egberink, F.G. Mugele, D.N. Reinhoudt, A. van den Berg, W. Verboom, H.J.G.E. Gardeniers, Chemical Engineering Journal 131 (2007) 163.
[97] S.C. Jacobson, R. Hergenröder, L.B. Koutny, J. Michael Ramsey, Analytical Chemistry 66 (1994) 1114.
[98] N.A. Lacher, K.E. Garrison, R.S. Martin, S.M. Lunte, Electrophoresis 22 (2001) 2526.
[99] V. Dolník, S. Liu, S. Jovanovich, Electrophoresis 21 (2000) 41.
[100] O. Hofmann, D. Che, K.A. Cruickshank, U.R. Muller, Analytical Chemistry 71 (1998) 678.
[101] W. Tan, Z.H. Fan, C.X. Qiu, A.J. Ricco, I. Gibbons, Electrophoresis 23 (2002) 3638.
[102] J.P. Kutter, S.C. Jacobson, J.M. Ramsey, Analytical Chemistry 69 (1997) 5165.
[103] C.T. Culbertson, S.C. Jacobson, J.M. Ramsey, Analytical Chemistry 72 (2000) 5814.

[104] D.J. Throckmorton, T.J. Shepodd, A.K. Singh, Analytical Chemistry 74 (2002) 784.
[105] J.P. Kutter, S.C. Jacobson, N. Matsubara, J.M. Ramsey, Analytical Chemistry 70 (1998) 3291.
[106] J. Eijkel, Lab on a Chip 7 (2007) 815.
[107] G. Jilge, K.K. Unger, U. Esser, H.J. Schafer, G. Rathgeber, W. Muller, Journal of Chromatography 476 (1989) 37.
[108] J.J. Kirkland, F.A. Truszkowski, C.H. Dilks, G.S. Engel, Journal of Chromatography A 890 (2000) 3.
[109] G. Ocvirk, E. Verpoorte, A. Manz, M. Grasserbauer, H.M. Widmer, Analytical Methods and Instrumentation 2 (1995) 74.
[110] A. Ishida, T. Yoshikawa, M. Natsume, T. Kamidate, Journal of Chromatography A 1132 (2006) 90.
[111] I.M. Lazar, P. Trisiripisal, H.A. Sarvaiya, Analytical Chemistry 78 (2006) 5513.
[112] A. Ishida, M. Natsume, T. Kamidate, Journal of Chromatography A 1213 (2008) 209.
[113] A. Gaspar, M.E. Piyasena, F.A. Gomez, Analytical Chemistry 79 (2007) 7906.
[114] A. Penrose, P. Myers, K. Bartle, S. McCrossen, Analyst 129 (2004) 704.
[115] M.T. Koesdjojo, C.R. Koch, V.T. Remcho, Analytical Chemistry 81 (2009) 1652.
[116] M. De Pra, W.T. Kok, P.J. Schoenmakers, Journal of Chromatography A 1184 (2008) 560.
[117] H. Yin, K. Killeen, R. Brennen, D. Sobek, M. Werlich, T. van de Goor, Analytical Chemistry 77 (2005) 527.
[118] H. Yin, K. Killeen, Journal of Separation Science 30 (2007) 1427.
[119] S. Ehlert, K. Kraiczek, J.A. Mora, M. Dittmann, G.P. Rozing, U. Tallarek, Analytical Chemistry 80 (2008) 5945.
[120] J.H. Knox, Journal of Chromatographic Science 18 (1980) 453.
[121] M.M. McEnery, J.D. Glennon, J. Alderman, S.C. O'Mathuna, Biomedical Chromatography 14 (2000) 44.
[122] M. McEnery, A. Tan, J. Alderman, J. Patterson, S.C. O'Mathuna, J.D. Glennon, Analyst 125 (2000) 25.
[123] P.G. Vahey, S.H. Park, B.J. Marquardt, Y. Xia, L.W. Burgess, R.E. Synovec, Talanta 51 (2000) 1205.
[124] A. Benvenuto, V. Guarnieri, L. Lorenzelli, C. Collini, M. Decarli, A. Adami, C. Potrich, L. Lunelli, R. Canteri, C. Pederzolli, Sensors and Actuators, B: Chemical 130 (2008) 181.
[125] H.V. Fuentes, A.T. Woolley, Lab on a Chip 7 (2007) 1524.
[126] C. Ericson, J. Holm, T. Ericson, S. Hjerten, Analytical Chemistry 72 (2000) 81.
[127] S.M. Ngola, Y. Fintschenko, W.Y. Choi, T.J. Shepodd, Analytical Chemistry 73 (2001) 849.

[128] D.S. Reichmuth, T.J. Shepodd, B.J. Kirby, Analytical Chemistry 77 (2005) 2997.
[129] B. He, N. Tait, F. Regnier, Analytical Chemistry 70 (1998) 3790.
[130] B. He, J. Ji, F.E. Regnier, Journal of Chromatography A 853 (1999) 257.
[131] F.E. Regnier, HRC Journal of High Resolution Chromatography 23 (2000) 19.
[132] B.E. Slentz, N.A. Penner, E. Lugowska, F. Regnier, Electrophoresis 22 (2001) 3736.
[133] H. Eghbali, W. De Malsche, D. Clicq, H. Gardeniers, G. Desmet, LC-GC Europe 20 (2007) 208.
[134] N. Kaji, Y. Tezuka, Y. Takamura, M. Ueda, T. Nishimoto, H. Nakanishi, Y. Horiike, Y. Baba, Analytical Chemistry 76 (2004) 15.
[135] K.B. Mogensen, F. Eriksson, O. Gustafsson, R.P.H. Nikolajsen, J.P. Kutter, Electrophoresis 25 (2004) 3788.
[136] P. Gzil, N. Vervoort, G.V. Baron, G. Desmet, Analytical Chemistry 75 (2003) 6244.
[137] J. De Smet, P. Gzil, M. Vervoort, H. Verelst, G.V. Baron, G. Desmet, Analytical Chemistry 76 (2004) 3716.
[138] N. Vervoort, J. Billen, P. Gzil, G.V. Baron, G. Desmet, Analytical Chemistry 76 (2004) 4501.
[139] M. De Pra, W.T. Kok, J.G.E. Gardeniers, G. Desmet, S. Eeltink, J.W. Van Nieuwkasteele, P.J. Schoenmakers, Analytical Chemistry 78 (2006) 6519.
[140] W. De Malsche, D. Clicq, V. Verdoold, P. Gzil, G. Desmet, H. Gardeniers, Lab on a Chip 7 (2007) 1705.
[141] W. De Malsche, H. Eghbali, D. Clicq, J. Vangelooven, H. Gardeniers, G. Desmet, Analytical Chemistry 79 (2007) 5915.
[142] W. De Malsche, H. Gardeniers, G. Desmet, Analytical Chemistry 80 (2008) 5391.

CHAPTER 3

An array of ordered pillars for pressure-driven liquid chromatography fabricated directly in cyclo olefin polymer

3.1 Abstract

The current chapter describes the development and characterization of a pillar array chip that is constructed out of a sandwich of cyclo olefin polymer (COP) sheets. The silicon master of a 5 cm long pillar array was embossed into the COP, yielding 4.3 μm deep pillars of 15.3 μm diameter with an external porosity of 43 % and a well designed sidewall region to avoid side wall induced band broadening. A closed channel configuration was obtained by pressure assisted thermal bonding to a non-processed COP lid. Injection of coumarin dye plugs and detection with a fluorescence microscope showed very close agreement of this channel configuration to theoretical expectations in terms of band broadening. This agreement is due to the low taper, the optimized sidewall region and the excellent bonding quality between the two polymer sheets, even at the pillar area. Under non-retained conditions (pure methanol as mobile phase), plate heights as low as 4 μm were obtained. Under retained conditions, using the native hydrophobic properties of the COP channel (in 70/30 v/v water/methanol mixture as mobile phase), a minimum plate height of 6 μm was obtained. A 4 component separation was successfully achieved, demonstrating that COP is a cheap and efficient alternative for silicon and silica based liquid chromatography formats.

3.2 Introduction

Pressure-driven liquid chromatography is, by far, the most prevalent separation technique. Until recent years, it has not been used in micro total analysis systems (μTAS) as the necessary micromachining technology was still not developed. The group of Fred Regnier [1] was the first to use microlithographic techniques in 1998 to produce chromatographic columns with a perfectly ordered array of micro-pillars. These columns where etched in quartz in order to avoid a short circuit through the support material when applying a potential to generate an electro-osmotic flow. Plate heights as low as 1.2 μm were obtained in these channels in CEC mode [2].

Few years later, pressure-driven experiments using pillar arrays were also conducted by other groups [3]. These authors used silicon as a support material because of the availability of the Bosch® process that allows the definition of nearly vertical pillars. This yielded reduced plate heights as low as 1 μm under retained conditions [4]. Another asset of the silicon material appeared to be the ability to increase the interaction surface by anodization of the silicon, resulting in the formation of porous silicon [5].

In parallel to this work, different techniques for polymer micromaching such as injection moulding [6], hot embossing [7] or nanoimprint lithography [8] have been developed. Interest for these materials has been increasing due to their wide variety of properties and functionalities. Nowadays, for nearly any application a polymer can be tailored.

Cyclo olefin polymer (COP) is a relatively new thermoplastic polymer. We have used it in this work because of its high organic solvent resistance (which is particularly useful when working with solvents used as mobile phase in liquid chromatography), low water adsorption, glass-like optical clarity and low background fluorescence [9]. Different types of cyclo olefin polymers are being commercialized nowadays, under varying commercial names, namely Zeonor,

Zeonex, Topas, Apel and Arton. Here, ZeonorFilm® prepared in DINA4 sheets has been used. Since COP was developed, it has been used to fabricate different μTAS such as microfluidic channels for capillary electrophoresis [10] and liquid chromatography using monolithic columns [11,12]. More recently, arrays of ordered pillars have been fabricated in cyclo olefin polymers to perform capillary and microchip electrochromatography [13] and to distribute the sample solution in an immunoassay chip [14].

In this work, we report the first unmodified COP chip used to perform a separation via pressure-driven reversed phase liquid chromatography, taking advantage of the hydrophobic properties of this polymer surface. The design of the chip, the fabrication of the master to mould the chip, the chip fabrication itself, the analysis of the column performance and finally, the separation of a mixture of four coumarins, is demonstrated.

3.3 Experimental

3.3.1 Chip design

A layout of the microchip is shown in Fig. 1a. It has been designed in a cross-like shape with a 5 cm long and 318 μm wide central channel which functions as the separation column and where the array of ordered pillars is positioned, and a 88 μm wide injection channel crossing it. The inlet and outlet channels cross the separation column in order to obtain a standard cross injection configuration [15,16].

The column consists of an array of cylindrical pillars designed to get an external porosity of $\varepsilon = 0.4$, with a diameter of 16 μm and an interpillar distance of 3.6 μm. In order to reduce the sidewall-induced band-broadening effect in the chip, a distance of 2.4 μm between the pillars and the column wall has been

designed, following the guidelines of computational simulation dynamics studies described in the literature [17].

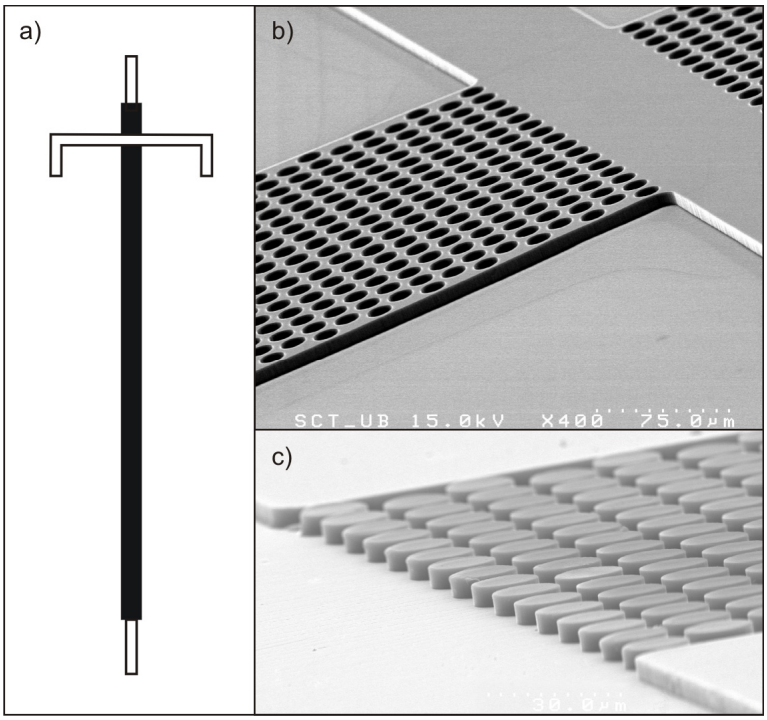

Fig. 1 (a) Layout of the chip with integrated separation column. (b) Scanning electron microscope (SEM) pictures of the injection zone of the etched silicon master and (c) the embossed COP sheet.

3.3.2 Microfabrication procedure

A silicon master for embossing the polymer film was fabricated via standard UV-photolitography and Bosch®-type deep reactive ion-etching [4] in a 4 inch silicon wafer. After the etching step, the resist was stripped leaving 4.3 µm deep holes in the master which defined the pillars after embossing the polymer. Before dicing the wafer, the fluorocarbons remaining from the Bosch process were removed in an ashing step at 800 °C. Then, the wafer was cleaned in nitric acid and finally dipped in hydrofluoric acid. The master obtained was a piece of silicon of 1.5 x 7 cm^2. A SEM picture of the fabricated master is shown in Fig. 1b. Before embossing, in order to avoid sticking and to ensure complete detachment

of the polymer sheet after embossing, the master surface was coated with a layer of 1H,1H,2H,2H-Perfluorooctyl-trichlorosilane (Fluka, Spain), in an evaporation method, as described by Mills *et al.* [18].

COP sheets (ZeonorFilm®, ZF 14-188, kindly provided by Zeon Corporation, Japan), 188 μm thick and with a glass transition temperature of T_g = 138 °C, were embossed using a HEX01 embossing system (Jenoptik AG, Germany), sandwiching the master and the polymer film between a pair of teflon sheets to avoid adhesion to the machine plates. Conditions used were 2000 N and 170 °C for 300 s. Demoulding temperature was set at 120 °C. After stripping the replicated polymer from the master with extreme care to avoid any damage to the pillars, the chip was cut and holes were drilled in it to get the inlet/outlet connections. Finally, to remove any remaining particles, the sample was cleaned with isopropanol (Fluka, Spain) in an ultrasound bath for 10 min. In Fig. 1c, a SEM picture of the injection part of the embossed channel is shown.

Pressure-assisted thermal bonding was applied for the adhesion of the embossed polymer to a non-processed COP lid. This process was done in a NIL apparatus (Obducat, Sweden) to allow for a perfect pressure uniformity along the column. Conditions found for satisfactory bonding are 40 bar and 123 °C during 600 s. In addition, to increase the strength of the bonding without applying more pressure to the chip that could deform the channel, the bonded chip was annealed for 10 min without applying any force on it at 145 °C, slightly above its polymer glass transition temperature.

3.3.3 Injection and separation procedure

To inject the sample on the separation column, the chip was placed in a home made holder consisting of an aluminum bottom-plate with a window to observe the microchannel, and a Delrin® top-plate with drilled through-holes compatible with commercially available Upchurch® nanoport connectors (Achrom, Belgium). Fused silica capillaries with an ID of 150 μm (Achrom, Belgium) were used to

connect the chip to valves used to switch between injection and flow propagation (see below).

Fig. 2 shows the two-step injection mechanism. First, the sample is forced to flow through the injection channel crossing the separation column (Fig. 2a). In the second step (Fig. 2b), the plug is defined by injecting the mobile phase on the separation column, transporting the sample plug along the column (Fig. 2c and 2d). Outlets of the separation column and the injection channel are kept open during the whole process in order to reduce the resistance of the channels, allowing that part of the injected sample flows into the separation column during the first step. Both steps were controlled by two external six-port valves (Rheodyne MX, Germany), closing the mobile phase inlet during the first step and closing the sample inlet during the second step.

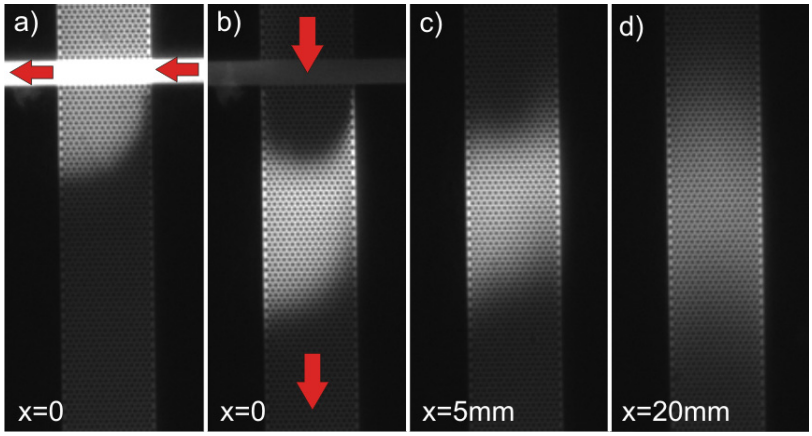

Fig. 2 Optical images from a frame sequence of an injected plug in the separation column. (a) The sample is first injected across the separation column, (b) the mobile phase is injected defining a plug that flows along the separation column. Images of the plug are taken at (c) 5 mm and (d) 20 mm from the injection point.

The home-made system used to pressurize the sample and the mobile phase is the same as the one explained in De Malsche *et al.* [4]. It consists of two pressurized stainless-steel vessels where pressure to the sample and the mobile phase is controlled by two independent pressure controllers (Bronkhorst, The Netherlands), fed by a nitrogen gas bottle. The maximum applied pressure at which no detachment of the Zeonor bond was observed was always above 15 bar.

In the experiments carried out to characterize the separation column, the employed mobile phase was a water/methanol mixture (70/30 (v/v) or 50/50 (v/v)), depending on the experiment), where the water phase was additionally buffered at pH=7 using a phosphate buffer. The used samples were different mixtures of 4 coumarin dyes [19,20]: C440, C450, C460 and C480 (Fluka, Belgium), prepared from individual stock solutions of 1 mM in methanol. Solutions of two coumarins (C440 and C480) were prepared to study the performance of the column, and a mixture of the four different coumarins was prepared to study a complete four component separation. In all the experiments, the solutions containing the coumarins had the same methanol/water ratio as the mobile phase used for that experiment to avoid viscous fingering [21].

The detection set-up consisted of a Hg-vapor lamp (U-LH100HGAPO, Olympus, Belgium) to excite the fluorescent coumarin dyes in the UV region and an inverted microscope (IX71, Olympus, Belgium) equipped with an UV-1 filter cube set (UV-2A DM400 Nikon, Cetec N.V., Belgium) to collect the emitted light. The microscope was mounted on a breadboard (M-IG 23-2, Newport, The Netherlands), together with a linear displacement stage (M-TS100DC) and a speed controller (MM, 4006 Newport). Visualization of the separations was performed using a CCD fluorescent camera (ORCA-ER4742, Hamamatsu Photonics, Belgium) mounted on the video adapter of the microscope and analyzed with the accompanying SimplePCI® 6 software.

3.4 Results and discussion

3.4.1 Microfabrication

Fig. 3a shows a top-view of the embossed channel in a region adjacent to the channel wall prior to the bonding process. The pillar diameter is 15.3 μm, the inter-pillar distance is 4.1 μm and the pillar-to-wall distance is 3.1 μm. This results in an external porosity of ε = 0.43, a value slightly above the 40 % porosity

designed on the photolithographic mask. These small differences between the designed and the experimental values are mainly because of the inaccuracy of the silicon master fabrication process, where the precision depends on unavoidable phenomena such as UV-light diffraction in micrometer-sized gaps and the under-etching of the silicon underneath the photoresist [22].

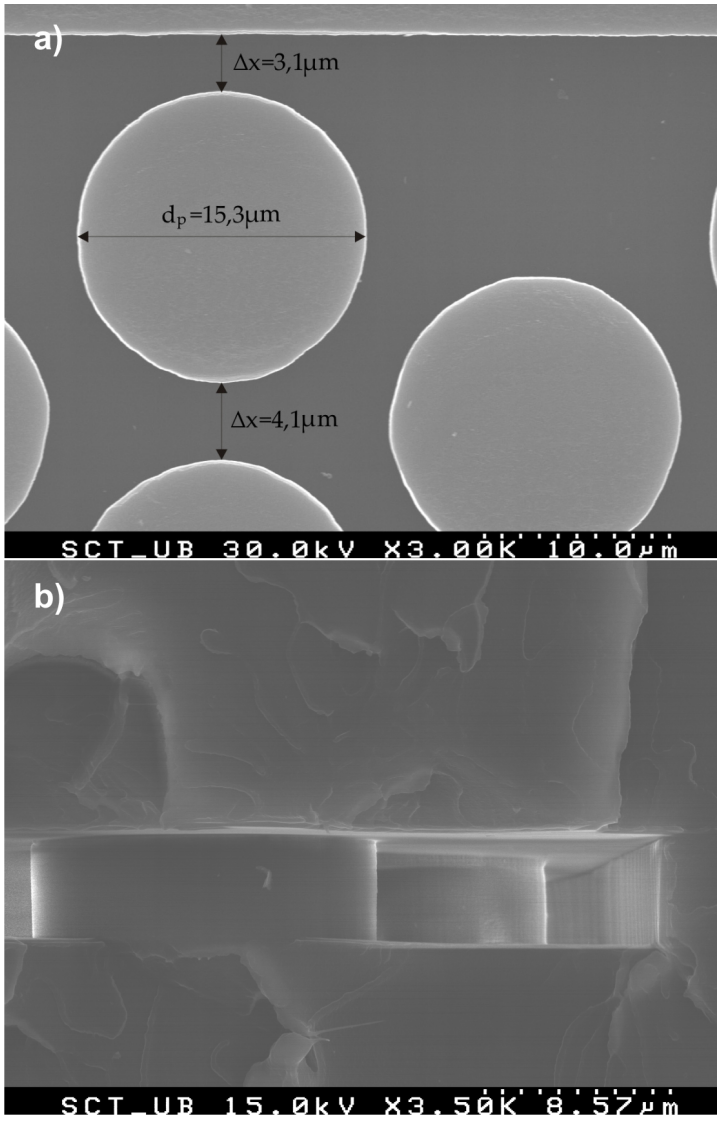

Fig. 3 (a) Bird's eye SEM picture of the pillars in the side-wall region with the calculated distances obtained after embossing the COP. (b) SEM picture of a cross-section of the bonded channel.

Fig. 3b shows the good quality of the thermally assisted bond between the micromachined COP sheet and a blank COP lid after the application of 15 bar on the inlet of the channel. The verticality of the pillars is nicely maintained, which is important for preventing a velocity gradient between the bottom and the top side of the channel (see below). It is also worth noticing that the channel depth in between the pillars is uniform, as often, during RIE etching, zones with different local surface areas can display different etch rates (the so-called RIE lag) [23]. Apparently, the surface in the current design is not large enough and/or the difference in surface area is not pronounced enough to allow for a RIE lag. Fig. 3b also shows that there is no gap between the pillars and the top lid, which is crucial to avoid stagnant zones at the bonding interface, which would be detrimental for the integrity of plugs flowing through the pillar array.

3.4.2 Band broadening

To study the quality and the potential performance of the fabricated column in terms of chromatography, the theoretical plate height values *H* of coumarin C440 were determined in 100 % methanol. This was done by analyzing a peak at two positions in the channel (Fig. 2c and 2d). It should be noticed that the peaks immediately after the injection were slightly asymmetric (see Fig 2b). When the peak had elapsed a sufficient distance, it became symmetrical. Peak shape could possibly be improved by the use of any of the other injection methods that have been described in the literature, all of which are compatible with the here-presented chip design [4,24]. The first position for detection was 5 mm downstream the injection slit and the second, at a distance of 20 mm. The plate height was calculated fitting the peak with a Gaussian function in the space domain. The obtained variances were used to calculate the plate height according to:

$$H = \frac{\sigma_{x,1}^2 - \sigma_{x,0}^2}{\Delta x} \qquad (1)$$

The plate height is strongly dependent on the mobile phase velocity u, as noted in the van Deemter equation [25]:

$$H = A + B/u + Cu \tag{2}$$

which is composed of three terms: the A-term represents the heterogeneity of the system, the B-term is linked to the axial dispersion due to the molecular diffusion and the C-term is related to the mass-transfer resistance between the stationary-phase and the mobile phase. To be able to compare the values of different packing (or differently sized pillars), the dimensional-less reduced plate height h expression introduced by Giddings et al. [26] is required:

$$h = A + B/\nu + C\nu \tag{3}$$

where ν is the reduced velocity, and h and ν are defined as:

$$h = \frac{H}{d_{pil}} \tag{4}$$

$$\nu = \frac{u d_{pil}}{D_m} \tag{5}$$

where d_p is the pillar diameter (set to 16 μm) and D_m the diffusion coefficient, which is 1.2 10^{-9} m^2 s^{-1} for coumarin C440 in a solution of pure methanol [27]. It can be argued that the interpillar distance should be used instead of the pillar diameter to normalize the plate height, but this would favor the pillar array even more [4]. Because of the tradition in the literature to represent reduced plate heights in particle (or pillar) diameter, this method is followed in the present chapter.

The experimental van Deemter curve obtained for coumarin C440 in non-retentive conditions is shown in Fig. 4, where it is compared to the theoretical values extracted from the computational fluid dynamics simulations made by De Smet et al. for a 5 μm deep channel [28]. It is noted that the obtained minimum value for the reduced plate height values is around 0.15 - 0.2, i.e. in close agreement with the simulations.

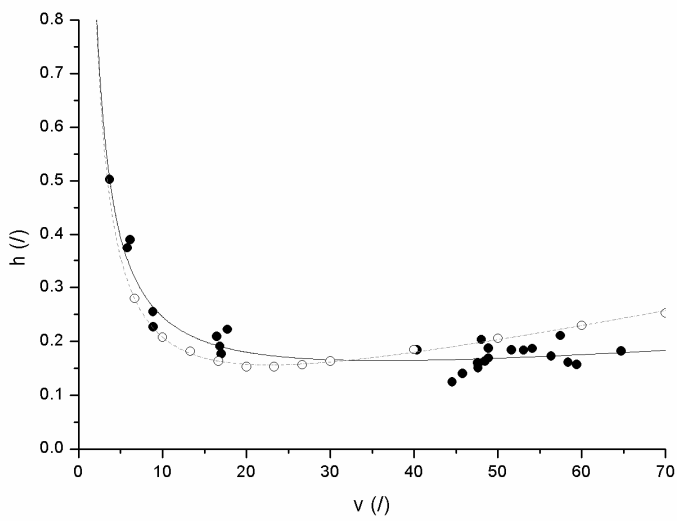

Fig. 4 Dimensionless Van Deemter curve for a solution of C440, using pure methanol as mobile phase (●) compared to the curve calculated by De Smet et al. using computational fluid dynamics simulations for a 5 μm deep channel (○) and the respective fits (◎) and (---).

The similarity between both van Deemter curves becomes also apparent by comparing the values of the constants of the experimental fitted curve (A = 0.075, B = 1.47, C = 0.0011) which are similar to the ones predicted in the simulations (i.e. A = 0.013, B = 1.64, C = 0.0032). It is also noticeable that the optimal velocity values corresponding to the lowest plate height values are shifted compared to the predicted values: the experimental results give an optimal velocity around 30, while the simulations predicted a value around 20.

In the same way, the retention properties of the column with different coumarin compounds (C440 and C480) have been studied using two different mobile-phase mixtures of water and methanol (70/30 (v/v) and 50/50 (v/v)). Fig. 5 shows two chromatograms of a separation of a mixture of 2 coumarins using a 70/30 (v/v) water/methanol mobile phase (water buffered with pH = 7) at different times after the injection. From these time-response intensity plots, a mobile phase velocity of u = 0.6 mm/s has been obtained using the C440 peak as a marker, as it is known that this coumarin is not retained [29]. Fig. 5b shows that even a small peak (appearing at 27 s), known to be an unidentified impurity of one of the coumarins, as also observed by Moore et al. [29], could be separated and detected.

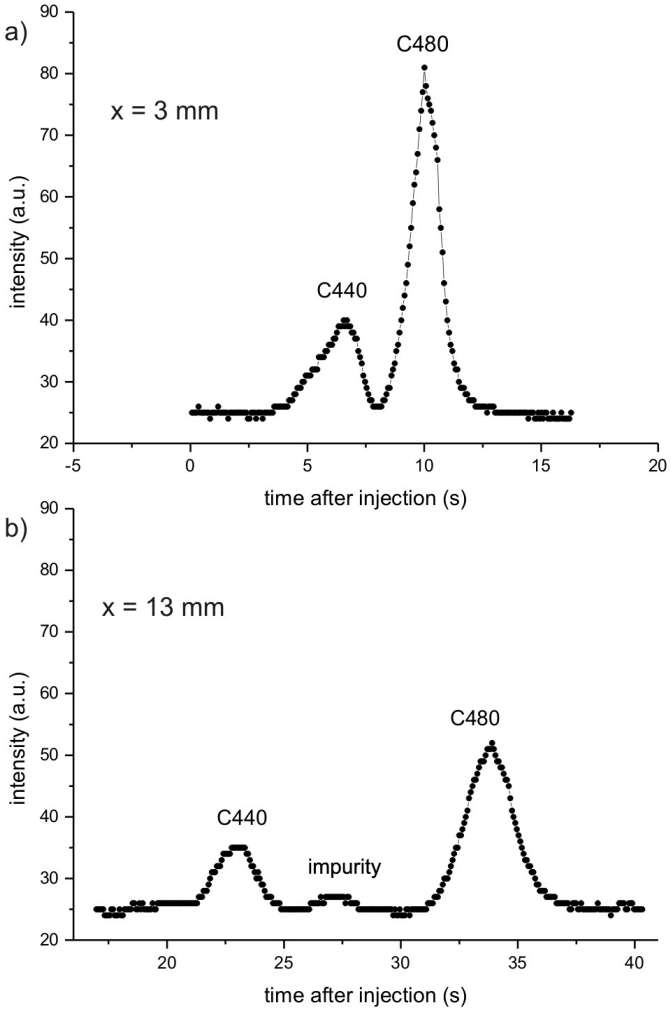

Fig. 5 Chromatograms of a C440 (1mM in methanol) and C480 (1mM in methanol) separation at 3 mm and 13 mm downstream the injection part. Mobile phase used is a 70/30 (v/v) mixture of water/methanol.

From Fig. 5, the retention factor of coumarin C480 has been calculated to be $k = 0.48$. This value is low, but enough to achieve an efficient separation in less than 15 s and 5 mm. At this point, one should remember that no modification has been done in the surface of the ZeonorFilm®, so separation is only due the high hydrophobicity of this polymer. Moreover, separations of the same two coumarin mixture using a 50/50 (v/v) water/methanol mobile phase at pH = 7 were performed, finding a similar behaviour

but with a retention factor of k = 0.09, lower than the first case and in agreement with expectations.

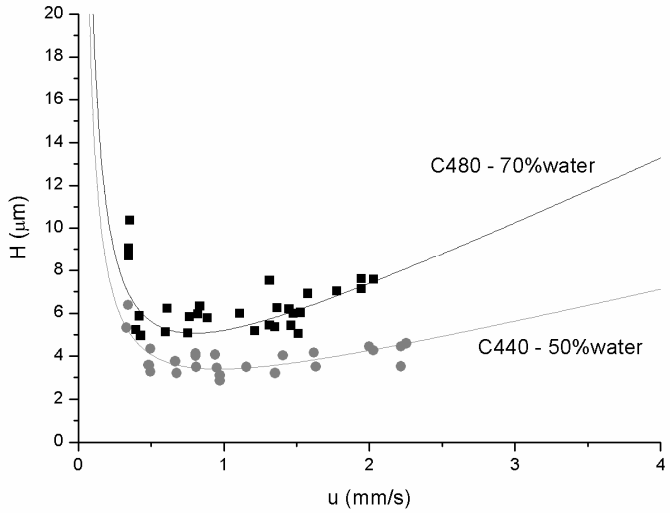

Fig. 6 Van Deemter curves of C440 (●) and C480 (■) in mobile phase compositions of 50/50 and 30/70 (v/v) methanol/water, respectively.

To complete the study concerning the chromatographic possibilities of the present COP chips, spatial intensity plots of the coumarin plugs, measured in a given video frame, were used to calculate the absolute plate height of both coumarins. Fig. 6 shows the absolute plate heights as a function of the measured velocity for the two coumarins in the two different mobile phase conditions where Van Deemter curves have been fitted. For C440, plate heights down to 3 μm were measured, and for C480, a plate height of 5 μm was achieved. Both values are surprisingly low, even though the pillars are as large as 15.3 μm in diameter, confirming the good result of the fabrication column and the high possibilities that COP has for liquid chromatography separations.

3.4.3 Four component separation

Finally, a separation of a mixture of 4 coumarins was achieved (C440, C450, C460 and C480), using a 70/30 (v/v) water/methanol mobile phase at pH=7. As can be seen

in Fig. 7, all bands are clearly separated at 25 mm downstream the injection slit. Also good symmetry can be observed, reflecting the absence of any side wall effects.

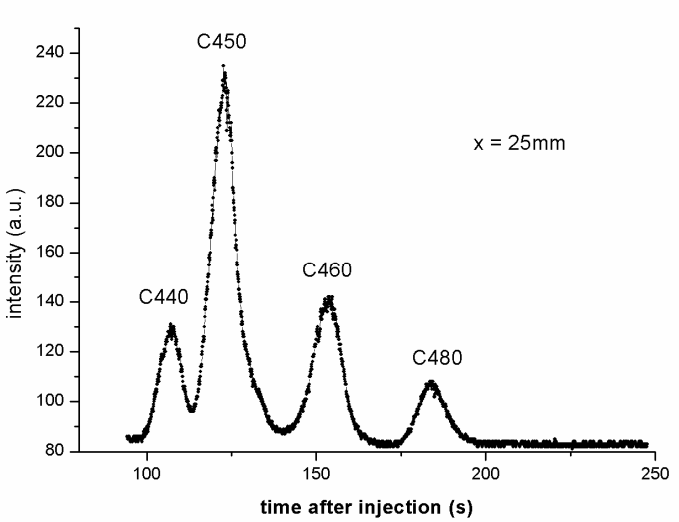

Fig. 7 Chromatogram of a separation of a four coumarin mixture, C440, C450, C460 and C480 (150/150/500/500 (v/v/v/v)) in a 70/30 (v/v) water/methanol (pH=7) mobile phase, monitored at 25 mm downstream the injection slit.

3.5 Conclusions

In this chapter, separation in a ZeonorFilm® column with an array of perfectly ordered pillars for pressure-driven reversed phase liquid chromatography is presented. This material displays good optical properties and is chemically compatible with the reagents used in the separation experiments, making it eminently suitable for this application. In addition, its hydrophobic surface, which interacts with the injected sample, allows to conduct reversed phase separations in an unmodified column. Mixtures of different coumarins were used to study the performance of the chip, but also to analyze the separations in different water/methanol (v/v) mobile phase mixtures. The analysis of the plate height obtained in non-retained conditions is in agreement with the results of previously published simulations, confirming the good quality of the fabricated column, and under retentive conditions, absolute plate heights of the order of 5 μm have been measured, which is surprisingly low, especially when considering

the large pillar size (15.3 μm). Finally, a mixture of four different coumarins was successfully separated, confirming the potential of cyclo olefin polymer for its use in pressure-driven reversed phase liquid chromatography.

These promising results open the door for future investigations using COP to build a LC platform. Since lithographic techniques are continuously improving, smaller pillar sizes and better injection systems may be achieved in the future to get a simple, fast fabricated and cheap separation tool.

3.6 References

[1] B. He, N. Tait, F. Regnier, Analytical Chemistry 70 (1998) 3790.

[2] F.E. Regnier, Journal of Separation Science 23 (2000) 19.

[3] M. De Pra, W.T. Kok, J.G.E. Gardeniers, G. Desmet, S. Eeltink, J.W. Van Nieuwkasteele, P.J. Schoenmakers, Analytical Chemistry 78 (2006) 6519.

[4] W. De Malsche, H. Eghbali, D. Clicq, J. Vangelooven, H. Gardeniers, G. Desmet, Analytical Chemistry 79 (2007) 5915.

[5] W. De Malsche, H. Gardeniers, G. Desmet, Analytical Chemistry 80 (2008) 5391.

[6] R.M. McCormick, R.J. Nelson, M.G. Alonso-Amigo, D.J. Benvegnu, H.H. Hooper, Analytical Chemistry 69 (1997) 2626.

[7] M. Heckele, W. Bacher, K.D. Müller, Microsystem Technologies 4 (1998) 122.

[8] L.J. Guo, Journal of Physics D: Applied Physics 37 (2004).

[9] R.R. Lamonte, D. McNally, Plastics Engineering 56 (2000) 51.

[10] J. Kameoka, H.G. Craighead, H. Zhang, J. Henion, Analytical Chemistry 73 (2001) 1935.

[11] Y. Yang, C. Li, J. Kameoka, K.H. Lee, H.G. Craighead, Lab on a Chip 5 (2005) 869.

[12] K.W. Ro, J. Liu, D.R. Knapp, Journal of Chromatography A 1111 (2006) 40.

[13] O. Gustafsson, K.B. Mogensen, J.P. Kutter, Electrophoresis 29 (2008) 3145.

[14] C. Jönsson, M. Aronsson, G. Rundström, C. Pettersson, I. Mendel-Hartvig, J. Bakker, E. Martinsson, B. Liedberg, B. MacCraith, O. Öhman, J. Melin, Lab on a Chip 8 (2008) 1191.

[15] S.C. Jacobson, R. Hergenröder, L.B. Koutny, R.J. Warmack, J. Michael Ramsey, Analytical Chemistry 66 (1994) 1107.

[16] G. Ocvirk, E. Verpoorte, A. Manz, M. Grasserbauer, H.M. Widmer, Analytical Methods and Instrumentation 2 (1995) 74.

[17] N. Vervoort, J. Billen, P. Gzil, G.V. Baron, G. Desmet, Analytical Chemistry 76 (2004) 4501.

[18] C.A. Mills, J.G. Fernandez, A. Errachid, J. Samitier, Microelectronic Engineering 85 (2008) 1897.

[19] J.P. Kutter, S.C. Jacobson, N. Matsubara, J.M. Ramsey, Analytical Chemistry 70 (1998) 3291.

[20] J.P. Kutter, S.C. Jacobson, J.M. Ramsey, Analytical Chemistry 69 (1997) 5165.

[21] R.A. Shalliker, B.S. Broyles, G. Guiochon, Journal of Chromatography A 865 (1999) 73.

[22] K. Ronse, Comptes Rendus Physique 7 (2006) 844.

[23] M. Elwenspoek, H.V. Jansen, Silicon Micromachining (1998).

[24] J. Vangelooven, W. De Malsche, H. Eghbali, K. Broeckhoven, H. Gardeniers, G. Desmet, Proceedings of the 32nd International Symposium on Capillary Chromatography and the 5th GCxGC Symposium, Riva del Garda, 2008.

[25] J.J. Van Deemter, F.J. Zuiderweg, A. Klinkenberg, Chemical Engineering Science 5 (1956) 271.

[26] J.C. Giddings, Dynamics of Chromatography, Part I, Principles and Theory (1965).

[27] K. Pappaert, J. Biesemans, D. Clicq, S. Vankrunkelsven, G. Desmet, Lab on a Chip 5 (2005) 1104.

[28] J. De Smet, P. Gzil, G.V. Baron, G. Desmet, Journal of Chromatography A 1154 (2007) 189.

[29] A.W. Moore Jr, S.C. Jacobson, J.M. Ramsey, Analytical Chemistry 67 (1995) 4184.

CHAPTER 4

Experimental study of the band broadening effect in a cyclo olefin polymer pillar array column

4.1 Abstract

An experimental study of a micromachined non-porous pillar array column performance under non-retentive conditions is presented. The same pillar structure has been fabricated in cyclo olefin polymer (COP) chips with three different depths *via* hot embossing and pressure-assisted thermal bonding. The influence of the depth on the band broadening along with the already known contribution arising from the top and bottom cover plates has been studied. The experimental results exhibit reduced plate heights as low as 0.2, which are in agreement with previous experimental work. Moreover, the constant values of the reduced Van Deemter expression are also in accordance with previous studies. A more exhaustive study of the C-term band broadening is also presented, showing that comparing the space between the pillars with different open tubular rectangular channels offers a good estimation of the C-term band broadening that is obtained experimentally. These experimental results, hence, confirm that micromachined pillar array columns fabricated in COP can achieve the same performance as the ones fabricated in silicon for the presently studied pillar channel design.

4.2 Introduction

The micromachined column concept proposed in 1998 by Regnier's group [1-3] has been widely studied during the past few years by different groups [4-7], as it has been demonstrated to be a very useful alternative to the typical packed beds that are being used in high performance liquid chromatography (HPLC) [8,9]. In this approach, and thanks to the micro-fabrication techniques of the microelectronics industry, the chromatographic support consists of an array of perfectly ordered etched pillars. The homogeneity that can be achieved with this structure leads to a substantial improvement of the column performance [10,11].

Using the ordered pillar array concept under pressure-driven flow conditions has appeared to be a challenge as they are more sensitive to slight imperfections in the bed structure than the electrically driven flows. Mainly, a good design of the sidewall zone and the definition of near vertical pillars are necessary to avoid a dramatic increase of the band broadening. This was first investigated by Vervoort *et al.* [12] using computational fluid dynamics (CFD), showing that an optimal design of the sidewall region could lead to a decrease in the band broadening by a factor of 4 near the optimal velocity. The first experimental realization of the concept has been achieved using the Bosch process to etch the pillars which was employed by De Pra *et al.* [5], demonstrating reduced plate heights as low as 0.2 for a non-retained component, and by De Malsche *et al.* [13], who, in addition, performed the first HPLC separations in a microfabricated pillar array column.

Besides the use of silicon-based materials to fabricate these structures, in the previous chapter, an entire cyclo olefin polymer (COP) chip containing an array of ordered pillars has been presented. Reduced plate heights as low as 0.2 in non-retained conditions were achieved, proving that a column with a perfectly ordered array of pillars can be also fabricated in a polymeric material. Finally, a high performance reversed-phase LC separation of four different components was also presented.

During the last few years, the performance limits of this column structure have been analyzed intensively. These studies are mainly on the investigation of the band broadening effect induced by the sidewall region [12,14,15] and by the top and bottom plates [16,17]. In the latter case, the additional band broadening effect cannot be eliminated, as can be accomplished in the former case by redesigning the sidewall region. It has been observed that this additional band broadening source can drastically increase the total band broadening in the commonly used velocity range. The exact contribution mainly depends on the ratio of the depth and the flow-through pores.

In the present chapter, experimental plate height data obtained from channels that were embossed in COP material, with the same structure but with different depths, is presented. The influence of pillar height on the theoretical plate height is studied for a non-retained dye and compared with the theoretical expectations.

4.3 Experimental

The microchip containing the ordered pillar array was designed in the same way as explained in the previous chapter. Briefly, the microchip consists of a separation channel, which is 5 cm long and 318 μm wide, filled with an array of ordered pillars (ε = 0.43, with a diameter of 15.3 μm). Distances between the pillars and to the column wall were designed according to the computational simulation dynamics studies described in the literature to avoid the sidewall-induced band-broadening effect [12]. This separation channel is crossed by a 88 μm wide injection channel turning up in a standard cross injection [18].

The fabrication process consists of two steps, the silicon master fabrication, which has been described in detail by De Malsche *et al.* [13], and the embossing and bonding of the polymer chip. In the first, silicon masters were fabricated via mid- UV photolitography and Bosch-type deep reactive ion-etching in a 4 inch wafer. Different etch times lead to different hole depths in the masters (2.7, 5.8

and 8.3 μm deep). Silicon wafers were diced, obtaining pieces of silicon of 1.5 x 7 cm^2.

For the second step, COP sheets (ZF 14-188, gently provided from Zeon Chemicals Co., Japan), were embossed using a HEX 01 embossing system (Jenoptik AG, Germany). To avoid sticking when detaching the polymer from the master, a fluoroalkylsilane monolayer [trichloro-(tridecafluoro-octyl-)silane] monolayer was evaporated on the silicon master before the embossing process [19]. Afterwards, holes were drilled in the microfabricated polymer before being bonded to another untreated COP sheet in a Nanoimprint Lithography equipment (Obducat, Sweden). More details of this process can be found in chapter 3. In Fig. 1, cross-section SEM pictures of the different bonded separation columns with the obtained depths are shown. One can observe that there is a slight difference between the master depths, indicated above, and the channel depths (2.5, 5.7 and 8.0 μm, respectively). This loss of a few tenths of microns is due to the pressure applied during the bonding process.

The experiments to characterize each column were carried out using an individual stock solution of 1 mM of C440 coumarin dye in methanol. The sample injection set-up used is the same as described in the previous chapter. Hence, to follow the plugs along the column, the stage of the inverted microscope (Eclipse Ti-S, Nikon) was moved through an external Motorized Linear Stage (UTS100CC, Newport). This was synchronized with the 6-port automated valves (MX Series II, Rheodyne), resulting in moving the stage just after the injection at the desired velocity. This was controlled with an in-house written LabView program (National Instruments). An Hg pre-centered fiber illuminator (Intesilight, Nikon) was used to excite the fluorescent dyes in the UV. To visualize them, the microscope was equipped with an UV filter cube set (UV-2A, Nikon) and an air-cooled CCD fluorescence camera (Orca-R2, Hamamatsu) mounted on the video adapter of the microscope in order to visualize the plugs. To analyze the recorded data, SimplePCI® 6 image analysis software (Hamamatsu) was employed.

To avoid background noise and to promote the absorbance of the background light, the chip was painted with a black permanent marker on the side facing the holder.

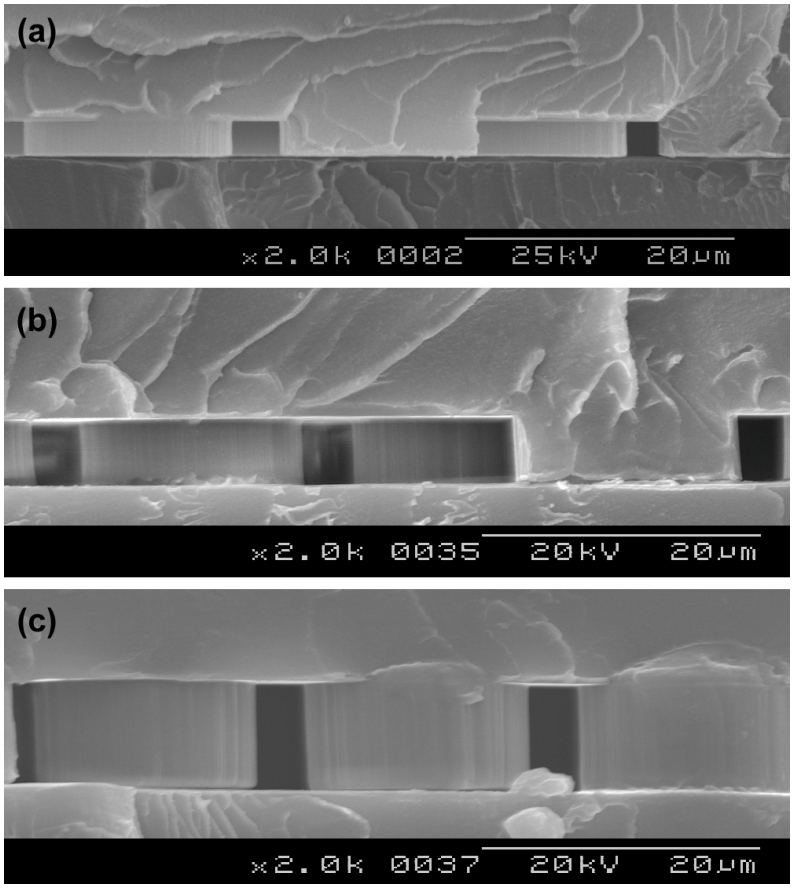

Fig. 1 SEM pictures of the different deep channel cross-sections; (a) 2.5 µm, (b) 5.7 µm and (c) 8.0 µm.

4.4 Results and discussion

In Fig. 2, a graphic description of the analysis procedure of an injected coumarin band is shown. An intensity average image of the whole channel with the plug centred on it, including the sidewall region, was taken (Fig. 2b) and plotted (Fig. 2c). That could be done due to the absence of sidewall effects as it is

demonstrated in Fig. 3, where ten points of each channel were measured taking and excluding the sidewall region respectively. The error between both measurements has been found to be less than 10%, being smaller than the dispersion of all the experimental values; so taking the whole channel will not affect the analysis of the data.

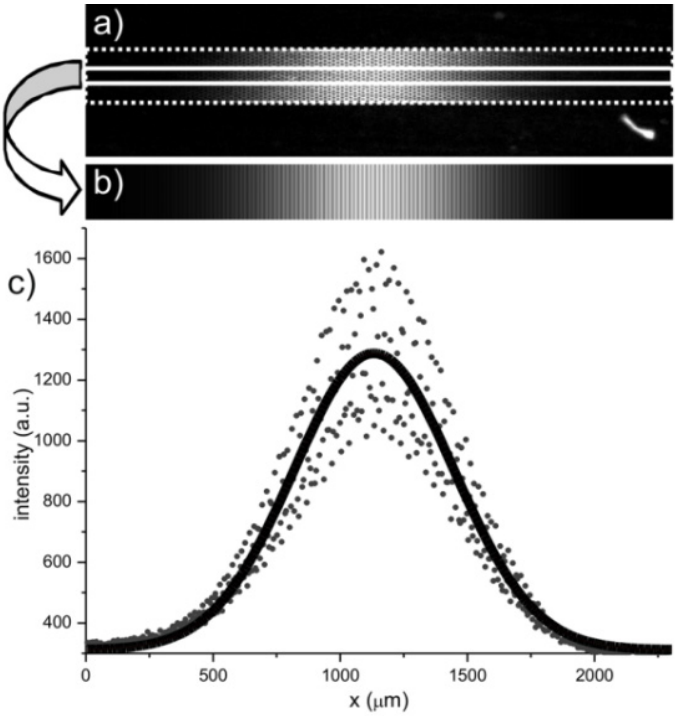

Fig. 2 Graphic description of an injected plug analysis. (a) Video frame with the injected plug centered on it. (b) Intensity average that can be done taking the whole channel (dash line) or excluding the sidewall region (solid line). (c) Plot with the data from the intensity average (scatter) and the Gaussian function fitting (line).

Moreover, and despite of the scattering due to the black spots in the figure that correspond to the pillars, the plug displays a good symmetry, allowing to be fitted with a Gaussian function:

$$C = C_{\max} \exp\left(-0.5 \left(\frac{x - x_0}{\sigma} \right)^2 \right) \qquad (1)$$

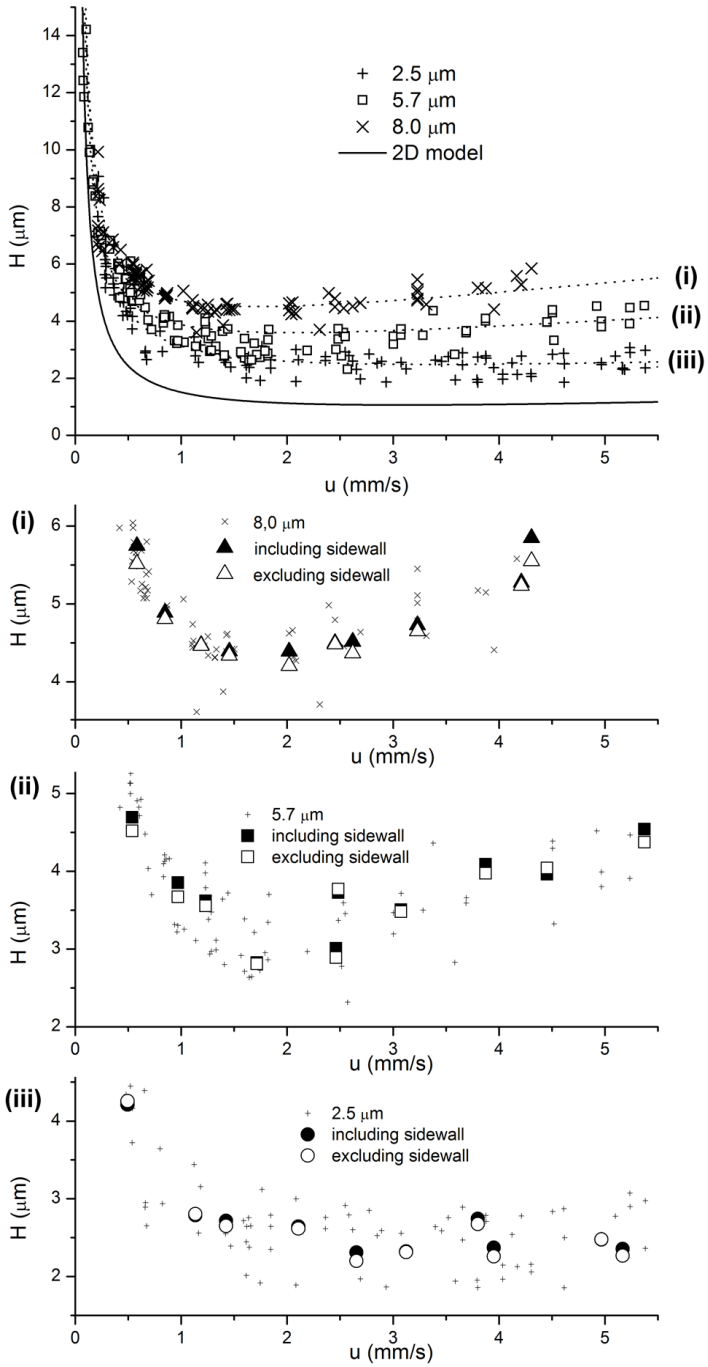

Fig. 3 Experimental data for the plate heights of the different deep channels ((+) 2.5 μm, (◎) 5.7 μm and (◎) 8.0 μm) with the respective fitted Van Deemter curves and the CFD simulated Van Deemter curve for the 2D model (top). Plate height values obtained analyzing a plug excluding the sidewall region (hollow figures) and their respective values obtained including the sidewall region (solid figures) for the 8.0 (i), 5.7 (ii) and 2.5 μm (iii) deep channels.

Then, the theoretical plate heights H for different velocities were calculated comparing the variances at two different points of the channel using:

$$H = \frac{\sigma_{x,1}^2 - \sigma_{x,0}^2}{\Delta x} \quad (2)$$

In this chapter, the plugs were analyzed at different points of the channel and compared simultaneously to show that there are no significant differences in the column performance along the channel. The value of Δx was always higher than 1 cm in order to have a good compromise between having a sufficient difference in spatial variance (to minimize the error on $\Delta\sigma_x^2$) and having enough intensity to allow an accurate determination of the whole peak.

The different plate heights values obtained for different mobile phase velocities were fitted with the basic van Deemter equation [20]:

$$H = A + B/u + Cu \quad (3)$$

Fig. 4 shows the different experimental values for the three different channels, and their fitted curves. Plate height values down to 2.5, 3.2 and 4.4 μm have been obtained for the 2.5, 5.7 and 8.0 μm deep channels, respectively. In the figure, we also added a curve that represents the plate heights values (H_{2D}) that would be obtained without top and bottom walls (pure 2D case), generated using CFD calculations [8,9].

The same experimental data in terms of the dimensionless reduced plate height h is shown in Fig. 3b. Giddings *et al*. [21] introduced this expression to be able to compare the values of different pillar geometries or different particle packing size:

$$h = A + B/\nu + C\nu \quad (4)$$

with the reduced velocity v and the reduced plate height h defined as:

$$h = \frac{H}{d_{pil}} \qquad v = \frac{u d_{pil}}{D_m} \tag{5}$$

where d_{pil} is the pillar diameter (15.3 μm) and D_m the diffusion coefficient, which corresponds to 1.2 10^{-9} m^2 s^{-1} for a solution of C440 in pure methanol [22].

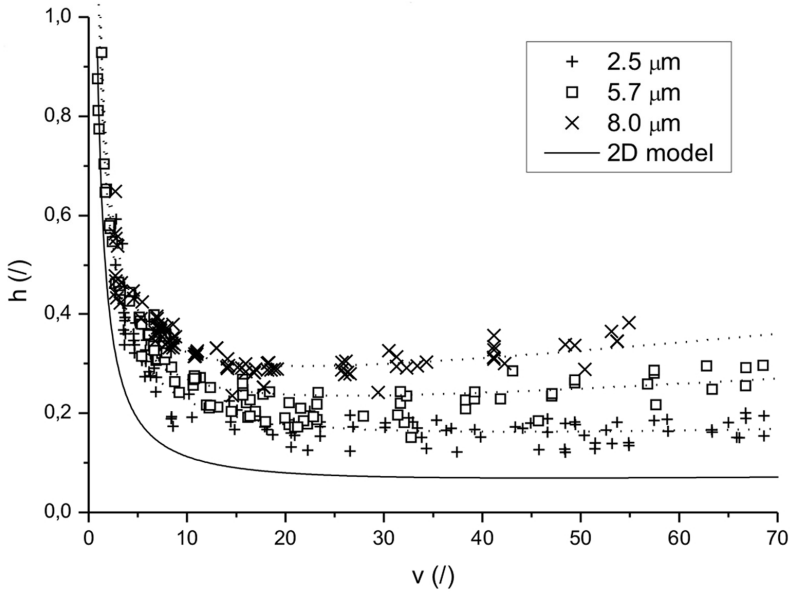

Fig. 4 Experimental data for the reduced plate heights of the different deep channels ((+) 2.5 μm, (□) 5.7 μm and (×) 8.0 μm) with the respective fitted Van Deemter curves and the CFD simulated Van Deemter curve for the 2D model

It can be observed that reduced plate heights of 0.2 have been reached and for the shallowest column, achieving the best predictions stated by De Pra *et al.* [5]. In Table 1 the *A*, *B* and *C* constant values obtained by fitting the experimental data to the reduced van Deemter equation (4) are compared to the values obtained by CFD simulations which predict minimum reduced plate heights as low as 0.1 [9].

The A-term value, which is related to the heterogeneity of the system, is similar to the obtained values in the silicon pillars of De Malsche *et al.* [13] and De Pra *et al.* [5]. The experimental values we obtained here are lower than the 0.24 achieved in the first study for a non-retained component, and in the same range of the

values achieved in the latter under non-retained conditions. The A-terms are, however, significantly larger than those obtained by CFD simulations for the 2D case (see Table 1), and, interestingly, are increasing with the pillar height. Even though we could not see any differences in pillar quality, it can be expected that more defects accumulate on the deepest pillar channels as compared to the more shallow channels. It also has to be reminded that we are using an imprint method to form the pillars, where the polymer pillars have to be gently removed from the etched holes in the silicon substrate. The deeper the gap is, the larger the chance that the polymer is damaged during removal after imprinting.

Table 1 Values of the experimental constant values of the Van Deemter curves obtained after fitting the experimental data and the constant values of the 2D simulated curve.

	w (μm)	*A-term*	*B-term*	*C-term*
Experimental data	2.5	0.11	1.06	0.00056
	5.7	0.17	0.88	0.00127
	8.0	0.21	0.95	0.00197
H_{2D} (CFD simulations)		0.03	0.81	0.00052

In agreement with the physical expectations, there is no much difference in the values of the B-term in relation to the 2D case. This constant can be seen as an empirical value that reflects the topological obstruction of axial molecular diffusion by the stationary phase support; therefore, it makes sense that it does not seem to be affected by the depth of the channels. In our experiments there are only slight differences between the different B-term values. An average value of 0.96 is obtained, which is close to the 0.81 predicted by the 2D simulations and the 0.9 obtained by De Pra *et al.* [5].

Finally, the C-term constant, which is in the present study purely related to the mass transfer resistance in the mobile phase (as it is conducted under non-

retentive conditions in non-porous pillar arrays), shows an increasing trend with the channel depth. Although there is no difference between the experimental value for the shallowest channel and the value obtained from the CFD simulations, this difference gets larger (up to 4 times) when increasing the channel depth. This behaviour of the C-term value may be explained by the additional contribution of the top and bottom plates on the band broadening, as it has been shown in previous studies [16,17]. There, this extra contribution was added to the 2D model, leading to a good agreement between the experimental results and the theoretical simulations. This can be done when the aspect ratio of the channel, w/d_{por} (where w is the channel height and d_{por} is the characteristic pore size, in this case the interpillar distance), is large enough, as it has been demonstrated in previous studies related to the sidewall band broadening in open tubular channels [23,24].

Table 2 C-term values of both experimental and estimated using Poppe's approximation. The aspect ratio that is larger than 1 (highlighted in black) was taken for this calculation.

w (μm)	w / d_{por}	d_{por} / w	*C-term experimental*	*C-term Poppe aproximation*
2.5	0.61	1.64	0.00056	0.00075
5.7	1.39	0.72	0.00127	0.00171
8.0	1.88	0.53	0.00197	0.00231

In the present study, the aspect ratios (see Table 2) are considerably smaller than 10, which does not allow the use of the above mentioned approach. As a means to rationalize the observed C-terms, we can, as a rough approximation, consider the space between the pillars as parallel plates. This case was studied by Poppe [25], and it allows to estimate the C-term that will arise in the 3 cases of differently rectangular 'open tubular channels' that are formed between the pillars.

The dimensionless contribution to the C-term under non-retained conditions is determined by [25]:

$$h_{mt} = \frac{1}{105} f_0 v \qquad (6)$$

with f_0 determined by the aspect ratio that is larger than 1 (values taken from Table 4 in [25]).

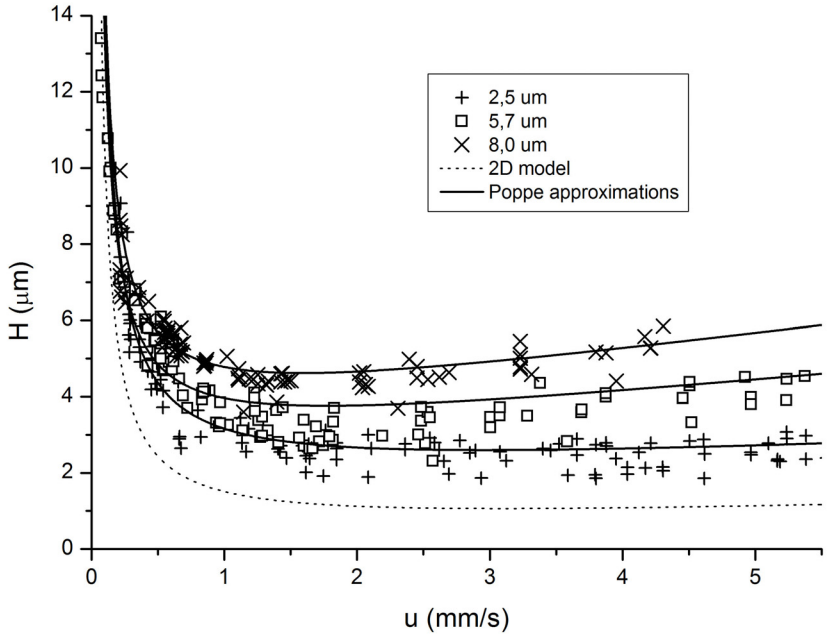

Fig. 5 Experimental data for the absolute plate heights of the different deep channels ((+) 2.5 μm, (□) 5.7 μm and (×) 8.0 μm) with the respective Poppe approximations which have been calculated using the experimental A- and B-term values and the C-term value calculated using the Poppe estimation.

These C-term values are listed in Table 2 and are in qualitative agreement to the experimentally obtained C-terms. It has to be stressed here that this approach is only valid as an estimation, as equation 6 describes the C-term for an open tubular rectangular shape, whereas the pillars in this study are considered as rectangular channels (defined by the top-wall flat walls and the virtual wall at the nearest point of two pillars).

In Fig 5, the van Deemter curves with these estimated C-terms and the fitted C-terms are depicted, showing a reasonable agreement between both data. With this final approach, we have demonstrated that the obtained experimental values are in agreement with what was expected theoretically; with A-term values which may be affected by the fabrication process, but achieve the best values obtained in previous work, B-term values close to the theoretical one, and C-term values, influenced by the different depths of the channels and also by the cover plates, which have been demonstrated to fit with the values obtained using the 'open tubular channel approximation' developed by Poppe.

4.5 Conclusions

In this chapter, the quality of micromachined non-porous pillar array column fabricated in COP is assessed using a fluorescent marker in non retained conditions. The influence of the channel depth in the band broadening is investigated using fabricated chips of 2.5, 5.7 and 8.0 μm deep columns with the same structure, i.e. external porosity, ε = 0.43 and pillar diameter d_{pil} = 15.3 μm. The experimental data for the reduced plate heights of the three columns are compared to the values obtained by CFD simulations for the 2D case. This comparison shows that the A-term is considerably larger in the experimental data than in the simulations but it is in the same range of the values obtained in previous work. An average value of 0.96 is obtained for the B-term which is close to the 0.81 value obtained in the 2D simulations.

A detailed study concerning the C-term to justify the difference between the experimental data and the simulation results taking in account the influence of the cover plates and the pillar walls is presented as well. It is shown that if the interpillar space is compared to rectangular open tubular channels, taking in account the approximations made by Poppe [25], both experimental and theoretical values are in an acceptable agreement leading to better efficiencies for low aspect ratio columns, hence, for shallower columns.

These results demonstrate that using a COP column with a pillar array the expected theoretical values concerning the band broadening are achieved as it is done in the 'silicon case', confirming the potential of this polymer-fabricated column.

4.6 References

[1] B. He, N. Tait, F. Regnier, Analytical Chemistry 70 (1998) 3790.

[2] F.E. Regnier, HRC Journal of High Resolution Chromatography 23 (2000) 19.

[3] B.E. Slentz, N.A. Penner, E. Lugowska, F. Regnier, Electrophoresis 22 (2001) 3736.

[4] K.B. Mogensen, F. Eriksson, O. Gustafsson, R.P.H. Nikolajsen, J.P. Kutter, Electrophoresis 25 (2004) 3788.

[5] M. De Pra, W.T. Kok, J.G.E. Gardeniers, G. Desmet, S. Eeltink, J.W. Van Nieuwkasteele, P.J. Schoenmakers, Analytical Chemistry 78 (2006) 6519.

[6] C. Aoyama, A. Saeki, M. Noguchi, Y. Shirasaki, S. Shoji, T. Funatsu, J. Mizuno, M. Tsunoda, Analytical Chemistry 82 (2010) 1420.

[7] X. Yan, Q. Wang, H.H. Bau, Journal of Chromatography A 1217 (2010) 1332.

[8] J. De Smet, P. Gzil, M. Vervoort, H. Verelst, G.V. Baron, G. Desmet, Analytical Chemistry 76 (2004) 3716.

[9] P. Gzil, N. Vervoort, G.V. Baron, G. Desmet, Analytical Chemistry 75 (2003) 6244.

[10] J.H. Knox, Journal of Chromatography A 831 (1999) 3.

[11] J. Eijkel, Lab on a Chip 7 (2007) 815.

[12] N. Vervoort, J. Billen, P. Gzil, G.V. Baron, G. Desmet, Analytical Chemistry 76 (2004) 4501.

[13] W. De Malsche, H. Eghbali, D. Clicq, J. Vangelooven, H. Gardeniers, G. Desmet, Analytical Chemistry 79 (2007) 5915.

[14] G. Desmet, G.V. Baron, Journal of Chromatography A 946 (2002) 51.

[15] K. Broeckhoven, G. Desmet, Journal of Chromatography A 1172 (2007) 25.

[16] J. De Smet, P. Gzil, G.V. Baron, G. Desmet, Journal of Chromatography A 1154 (2007) 189.

[17] H. Eghbali, W. De Malsche, J. De Smet, J. Billen, M. De Pra, W.T. Kok, P.J. Schoenmakers, H. Gardeniers, G. Desmet, Journal of Separation Science 30 (2007) 2605.

[18] S.C. Jacobson, R. Hergenröder, L.B. Koutny, R.J. Warmack, J. Michael Ramsey, Analytical Chemistry 66 (1994) 1107.

[19] C.A. Mills, E. Martinez, F. Bessueille, G. Villanueva, J. Bausells, J. Samitier, A. Errachid, Microelectronic Engineering 78-79 (2005) 695.

[20] J.J. Van Deemter, F.J. Zuiderweg, A. Klinkenberg, Chemical Engineering Science 5 (1956) 271.

[21] J.C. Giddings, Dynamics of Chromatography, Part I, Principles and Theory (1965).

[22] K. Pappaert, J. Biesemans, D. Clicq, S. Vankrunkelsven, G. Desmet, Lab on a Chip 5 (2005) 1104.

[23] R. Aris, Proceedings of the Royal Society London 235 (1956) 67.

[24] A. Cifuentes, H. Poppe, Chromatographia 39 (1994) 391.

[25] H. Poppe, Journal of Chromatography A 948 (2002) 3.

CHAPTER 5

Experimental study of the retention properties of a cyclo olefin polymer pillar array column in reversed phase mode

5.1 Abstract

Experimental measurements to study the retention capacity and band broadening under retentive conditions using micromachined non-porous pillar array columns fabricated in cyclo olefin polymer (COP) are presented. In particular, three columns with different depths but with the same pillar structure have been fabricated *via* hot embossing and pressure-assisted thermal bonding. Separations of a mixture of 4 coumarins using varying mobile phase compositions have been monitored to study the relation between the retention factor and the ratio of organic solvent in the aqueous mobile phase. Moreover, the linear relation between the retention and the surface/volume ratio predicted in theory has been observed, achieving retention factors up to k = 2.5. Under the same retentive conditions, minimal reduced plate height values of h_{min} = 0.4 have been obtained at retention factors of k = 1.2. These experimental results are compared to the case of non-porous and porous silicon pillars. Similar results for the plate heights are achieved while retention factors are higher than the non-porous silicon column and considerably smaller than the porous pillar column, given the non-porous nature of the used COP. The feasibility of using this polymer column as an alternative to the pillar array silicon columns is corroborated.

5.2 Introduction

Since the launch of Regnier's and co-workers's concept of collocated monolithic support structures (COMOSS) [1-3] introducing the micromachined pillar array concept as a revolutionary alternative to the typical packed beds, over a decade has passed. The theoretical studies of this column structure that followed Regnier's work [4,5] described the potential of this column configuration for its use in pressure-driven liquid chromatography, which has been confirmed lately with the publication of several papers [6-11]. Particularly, De Pra *et al.* reported reduced plate heights as low as h_{min} = 0.2 under non-retentive conditions while De Malsche *et al.* achieved reduced plate heights of h_{min} = 1 under retentive conditions, with the largest retention factors being k = 0.65 – 1.2.

As examples, improvements in the performance of this column configuration have been achieved by redesigning the sidewall region [12] and an explanation of the influence of the top and bottom plates has been given [13,14]. But one of the major challenges to overcome for this column format, to be competitive with the commercial packed bed or monolithic HPLC-columns, is the need to increase the surface area to enhance the chromatographic exchange between the stationary and the mobile phase [15]. This increase of the retention has already been achieved by the fabrication of porous silicon shells over the pillars using electrochemical anodization of the solid silicon pillars [16-18]. With this method, retention factors up to k = 12 have been achieved [17].

Other attempts to increase the surface of the pillar array structure have been also performed, albeit not much success has been achieved with these other strategies. The use of xerogel films [19] to etch the pillars on it [20] has been tested, where it appeared difficult to avoid tapering of the porous walls [21]. The formation of porous glass by plasma etching for electrically-driven flows has also been used as a strategy to increase the surface, but the pressures the chips can withstand showed to be not sufficient for being used under pressure-driven HPLC conditions [22]. Finally, the synthesis of siloxane-based monoliths in the presence of a two-dimensional perfectly

ordered array of micropillars has also been reported [23], however no data concerning the retention have yet been published.

Later, exploration of polymers for the fabrication of the pillar array column structure has been carried out. Among the variety of polymers available on the market, the recently introduced cyclo olefin polymers (COPs) deserves special attention as they show very promising properties, such as, high chemical resistance, low water absorption, good optical transparency near the UV range and ease of fabrication to be used in microfluidics [24]. A lot of work concerning the fabrication of chromatography chips in COPs has been presented since 2001. Kameoka *et al.* [25] reported a capillary electrophoresis microchannel with a coupled microsprayer for mass spectroscopy analysis fabricated in COP. Ro *et al*. [26] have developed a COP microfluidic device with an array of methacrylate monolithic LC columns prepared by UV-initiated polymerization inside the microfluidic channels, and recently, Liu *et al*. [27] have fabricated COP chips containing in situ photopolymerized polymethacrylate monolithic stationary phases for LC. Concerning the idea of the pillar structure, Gustafsson *et al*. [28] were the first to fabricate arrays of ordered pillars in a COP by nanoimprint lithography (NIL). They used the hydrophobic surface of the COP directly as the stationary phase to separate three fluorescently labelled amines by reversed phased electrochromatography.

In chapter 3, a chip containing a pillar array column fabricated in COP for pressure-driven reversed phase liquid chromatography is described. There, reduced plate heights of 0.2 under non-retentive conditions were achieved and a separation of four different coumarins was obtained with retention factors up to $k = 0.5$.

In the present chapter, an exhaustive study of the column performance under retentive conditions is presented. Particularly, the retention in three identical columns with different depths is compared to allow for a more general evaluation of COP as an alternative material to the silicon and porous silicon based columns.

5.3 Experimental

The fabrication of the COP chip with a 5 cm long and 318 μm wide separation column containing the pillar array (external porosity, ε = 0.43, pillar diameter, d_{pil} = 15.3 μm and a proper sidewall region designed to avoid the sidewall-induced band broadening effect [12]) has been already described in chapter 3. In short, silicon masters with 2.7, 5.8 and 8.3 μm deep holes were fabricated via standard UV-photolithography and Bosch-type reactive ion-etching [8]. Then, the masters were used to emboss the COP sheets (ZF 14-188, Zeon Chemicals Co, Japan) in a HEX 01 embossing equipment (Jenoptik AG, Germany). Finally, the microstructured COP sheets were bonded to non-processed COP sheets via pressure-assisted thermal bonding in a Nanoimprint Lithography equipment (Obducat, Sweden). After the bonding, some of the fabricated channels were examined to check their depths, observing that some hundreds of nanometers were lost due to the pressure applied during the bonding, resulting in 2.5, 5.7 and 8.0 μm deep channels. In Fig. 1, a SEM image of the bonded channel with part of the pillars out of the bonded zone is shown.

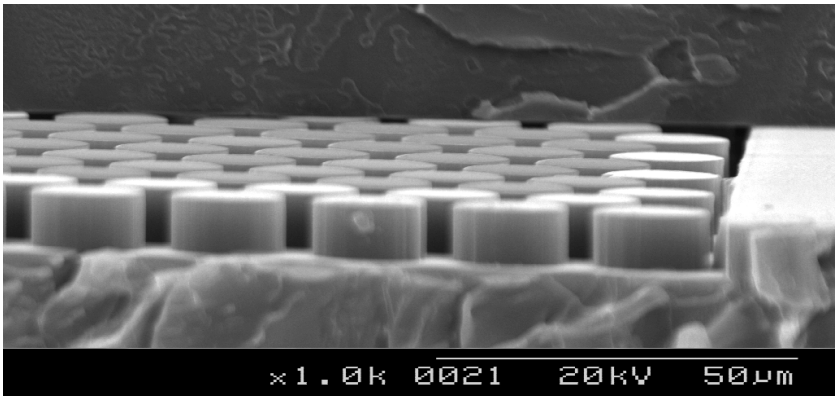

Fig. 1 SEM image of the pillars at the bonding interface in a 8.0 μm deep channel.

A home-built holder, consisting in an aluminum bottom-plate, with an open window to allow the observation of the microchannel, and a Delrin® top-plate, where through-holes compatible with commercially available Upchurch nanoport connectors were drilled, was used to place the COP chip. Fused silica capillaries with an inner diameter of 150 μm were used to connect the chip to the injection set-up.

Also, significant care in order to avoid background noise and to promote the absorbance of the background signal was taken when painting with a black permanent marker the side of the chip facing the top plate of the holder.

The sample injection was performed using an automated 6-valve system (MX Series II, Rheodyne), monitored with an in-house written LabView program. This program also controls an external motorized linear stage (UTS100CC, Newport) that moves the stage of an inverted microscope (Eclipse Ti-S, Nikon) following the injected plugs as it is already described in chapter 3. An Hg precentered fiber illuminator (Intesilight, Nikon) was used to excite the fluorescent dyes in the UV. The peaks were visualized using an air-cooled CCD fluorescence camera (Orca-R2, Hamamatsu) and a UV filter cube set (UV-2A, Nikon). The peak intensity profiles were subsequently analyzed using the Simple PCI 6 (Hamamatsu) image analysis software.

Two types of experiments have been performed in this study. Separation experiments of four different coumarin mixtures, C440 (CAS no. 26093-31-2, Acros Organics, Belgium), C450 (CAS no. 26078-25-1), C460 (CAS no. 91-44-1) and C480 (CAS no. 41267-76-9) have been carried out to study their retention as a function of the column depth and the mobile phase composition. Each coumarin was individually dissolved in HPLC-grade methanol at a concentration of 1 mM. For the mobile phase, different water/methanol mixtures, varying from 70/30 v/v to 50/50 v/v, and with the water phase additionally buffered at pH = 7 using a phosphate buffer, were used. It is also worthy to point out that for each experiment the coumarin mixtures were also dissolved in the same ratio of water/methanol as the mobile phase to avoid viscous fingering which has been also studied for perfectly ordered pillar array columns [29]. As a marker for the mobile phase velocity to determine the different retention factors, coumarin C440 was used, as it has been observed that its migration time is not significantly affected by changing the methanol concentration [30].

Finally, and to establish van Deemter curves under retentive conditions, coumarin C480 was injected using different water/methanol mixtures as mobile phases. Again,

coumarin C440 was used to determine the mobile phase velocity and the same considerations that have been described above were taken to avoid viscous fingering.

5.4 Results and discussion

Separation experiments were performed in the three channels with different depths using varying water/methanol ratios as the mobile phase. In these experiments, the four different coumarins were mixed, injected and separated. Chromatograms are time-response intensity plots that have been obtained after analyzing the same the fluorescent intensity of the same row of pixels during the whole video caption that was recorded during the separation experiments. With these time-response intensity plots the retention factor k of each component can be determined measuring its residence time, as follows:

$$k = \frac{t_r - t_0}{t_0} \qquad (1)$$

where t_r is the residence time for the retained component and t_0 is the residence time for the non-retained component, which in our case is coumarin C440.

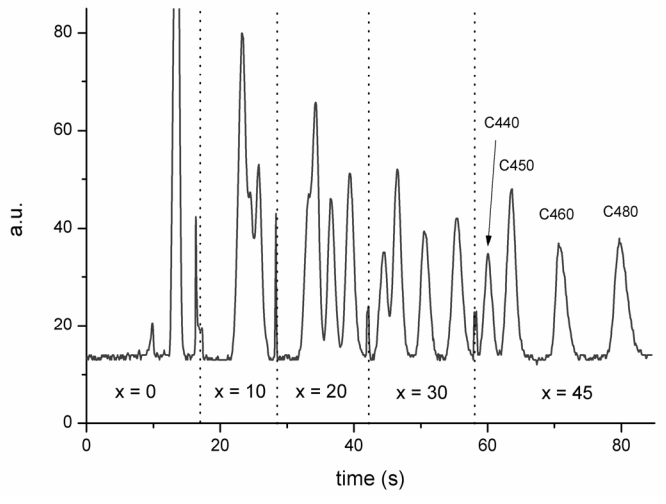

Fig. 2 Chromatogram of coumarins C440, C450, C460 and C480 in 60/40 (v/v) water/methanol (pH 7) in a 8.0 μm deep channel, monitored at 10, 20, 30 and 45 mm downstream the injection slit (0 mm). The mobile phase velocity was 0.95 mm/s.

In Fig. 2 an example of a chromatogram is shown. There, measurements have been taken at different positions downstream the injection slit, in a way that the microscope stage was moved to the next stop after all the components passed by the focus of the microscope. It can be observed that the four components have a different retention, leading to a perfectly based-line separation at the end of the column (45 mm downstream the injection slit).

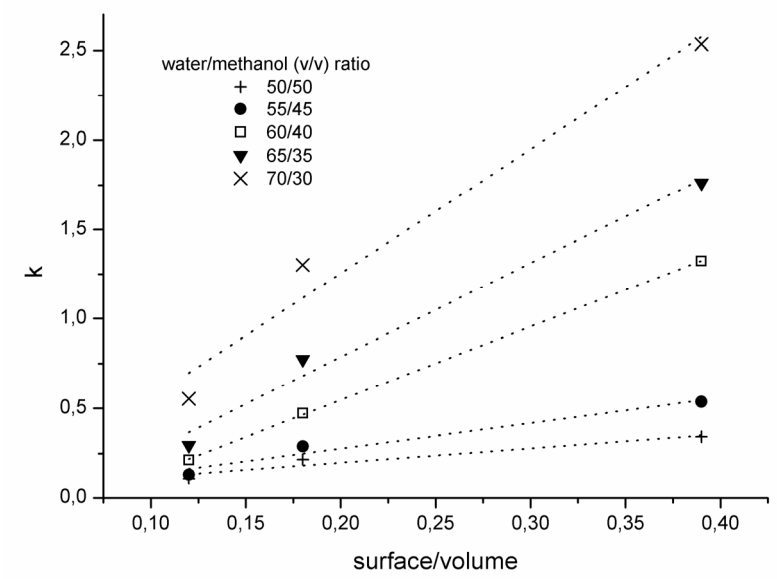

Fig. 3 Values of the retention factor *k* in terms of the surface/volume ratio for the 2.5, 5.7 and 8.0 μm deep channels (from right to left) for the different water/methanol (v/v) mobile phase ratios.

Next, the influence of the column depth on the retention is studied in detail. As the pillar array structure is the same for all columns, an increase of the column depth leads to a decrease of the surface/volume ratio, which is expected to have a strong influence on the retention. To assess the retention behaviour of the different species in terms of the surface/volume ratio, the retention of coumarin C480 was measured for various mobile phase compositions, ranging from 70/30 to 50/50 (v/v), water/methanol mixtures. Results are depicted in Fig. 3, where it is clearly seen that retention increases with the surface/volume ratio, hence, with decreasing the column depth. Retention factors up to $k = 2.5$ have been achieved for the shallowest channel in the most favourable conditions, doubling the retention factors achieved by De Malsche *et al.* for a non-porous silicon pillar array column [8]. A linear trend between

the retention and the surface/volume ratio can be observed and is pointed out by the dotted lines in Fig. 3. This linear relation is in accordance to the retention mechanism in reversed-phase LC, where the retention depends on the surface of the stationary phase [31]. This linear behaviour is also an indication of the absence of overloading at the applied conditions. It can be noticed, however, that at the highest retention measured (70 % water) the quality of the linear fit decreases, indicating possible overloading at the applied concentration. This linear relation also confirms the nonexistence of a dual retention mechanism which may alter the retention behaviour of the column.

Moreover, specifically in the case of reversed-phase liquid chromatography, a linear relationship between *lnk* and the fraction of organic modifier φ in aqueous binary mobile phase systems has been described [32]:

$$\ln k = \ln k_0 - S\phi \qquad (2)$$

where *S* is the solvent strength, which for reversed-phase coatings with methanol as the organic modifier present values of *S* = 7-10. In Figs. 4a, b and c the data of the retention of the three retained coumarins (C440, C450 and C480) in the 2.5, 5.7 and 8.0 μm deep columns as a function of the fraction of methanol used in the mobile phase is shown. The best fits to eq. (2) achieved for the presented experimental data have been added to the figures showing solvent strength values inside the predicted range and increasing with the surface/volume ratio.

An in-depth study of the efficiency of the columns used in the present work under non-retentive conditions is given in the previous chapter. However, and in order to give an example of the chromatographic performance of the column under retentive conditions, van Deemter curves of coumarin C480 for the 2.5 μm deep channel using water/methanol mixtures of 60/40 and 50/50 v/v as the mobile phase have been determined. For that, coumarin plugs were injected and monitored at two different distances far enough from the injection slit (e.g. 10 and 25 mm) to allow coumarins C440 and C480 to be separated. As stated above, coumarin C440 was used to determine the mobile phase velocity. Then, given their symmetrical shape, both plugs

could be fitted to a Gaussian distribution. The Gaussian fittings were, afterwards, used to calculate the absolute plate height H as follows:

$$H = \frac{\Delta\sigma_x^2}{\Delta x} \tag{3}$$

with $\Delta\sigma_x$ as the difference between both spatial standard deviations of the Gaussian fit of the plug after traveling a distance Δx.

The van Deemter equation relates the absolute plate height with the mobile phase velocity, u [33]:

$$H = A + B/u + Cu \tag{4}$$

where A, B and C are constants related to the heterogeneity of the system, the dispersion due to the molecular diffusion and the mass-transfer resistance between the stationary and the mobile phase, respectively. In Fig. 5, van Deemter curves of the retained components are compared to the curve for the same component under non-retentive conditions, i.e., using pure methanol as the mobile phase. It is observed that under retentive conditions the optimal velocity is shifted to lower velocities while the plate height minimum slightly increases. Taking the reduced coordinates in order to cancel the effect of changing the molecular diffusion coefficient, shown in the inset of Fig. 5, embedded, it is clear that the reduced plate heights in the C-term dominated part of the curve increase with the retention factor. Moreover, the abrupt increase of the plate heights when passing from no retention to only a retention factor of $k = 0.3$ is noticeable. This effect is also found for coumarins C450 and C460 and coincides with the results obtained by De Malsche *et al.* [17], where an initial increase in the plate height was found when moving from a retention coefficient of $k = 0$ to $k = 1.2$. In both cases, further increases in k lead to a less strong increase of the plate height in the C-term dominated part of the curve. However, the minimum values for the reduced plate height under retentive conditions is only about $h_{min} = 0.4$ for a mobile phase composition of 60/40 v/v water/methanol ($k = 1.2$), smaller than the values around $h_{min} = 0.9$ obtained under the same retentive conditions ($k = 1.2$) by De Malsche *et al.* for the case of pillars with a porous shell of 1 μm [17].

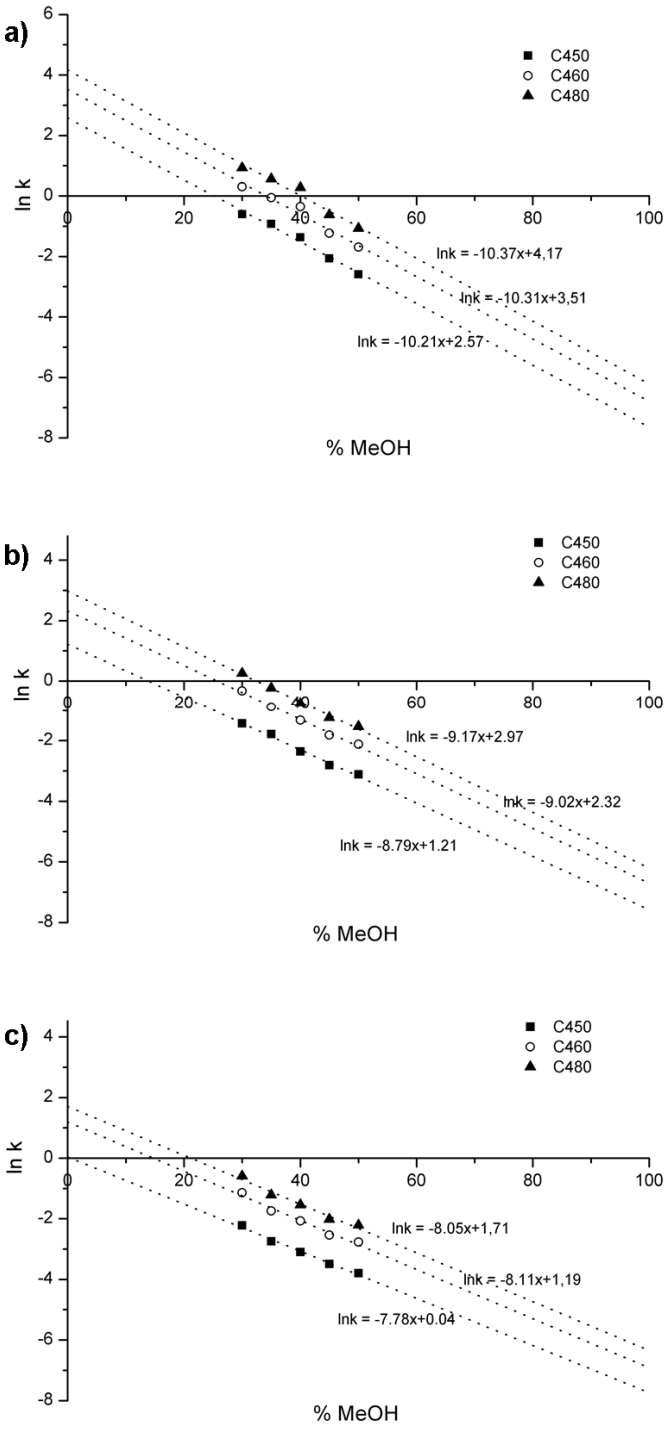

Fig. 4 Relations between the retention factors of the (a) 2.5, (b) 5.7 and (c) 8.0 μm deep channels and the methanol content of the mobile phase.

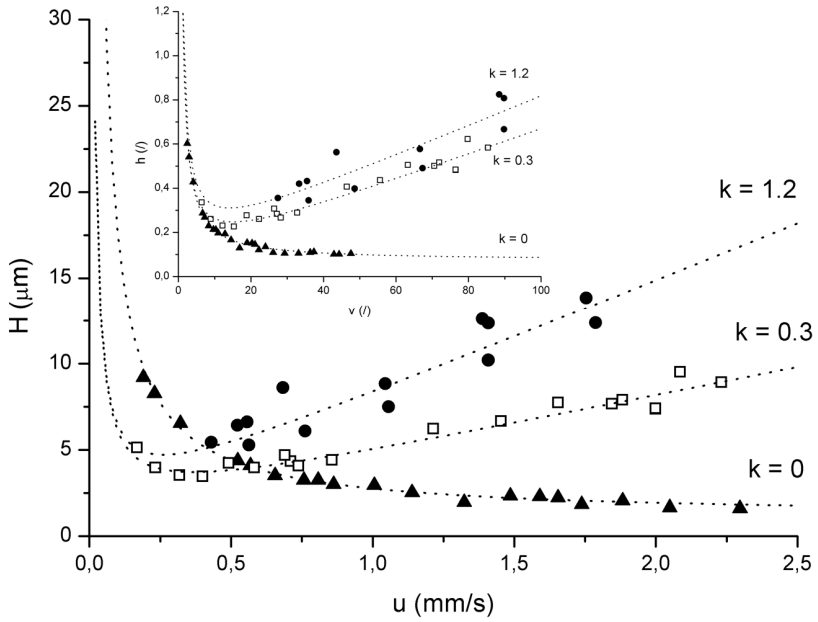

Fig. 5 Experimental data for the plate heights of coumarin C480 in the 2.5 μm deep channel under non-retentive conditions (▲) and retentive conditions, corresponding to water/methanol mobile phase ratios of 50/50 (□) and 60/40 (●) (v/v). In the embedded graph the same data is shown in reduced coordinates. Dashed lines correspond to the best fitted Van Deemter curves.

These low values for the reduced plate heights are, in addition, lower than the best values achieved for the best commercially available packed bed columns (h_{min} = 1.6), which use porous shell particles of 2.7 μm in diameter [34]. When using the reduced coordinates it is also observed that the values for the minimum of the reduced van Deemter curves under retentive conditions are slightly larger and shifted to smaller reduced velocities in comparison with the values obtained under non-retentive conditions; moreover, there is a considerable difference in the C-term dominated part of the curve, as expected.

5.5 Conclusions

Use of COP is a cheap alternative to silicon for the fabrication of micropillar array columns, as has already been demonstrated in the previous chapters. In this one,

moreover, the retention power of this polymer column was investigated and compared with the silicon case. Different chips containing 2.5, 5.7 and 8.0 μm deep columns with the same structure, i.e., external porosity, ε = 0.43 and pillar diameter d_{pil} = 15.3 μm, have been fabricated to study both the influence of the channel depth (i.e. surface/volume ratio) and the mobile phase composition on the retention factor. Both experiments show good agreement with the theory described for reversed-phase liquid chromatography, with best achieved retention factors of k = 2.5 using the shallowest column and a mobile phase composition of 70/30 v/v water/methanol.

Also the study of the band broadening under retentive conditions has been carried out. Injections of coumarin C480 have been done under different mobile phase conditions obtaining minimum values for the reduced plate height of h_{min} = 0.4 for a mobile phase composition of 60/40 v/v water/methanol (k = 1.2). As expected, increasing the retention factor leads to a strong increase of the plate height in the C-term dominated part of the curve, especially when moving from a retention coefficient of k = 0 to k = 0.3.

These obtained values for the retention and the reduced plate height place the performance of this pillar array column fabricated in COP between the performance of the non-porous and the porous silicon micropillar array. Reduced plate heights are similar to those of the silicon non-porous case, while the achieved retention factors are slightly larger. The analysis of the retention dependence on the surface-to-volume ratio shows that better performances are achieved for shallower columns, which are an explanation for the differences to the silicon case where high aspect ratio columns were fabricated. Regarding the porous silicon case, the COP column has smaller reduced plate heights while retention factors are still far from the porous silicon shell pillars. As a summary, the good performance of the COP column has been demonstrated, making it a reasonable alternative to the expensive pillar array columns fabricated in silicon, also in terms of performance. Specifically, this non-porous column format may be ideally suited applications like protein and nucleic-acid separations, where non-porous columns still play a major role.

5.6 References

[1] B. He, N. Tait, F. Regnier, Analytical Chemistry 70 (1998) 3790.

[2] F.E. Regnier, HRC Journal of High Resolution Chromatography 23 (2000) 19.

[3] B.E. Slentz, N.A. Penner, E. Lugowska, F. Regnier, Electrophoresis 22 (2001) 3736.

[4] J. De Smet, P. Gzil, M. Vervoort, H. Verelst, G.V. Baron, G. Desmet, Analytical Chemistry 76 (2004) 3716.

[5] P. Gzil, N. Vervoort, G.V. Baron, G. Desmet, Analytical Chemistry 75 (2003) 6244.

[6] M. De Pra, W.T. Kok, J.G.E. Gardeniers, G. Desmet, S. Eeltink, J.W. Van Nieuwkasteele, P.J. Schoenmakers, Analytical Chemistry 78 (2006) 6519.

[7] H. Eghbali, W. De Malsche, D. Clicq, H. Gardeniers, G. Desmet, LC-GC Europe 20 (2007) 208.

[8] W. De Malsche, H. Eghbali, D. Clicq, J. Vangelooven, H. Gardeniers, G. Desmet, Analytical Chemistry 79 (2007) 5915.

[9] X. Yan, Q. Wang, H.H. Bau, Journal of Chromatography A 1217 (2010) 1332.

[10] N.V. Lavrik, L.C. Taylor, M.J. Sepaniak, Lab on a Chip 10 (2010) 1086.

[11] C. Aoyama, A. Saeki, M. Noguchi, Y. Shirasaki, S. Shoji, T. Funatsu, J. Mizuno, M. Tsunoda, Analytical Chemistry 82 (2010) 1420.

[12] N. Vervoort, J. Billen, P. Gzil, G.V. Baron, G. Desmet, Analytical Chemistry 76 (2004) 4501.

[13] J. De Smet, P. Gzil, G.V. Baron, G. Desmet, Journal of Chromatography A 1154 (2007) 189.

[14] H. Eghbali, W. De Malsche, J. De Smet, J. Billen, M. De Pra, W.T. Kok, P.J. Schoenmakers, H. Gardeniers, G. Desmet, Journal of Separation Science 30 (2007) 2605.

[15] J. Eijkel, Lab on a Chip 7 (2007) 815.

[16] W. De Malsche, D. Clicq, V. Verdoold, P. Gzil, G. Desmet, H. Gardeniers, Lab on a Chip 7 (2007) 1705.

[17] W. De Malsche, H. Gardeniers, G. Desmet, Analytical Chemistry 80 (2008) 5391.

[18] R.M. Tiggelaar, V. Verdoold, H. Eghbali, G. Desmet, J.G.E. Gardeniers, Lab on a Chip 9 (2009) 456.

[19] K. Kanamori, M. Aizawa, K. Nakanishi, T. Hanada, Advanced Materials 19 (2007) 1589.

[20] V. Verdoold, P. Gzil, F. Detobel, K. Wyns, G. Desmet, H. Gardeniers, in 34th International Conference on Micro & Nano Engineering, Athens, 2008.

[21] T.E.F.M. Standaert, E.A. Joseph, G.S. Oehrlein, A. Jain, W.N. Gill, P.C. Wayner Jr, J.L. Plawsky, Journal of Vacuum Science and Technology A: Vacuum, Surfaces and Films 18 (2000) 2742.

[22] R.C. De Andrade Costa, K.B. Mogensen, J.P. Kutter, Lab on a Chip 5 (2005) 1310.

[23] F. Detobel, H. Eghbali, S. De Bruyne, H. Terryn, H. Gardeniers, G. Desmet, Journal of Chromatography A 1216 (2009) 7360.

[24] P. Nunes, P. Ohlsson, O. Ordeig, J. Kutter, Microfluidics and Nanofluidics (2010).

[25] J. Kameoka, H.G. Craighead, H. Zhang, J. Henion, Analytical Chemistry 73 (2001) 1935.

[26] K.W. Ro, J. Liu, D.R. Knapp, Journal of Chromatography A 1111 (2006) 40.

[27] J. Liu, C.-F. Chen, C.-W. Tsao, C.-C. Chang, C.-C. Chu, D.L. DeVoe, Analytical Chemistry 81 (2009) 2545.

[28] O. Gustafsson, K.B. Mogensen, J.P. Kutter, Electrophoresis 29 (2008) 3145.

[29] W. De Malsche, J. Op De Beeck, H. Gardeniers, G. Desmet, Journal of Chromatography A 1216 (2009) 5511.

[30] A.W. Moore, S.C. Jacobson, J.M. Ramsey, Analytical Chemistry 67 (1995) 4184.

[31] J.C. Giddings, Dynamics of Chromatography, Part I, Principles and Theory, Marcel Dekker, New York, 1965.

[32] U.D. Neue, HPLC Columns: Theory, Technology, and Practice, Wiley-VCH, New York, 1997.

[33] J.J. Van Deemter, F.J. Zuiderweg, A. Klinkenberg, Chemical Engineering Science 5 (1956) 271.

[34] S. Fekete, J. Fekete, K. Ganzler, Journal of Pharmaceutical and Biomedical Analysis 49 (2009) 64.

CHAPTER 6

A cyclo olefin polymer microfluidic chip with integrated gold microelectrodes

6.1 Abstract

This chapter presents an entirely polymeric microfluidic system, made of cyclo olefin polymer (COP), with integrated gold microband electrodes for electrochemical applications in organic media. In the present study, we take advantage of the COP's high chemical stability to polar organic solvents in two different ways: (i) to fabricate gold microelectrodes using COP as a substrate by standard lithographic and lift-off techniques; and (ii) to perform electrochemical experiments in organic media. In particular, fourteen parallel gold microelectrodes with a width of 14 μm and separated from their closest neighbour by 16 μm were fabricated by lithographic and lift-off techniques on a 188 μm thick COP sheet. A closed channel configuration was obtained by pressure-assisted thermal bonding between the COP sheet containing the microelectrodes and a microstrutured COP sheet, where a 3 cm long, 50 μm wide and 24 μm deep channel was fabricated *via* hot embossing. Cyclic voltammetric measurements were carried out in aqueous and organic media, using a solution consisting of 5 mM ferrocyanide/ferricyanide in 0.5 M KNO_3 and 5 mM ferrocene in 0.1 M TBAP/acetonitrile, respectively. Experimental currents obtained for different flow rates ranging from 1 to 10 μL min^{-1} were compared to the theoretical steady state currents calculated by the Levich equation for a band

electrode [1]. In both cases, the difference between the experimental and the predicted data is less than 5%, thus validating the behaviour of the fabricated device. This result opens for the possibility to use a microfluidic system entirely made from COP with integrated microband electrodes in organic electroanalysis and in electrosynthesis

6.2 Introduction

The last decade has seen a substantial rise in the use of microfluidic systems for electroanalysis [2,3]. This is mainly due to the fact that hydrodynamic devices (flow cells [4,5], rotating electrodes [6], and electrochemical cells in presence of ultrasonic forces [7]) offer significant advantages over electrochemical techniques operated in stagnant solutions. Basically, these systems use convection to enhance the rate of mass transport to the electrodes resulting in increased currents and sensitivities compared to voltammetric measurements performed in still solutions. Moreover, electrochemical techniques offer great advantages over other common detection techniques to be used in so-called micro-total analysis systems (μTAS), because of their low power requirements, low limits of detection, remarkable sensitivity, and high compatibility with advanced micromachining and microfabrication technologies [8].

The first approaches to integrate electrochemistry in microfluidics used silicon and/or glass based substrates and standard lithographic and micromachining techniques. In particular, capillary electrophoresis chips made in glass with integrated electrodes were the first devices to be reported [9] and have also been the most widely used [10,11]. The main drawbacks of using the traditional materials (silicon or glass) for the fabrication of microfluidic systems are the high fabrication costs and often tedious fabrication processes. With the goal of fabricating cheap, portable and disposable microsystems, polymeric materials have been identified as a good alternative.

The first attempts to move to total polymeric microsystems with integrated electrochemical detection were hybrid devices combining glass and poly (dimethyl siloxane) (PDMS); such systems are still extensively used [12,13]. It was not until 1999 that the first report of an entirely polymeric chip with integrated microelectrodes was presented [14]. Microchannels in poly (ethylene terephthalate) (PET) were laser-photoablated and then filled with carbon polymer ink. Later, microelectrodes in polymer microchips have been fabricated using different techniques: (i) assembly, where the electrode material is inserted into the device [15-17]; (ii) screen-printing [18-20] and airbrushing [21], where a paste containing metal particles is deposited onto the polymer either over a screen containing the geometrical pattern of the electrode or being sprayed through a patterned thin film; (iii) direct electrodeposition [22], where the metal deposition takes place through a metal shadow mask via sputtering or evaporation; (iv) surface modification of the polymer surface and electrodeposition [23]; and (v) photolithography [24].

As mentioned above, photolithography is the most widely and commonly used technique to fabricate metal electrodes in silicon- or glass-based devices due to the near perfect control of the size, shape and interelectrode distance between two adjacent electrodes it affords [25]. Unfortunately, as stated by Becker *et al*. [26], most thermoplastic polymers are chemically incompatible with the common photolithographic techniques that involve the use of photoresists (which, typically, are solvent-based) and organic solutions, like acetone, for the lift-off process. Because of this, the fabrication of microelectrodes by photolithography in polymer substrates has been limited mainly to thermosetting polymers (polyimide, SU-8, etc.) [27,28], although there are few works using compatible processes with thermoplastics such as poly (methyl methacrylate) (PMMA) [29,30] and polycarbonate (PC) [31].

This issue related to the chemical compatibility with organic solvents can now be overcome using the relatively new thermoplastic polymers called either cyclo olefin polymer or copolymer (COP/COC) with the brand names Zeonor® and

Topas®, respectively. COP and COC, apart from presenting low water absorption, good optical properties and excellent biocompatibility, are highly resistant to acids, bases and polar organic solvents [32,33]. It is the latter that makes them really promising for lithography processes, as it has already been shown by Yang *et al.* [34] and Nielsen *et al.* [35], as well as for organic media applications.

Up to now COC and COP have been used as materials to fabricate microchips for different applications such as capillary electrophoresis [15,36], chromatography [37,38] (as it has been also demonstrated in the previous chapters), isoelectric focusing [39,40], and blood [41,42] and DNA analysis [43,44]. Several different detection methods have been employed in those chips, e.g., electrochemical detection [15,45], optical detection [40,46] and mass spectrometry [47,48]. Surprisingly, to date only a few works have been published that take advantage of the beneficial properties of these polymers (COP/COC) as a substrate material to integrate microelectrodes in microfluidics. Lee e*t al*. [49] were the first to fabricate and test a 5 μm band gold electrode on a COC substrate by cyclic voltammetry. Later, Zou *et al*. [50] patterned a gold nano interdigitated electrode array (nIDA) on COC for direct bio-affinity sensing using impedimetric measurements. And, more recently, Shim *et al.* [51] fabricated interdigitated array electrodes with nano gaps using optical lithography and a controlled undercut method over a COC substrate.

In the present chapter, our aim was to use the high chemical resistance of COP to polar organic solvents in two different ways: (i) to fabricate the electrodes by lithographic techniques, and (ii) to perform, for the first time to the best of our knowledge, electrochemical experiments in organic media within an entirely polymeric microfluidic cell. So far, despite the promising potential of microfluidics in organic media, e.g., the two-phase flow microfluidic systems employed in electrosynthesis [52,53], its use has been limited due to the lack of substrates/passivants resistant to organic solvents.

For that, a microfabricated COP fluidic system containing fourteen microband electrodes, each 50 μm wide and 14 μm long, is presented. A sketch of this microfluidic system is shown in Fig. 1. The microband electrodes were characterized in aqueous media and in acetonitrile using cyclic voltammetry at different flow rates. Acetonirtile has been the organic solvent chosen for the experiments as it is the most extensively used in organic electrochemistry and the one that so far has been tested the most in microfluidics [54,55]. In any case, according to the specifications provided by the Zeon Corporation [33], the reported COP cell is expected to be resistant to other solvents of interest in organic electrochemistry as well, such as dimethylformamide (DMF), dimethylsulfoxide (DMSO) and propylene carbonate.

The experimental limiting current values were compared with the state limiting currents predicted by Levich [56]. Based on the agreement between our results and theory, we strongly believe that COP will be extremely useful for organic electrosynthesis as well as electronalysis using microfluidics.

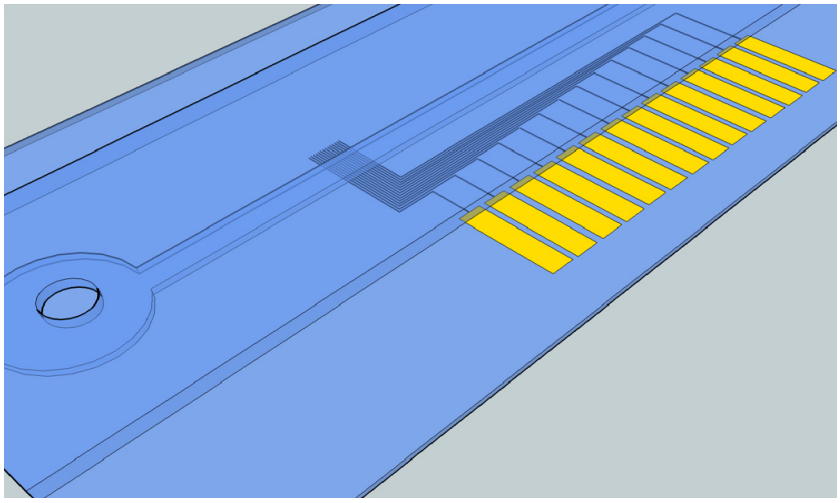

Fig. 1 Sketch of the microfluidic system containing the microchannel and the gold microband electrodes.

6.3 Experimental

6.3.1 Fabrication

In the present study, COP sheets (grade ZF 14-188) were used. They are 188 μm thick and have a glass transition temperature of T_g = 138 °C. The ZF 14–188 sheets were kindly provided by Zeon Corporation, Japan.

The microfluidic devices were fabricated through the assembly of two separated parts, an upper COP part containing the microfluidic channel and a lower part containing the microband gold electrodes patterned also on COP. slightly above its polymer glass transition temperature.

6.3.1.1 Electrode Fabrication

The lower COP part of the microfluidic system containing 14 parallel gold band microelectrodes, each with a width of 14 μm and separated from their closest neighbour by 16 μm, was produced by conventional lithographic and lift-off techniques.

First of all, the COP sheets were cut in a 4 inch wafer shape and cleaned in a piranha bath (1:3 hydrogen peroxide (45%) / sulphuric acid (96%)) for 10 min to remove any possible contamination. After rinsing the wafers in deionized water and drying them in a spin dryer, 1.5 μm of AZ5214E photoresist was spun onto the COP wafers and baked at 90 °C for 60 s on a hotplate. AZ5214E positive resist has been chosen due to its capability of image reversal, resulting in a negative pattern of the mask with a negative wall profile ideally suited for the lift-off step [57]. The image reversal process consists of three steps: (i) exposure of the wafer through the mask with UV-light, (ii) reversal bake at 120 °C for 2 min on a hotplate, and (iii) flood exposure of the entire wafer without any mask. The most critical step of the image reversal process is the reversal bake step. In our case, it was necessary to perform this step in a furnace for 25 min instead of on a hotplate for 2 min. This is mainly because of the small thickness of the COP sheet, which,

at the temperature used (18 °C below T_g), was found to bend or warp resulting in not all the zones in the COP reaching the same temperature. This, in turn, leads to problems in the negative lithography process. Finally, the COP sheets were developed on a wet bench using the recommended developer for this photoresist.

Once the lithography step was finished, a thin gold film (200 nm) was evaporated by e-beam (QCL 800, Wordentec Ltd., United Kingdom) over the developed resist pattern. Afterwards, the lift-off was performed in acetone in order to strip the underlying resist. It was at this step of the fabrication process that we took advantage of the image reversal lithography, as the negative slope of the photoresist greatly simplified the removal of the photoresist. Yields of 80-90% were easily achieved with the lithography process described above. Remaining impurities in the COP surface after the cleaning step; or small inhomogeneities of the COP surface itself, are probably the main reasons for not achieving 100% yield. In Fig. 2 a detailed view of the fabricated electrodes is shown.

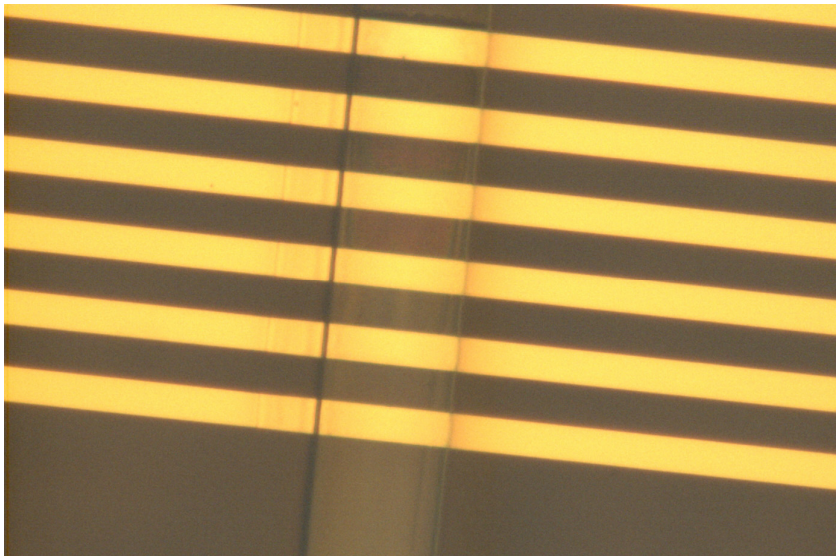

Fig. 2 Optical image of the microfluidic channel crossing the set of gold microband electrodes. The working area of the electrodes is determined by the width of the gold bands (14 μm) and the width of the channel (50 μm).

It is important to point out that no adhesion layer, such as Ti or Cr, was needed to improve the adhesion between gold and COP, as it has already been reported

by Lee et al. [49]. The gold adhesion to the COP was evaluated by using Scotch tape on several different chips. Scotch tape was applied firmly over the electrodes area at room temperature and subsequently stripped off. Inspection of the Scotch tape under an optical microscope revealed no evidence of metal in any of the cases.

The absence of a necessity for an adhesion layer, together with the fact that the length of the electrodes in our system is determined by the width of the channel (see below), eliminates the need of a passivation layer to define the electrode area and to protect the edges of the electrodes that otherwise would expose the adhesion layer to the solution. The absence of a passivation layer thus (i) simplifies the fabrication process, (ii) expands the number of chemicals that can be studied in the system, and (iii) eliminates the need for having recessed electrodes that diminish the output signal [58].

6.3.1.2 Microfluidic channel fabrication

In parallel to the electrodes fabrication, a 3 cm long, 50 μm wide and 24 μm deep channel was structured on another COP sheet via hot embossing. For this, a silicon master was fabricated using standard UV-lithography and Bosch-type deep reactive ion etching. More details regarding the master fabrication process can be found in [59]. The last step was the deposition of a 1H,1H,2H,2H-perfluorodecyltrichlorosilane layer by chemical vapour deposition (MVD 100, Applied Microstructures Inc., USA) as an antisticking coating. This facilitates the release of the COP microfluidic channel from the master during the embossing. The chips were individually cut from the wafer with a dicing saw and cleaned with isopropanol before being used as a master for hot embossing.

The master and a clean COP sheet, previously cut to the chip dimensions (8 x 2 cm), were placed in a manual laboratory bonding press with hot/cooling plates (TEMPRESS, Paul-Otto Weber GmbH, Germany). COP was embossed at 170ºC and 10 kN for 10 min. Demoulding of the system was performed at 120ºC to avoid

accumulation of material in the top of the microstructures due to the different thermal expansion coefficients of silicon and COP [60]. Finally, 1 mm holes were manually drilled at the beginning and at the end of the microchannel in the microstructured COP sheet.

6.3.1.3 Bonding

The final closed channel configuration, with the integrated electrodes was achieved by bonding together the two fabricated COP parts, the one with microchannel and the one with the microelectrode array. Prior to this step, the surfaces of both parts were carefully cleaned with isopropanol for 15 min in an ultrasonic bath. After rinsing them in deionised water and drying with a N_2 gun, the microchannel part was placed perpendicularly over the set of parallel microbands on the other COP sheet. The bonding took place at 120 °C and 8 kN for 15 min in the same hot press as used for the embossing. The bonding temperature was chosen slightly below the glass transition temperature of the COP (T_g = 138 °C) to avoid the collapse of the channel. Fig. 3 shows a SEM image of a bonded fluidic channel cross-section. There, the height of the channel has been measured and found to be slightly smaller (22 μm) than the expected value (24 μm).

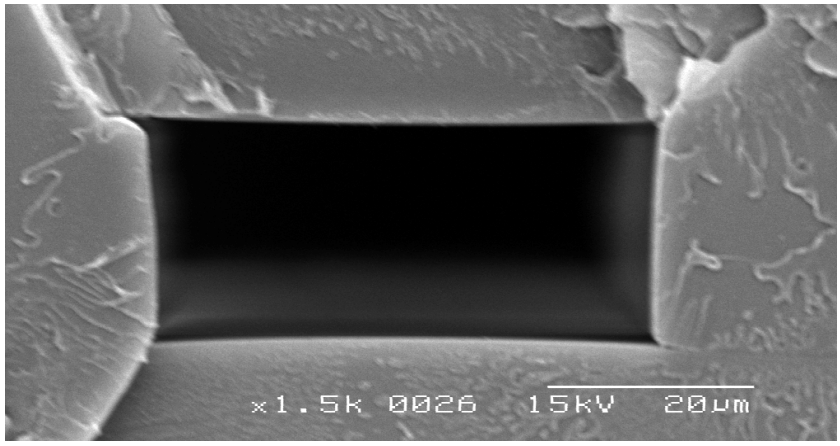

Fig. 3 SEM image of a cross-section of the bonded COP microchannel. The real dimensions of the closed channel are 50.4 μm wide and 22.0 μm height.

As it can be seen in Fig. 2, the effective width of the microband electrodes in the microchannel was defined by the microchannel width. The area of each microband electrode was, hence, 700 μm². The optical transparency of the COP allowed microscopic examinations of the state of the band electrodes during the experiments.

6.1.3.4 Holder

For an easier handling of the chip a three part holder was micro milled. As it is shown in Fig. 4, the middle part holds a commercial spring-loaded connector (8PD Series, Preci-Dip, Switzerland) used to provide contact between the electrode pads and a commercial potentiostat. For this part of the holder, PMMA was used. The transparency of the PMMA top-plate was needed because the pins of the connector need to be placed precisely over the electrode pads as they must be in contact when the screws are tightened.

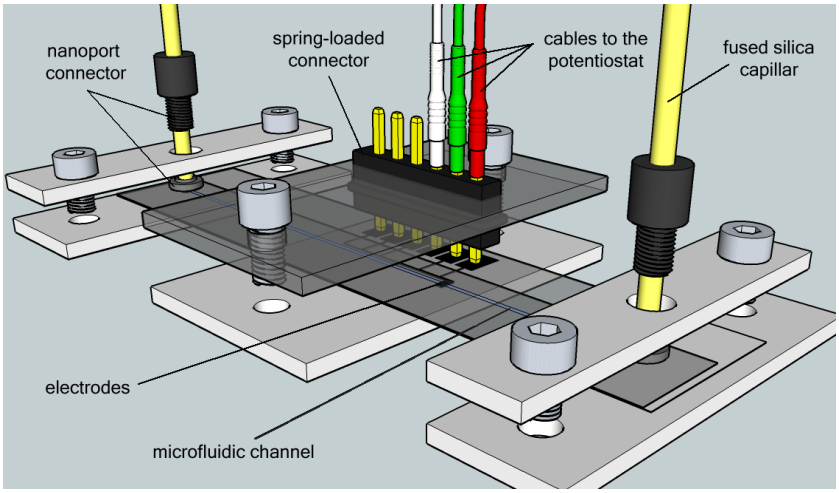

Fig. 4 Sketch of the holders used to connect the microfluidic chip.

The other two parts of the holder were used to connect fused silica capillaries with an ID of 50 μm (Polymicro, Germany) through nanoport connectors to the inlet and the outlet of the microchannel. Unlike the middle part of the holder, these parts were made of Delrin® to avoid corrosion of the holder material in case of leakage when organic solvents are infused.

6.3.2 Chemicals and instrumentation

Potassium hexacyanoferrate (II) (K_4FeCN_6), potassium hexacyanoferrate (III) (K_3FeCN_6), ferrocene ($Fe(C_5H_5)_2$), tetrabutylammonium perchlorate (TBAP), potassium nitrate (KNO_3) and acetonitrile (99.9%) were purchased from Sigma-Aldrich. All chemicals were of analytical reagent grade, and all aqueous solutions were prepared using ultrapure deionised water (DI) (18 MΩ cm at 298 K).

Cyclic-voltammetric experiments were carried out with a potentiostat (CHI1010A, CH Instruments Inc., USA) using a three electrode cell configuration with two of the microbands acting as working and counter electrodes, respectively, and the third one as a quasi-reference electrode. The counter and the reference electrodes were located downstream with respect to the working electrode to avoid interferences due to the counter electrode reactions [61].

A NE-1000 syringe pump (TSE Systems, Germany) was used to obtain a solution flow through the microfluidic channel. The volumetric fluidic flows used in this work range from 1 to 10 μL min^{-1}. To connect the inlet capillary to the Gastight syringe (Hamilton, Switzerland), a commercial luer adapter from Upchurch was employed. The outlet of the microfluidic channel was connected to a waste septum.

6.4 Results and discussion

To validate the feasibility of using gold microelectrodes deposited on COP in a microfluidic system, cyclic voltammetric measurements were first carried out in aqueous media. Fig. 5 shows cyclic voltammograms recorded at 100 mV s^{-1} for different flow rates ranging from 2 to 10 μL min^{-1} in a solution consisting of 5 mM ferrocyanide/ferricyanide in 0.5 M KNO_3. Note that each voltammogram presents a perfect sigmoidal shape and that the limiting current depends on the flow rate. This behaviour was expected considering the laminar flow conditions in the microchannel [1]. Under these conditions, the diffusion layer thickness is stable

and reproducible and steady state voltammograms are observed. Moreover, it has also been checked that the limiting current does not depend on the scan rate (in the interval from 25 to 100 mV s^{-1} [62,63]; results not shown). In all the experiments, one of the gold bands was used as a quasi-reference electrode. The potential of the quasi-reference electrode was found to be -147 ± 8 mV vs SCE and it was stable during the experiments.

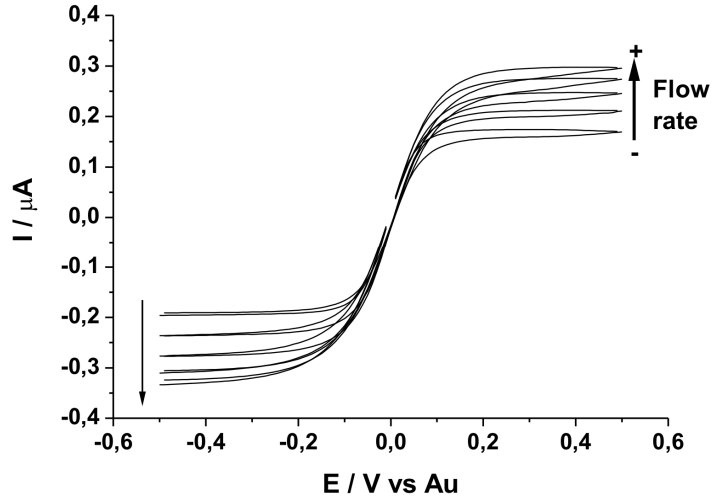

Fig. 5 Cyclic voltammograms recorded at various flow rates (2, 4, 6, 8 and 10 μL min^{-1}) in a solution of 5 mM ferrocyanide/ferricyanide in 0.5 M KNO_3. The scan rate for all the CVs was 100 mV s^{-1}. The microbands were 14 μm wide, and the interelectrode distance was 16 μm.

Taking into account that the electrodes are positioned in a region of the flow cell where the flow profile is fully developed, the current data can be interpreted according to Levich's equation [56]. For a microband electrode inside a channel with a rectangular cross-section, it can be expressed as [1]:

$$I = 0.925nFcw\left(x_e D\right)^{2/3}\left(\frac{U}{h^2 d}\right)^{1/3} \qquad (1)$$

where n is the number of exchanged electrons, F is the Faraday constant (96485 C mol^{-1}), c and D are the concentration and the diffusion coefficient of the electroactive species, respectively, d is the channel width, h is half –the height of the channel, x_e and w are the length and the width of the microband electrodes, respectively, and U is the flow rate. In the particular geometry used in this study,

a microband electrode covers the entire width of the channel and, thus, w and d take on the same value.

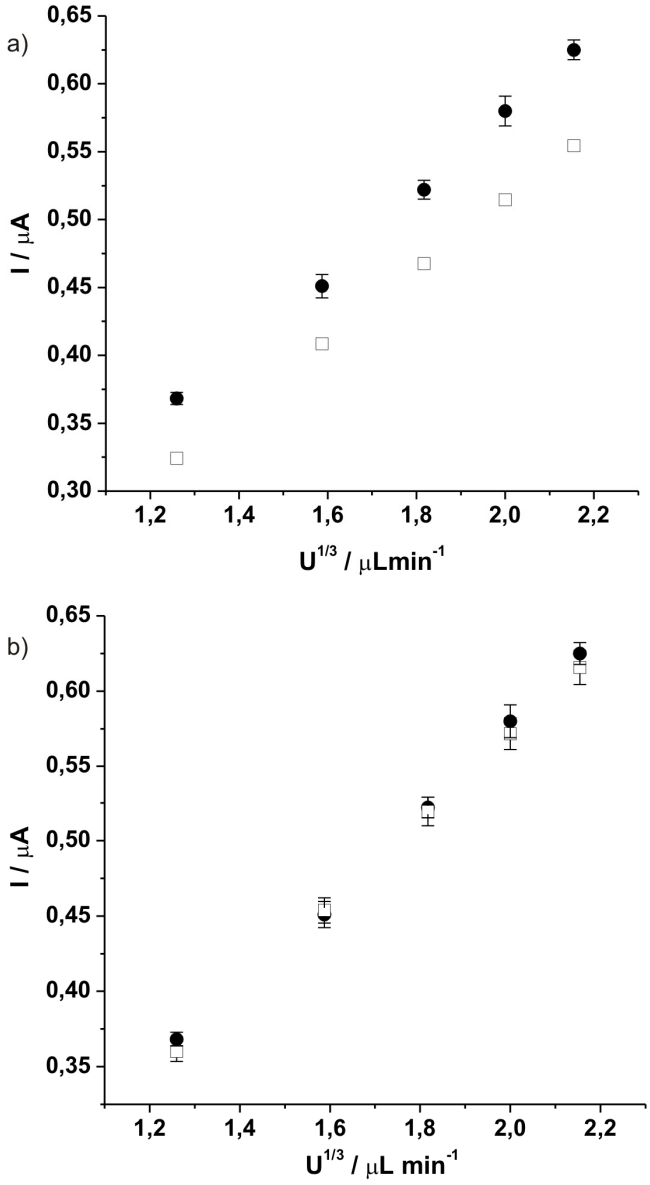

Fig. 6 The experimental limiting voltammetric currents (●) and the corresponding predicted currents according to the Levich equation (□) as a function of the cubic root of the volumetric flow rate (a) before and (b) after correction for the real channel dimensions. The theoretical channel dimensions in (a) were 50 x 24 μm while the real channel dimensions determined by SEM images in (b) were 50 x 20.5 ± 0.6 μm. The solution contained 5.0 mM ferrocyanide, 5.0 mM ferricyanide, and 0.5 M KNO3, and the experimental results were obtained using a three-electrode configuration and a scan rate of 100 mV s^{-1}.

In Fig. 6a, the expected steady state currents calculated by the Levich equation (1) are represented next to the experimental values obtained from the experiment described above plotted as a function of the cubic root of the volumetric flow rate. The values used for the diffusion coefficients of ferrocyanide and ferricyanide were in both cases $D = 6.5 \times 10^{-10}$ m^2 s^{-1} [64], the microband electrode dimensions were set to be w = 50 μm, x_e = 14 μm and the channel dimensions to d = 50 μm and $2h$ = 24 μm. The experimental data represented for each flow rate correspond to the average limiting current value from at least four consecutive cyclic voltammograms. The variations within each set of data (<1%) can be due to small fluctuations in the flow rate. Notice that the experimental limiting current values present a linear dependence with the cubic root of the flow rate, as predicted by Levich equation, but that all experimental values are around 12% higher than the theoretical values. As it has already been mentioned in the fabrication section, the dimensions of the channel can become slightly reduced during the bonding process. For this reason, we attribute these deviations in the current to an overestimation of the channel cross-section, which resulted in lower currents predicted by Levich. In order to confirm this assumption, after performing the experiments, the microchannel was cut and the cross-section explored in a SEM. The real height of the channel used for the experiments shown in Fig. 5 was found to be 20.5 $\pm$ 0.6 μm instead of the expected 24 μm. Therefore, the estimated limiting currents by Levich were recalculated with the new channel dimensions and compared with the experimental values. These new values are shown in Fig. 6b and it can be noted that, after the correction, the difference between both sets of data is below 2%. The origin of this remaining difference between the real behaviour of our system and the limiting currents predicted by Levich could be due to the fact that the axial diffusion contribution is not accounted in Levich's approximation [65]. Levich's equation describes the behaviour of a band electrode inside a macroscopic system where just axial convection and diffusion in the perpendicular direction toward the electrode are considered.

The same set of gold microband electrodes used for the experiments illustrated in Fig. 6 was used over several days without any evidence of damage or delaminating

problems. Moreover, comparing the limiting current values obtained from cyclic voltammograms carried out under the same experimental conditions at different days yielded a variation of less than 10%. Table 1 lists thes experimental limiting currents, I^{exp}, obtained for three non-consecutive days at different flow rates ranging from 2 to 10 μL min^{-1}. The solution contained 5 mM ferrocyanide in 0.5 M KNO_3 and the scan rate was 100 mV s^{-1} in all cases. Table 1 also lists the average limiting current, $I^{average}$, for the three different days and the expected limiting current by Levich's equation (1), I^{levich}. Although further studies are necessary to characterize the long-term stability of the electrodes, these results suggest a sufficient stability of the electrodes without the need of an adhesion layer between gold and the COP surface. Also, given the simple and inexpensive fabrication possibility, the chips are not really intended for long-term use, and electrodes that are stable over several days are deemed more than sufficient for most envisioned applications of the polymer devices.

Table 1 Experimental limiting currents, I^{exp}, obtained for a set of band microelectrodes (x_e = 14 μm, w = 50 μm) inside a microfluidic cell (d = 50 μm wide, 2h = 20.5 μm) containing 5mM ferrocyanide in 0.5 M KNO_3. Each data is the average of at least four consecutive voltammograms recorded at 100 mV s^{-1}. $I^{average}$ is the average of the limiting currents obtained for each flow rate for three different days and I^{levich} represents the predicted limiting currents for the system calculated by the Levich equation (1).

U / $\mu L min^{-1}$	I_1^{exp}/ μA	I_2^{exp}/ μA	I_3^{exp}/ μA	$I^{average}$/ μA	I^{levich} / μA
2	0.172 ± 0.001	0.169 ± 0.010	0.172 ± 0.002	0.171 ± 0.005	0.180 ± 0.004
4	0.220 ± 0.004	0.202 ± 0.007	0.229 ± 0.004	0.215 ± 0.010	0.227 ± 0.005
6	0.250 ± 0.008	0.245 ± 0.007	0.248 ± 0.004	0.248 ± 0.005	0.260 ± 0.005
8	0.274 ± 0.005	0.272 ± 0.004	0.270 ± 0.005	0.272 ± 0.004	0.286 ± 0.006
10	0.305 ± 0.006	0.289 ± 0.004	0.299 ± 0.006	0.296 ± 0.006	0.308 ± 0,006

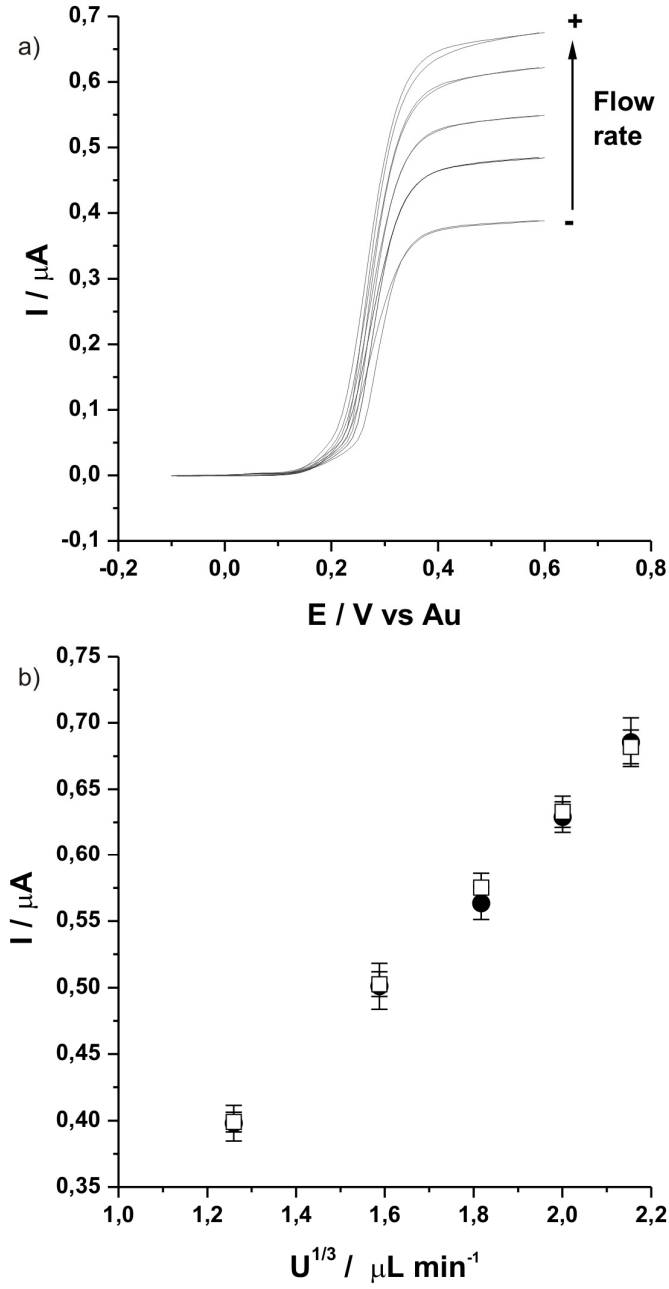

Fig. 7 (a) Cyclic voltammograms at different flow rates (2, 4, 6, 8 and 10 μL min^{-1}) recorded at 100 mV s^{-1} with a microband electrode (x_e = 14 μm, w = 50 μm) in a microchannel (d = 50 μm wide, 2h = 22 ± 1 μm) containing a solution of 5 mM ferrocene and 0.1 M TBAP/acetonitrile. (b) Analysis of the experimental voltammetric curves (●) and the predicted limiting currents according to Levich (□) as a function of the cubic root of the volumetric flow rate.

The experiments and results presented above thus prove the following points: (i) the gold microband electrodes integrated in the COP microfluidic channel work perfectly in aqueous media and their behaviour is in good agreement with Levich's predictions, proving that the bonding process does not affect the electrodes. (ii) Adhesion of the gold electrodes to the COP seems to be strong enough without the presence of any adhesion layer and, as a consequence, no kind of passivation layer was necessary. And finally, (iii) the electrodes work perfectly without any kind of electrochemical activation, probably due to the absence of any passivation layer.

In the second part of this work, we wanted to take advantage once more of the high chemical resistance of the COP, demonstrating the feasibility to use our microfluidic system in organic media. As it has been mentioned in the introduction, the use of microelectrodes and microfluidic systems in organic electrochemistry has been hampered by a lack of suitable substrates/insulators resistant to (organic) solvents. As COP has a high chemical stability against the most common solvents used in organic electrochemistry (e.g., acetonitrile, DMSO, and DMF), we suggest that COP could turn out to be a revolutionary material for organic electrochemistry. In order to prove that, cyclic voltammetric experiments of ferrocene in acetonitrile (D = 2.3 × 10^{-9} m^2 s^{-1}) [66] were performed.

Fig. 7a shows cyclic voltammograms obtained at different flow rates (2, 4, 6, 8, 10 μL min^{-1}) in a solution containing 5 mM ferrocene in 0.1 M TBAP/acetonitrile at 100 mV s^{-1}. In this case, it is also noticeable, similar to the results shown in Fig. 5, that the voltammograms have a perfect sigmoidal shape with limiting currents depending on the flow rate. The comparison between the experimental and the estimated liming currents calculated by the Levich equation (1) as a function of the cubic root of the flow rate are shown in Fig. 7b. For the latter calculations, the dimensions of the channel were set to be d = 50 μm and $2h$ = 22.0 ± 1 μm, values obtained from SEM images of the cross-section of the channel (Fig. 3). Also in this case, the experimental and the estimated values are in complete agreement for all flow rates, proving for the first time (to the best of our knowledge) the capability

to use an entirely polymeric microfluidic system with gold microband electrodes in organic media, in particularly acetonitrile. Therefore, the excellent chemical properties of COP render this material an interesting substrate to open the door for organic electroanalysis and electrosynthesis to the microfluidic world.

6.5 Conclusions

In this chapter, an entirely polymeric microfluidic platform with integrated microelectrodes for experiments concerning organic electrochemistry is presented. This has been possible due to the extraordinary chemical properties of the COP, which apart from making it suitable for organic electrosynthesis and electroanalysis, also allow the use of standard photolithographic techniques.

From the fabrication point of view, the gold electrode fabrication *via* lithography on COP is simpler and faster than with other materials because neither an adhesion layer between the gold and the COP nor a passivation layer are needed. Moreover, the thermal bonding of the COP substrate that contains the microelectrodes to the microfluidic channel doesn't seem to damage the electrodes, which, in addition, do not require any kind of electrochemical activation.

The good performance of the device presented has been shown in aqueous media and in acetonitrile. Here, experimental steady state currents obtained by cyclic voltammetry at different flow rates have been compared with the estimated values predicted by Levich's equation; in both cases (aqueous and non-aquoeus) the differences between experimental and theoretical values were lower than 5%.

Although acetonitrile was the solvent chosen to prove the good performance of our device in organic media, according to the chemical stability specifications of the COP provided by the Zeon Corporation,[33] the COP microfluidic system fabricated in this project should also be resistant to other organic solvents of

interest, such as DMF, DMSO and propylene carbonate. Moreover, it should also be possible to take advantage of the high optical transparency of the COP over a wide wavelength range (from 300 to 1200 nm) [33] and use the system for photoelectrochemistry [5].

It is for all these reasons that we strongly believe in the great potential of COP as a substrate material to integrate electrochemistry and microfluidics for organic electrosynthesis as well as electroanlysis.

6.6 References

[1] R.G. Compton, A.C. Fisher, R.G. Wellington, P.J. Dobson, P.A. Leigh, Journal of Physical Chemistry 97 (1993) 10410.

[2] M. Pumera, A. Merkoçi, S. Alegret, TrAC Trends in Analytical Chemistry 25 (2006) 219.

[3] L. Nyholm, Analyst 130 (2005) 599.

[4] J.A. Cooper, R.G. Compton, Electroanalysis 10 (1998) 141.

[5] R.G. Compton, R.A.W. Dryfe, Progress in Reaction Kinetics 20 (1995) 245.

[6] W.J. Albery, M.L. Hitchman, Ring-disc electrodes, Clarendon Press, Oxford, 1971.

[7] R.G. Compton, J.C. Eklund, S.D. Page, T.J. Mason, D.J. Walton, Journal of Applied Electrochemistry 26 (1996) 775.

[8] J. Wang, Talanta 56 (2002) 223.

[9] D.J. Harrison, A. Manz, Z. Fan, H. Luedi, H.M. Widmer, Analytical Chemistry 64 (1992) 1926.

[10] R.P. Baldwin, T.J. Roussel, M.M. Crain, V. Bathlagunda, D.J. Jackson, J. Gullapalli, J.A. Conklin, R. Pai, J.F. Naber, K.M. Walsh, R.S. Keynton, Analytical Chemistry 74 (2002) 3690.

[11] A.T. Woolley, K. Lao, A.N. Glazer, R.A. Mathies, Analytical Chemistry 70 (1998) 684.

[12] R.S. Martin, A.J. Gawron, S.M. Lunte, C.S. Henry, Analytical Chemistry 72 (2000) 3196.

[13] O. Ordeig, N. Godino, J. del Campo, F.X. Munoz, F. Nikolajeff, L. Nyholm, Analytical Chemistry 80 (2008) 3622.

[14] J.S. Rossier, M.A. Roberts, R. Ferrigno, H.H. Girault, Analytical Chemistry 71 (1999) 4294.

[15] M. Castano-Alvarez, M.T. Fernandez-Abedul, A. Costa-Garcia, Electrophoresis 26 (2005) 3160.
[16] A.J. Gawron, R.S. Martin, S.M. Lunte, Electrophoresis 22 (2001) 242.
[17] J.C. Sanders, M.C. Breadmore, P.S. Mitchell, J.P. Landers, Analyst 127 (2002) 1558.
[18] R.O. Kadara, N. Jenkinson, C.E. Banks, Electrochemistry Communications 11 (2009) 1377.
[19] D.-M. Tsai, K.-W. Lin, J.-M. Zen, H.-Y. Chen, R.-H. Hong, Electrophoresis 26 (2005) 3007.
[20] J. Wang, B. Tian, E. Sahlin, Analytical Chemistry 71 (1999) 5436.
[21] C.E. Walker, Z. Xia, Z.S. Foster, B.J. Lutz, Z.H. Fan, Electroanalysis 20 (2008) 663.
[22] N. Takano, et al., Journal of Micromechanics and Microengineering 16 (2006) 1606.
[23] Y. Kong, H. Chen, Y. Wang, S.A. Soper, Electrophoresis 27 (2006) 2940.
[24] B. Graß, A. Neyer, M. Jöhnck, D. Siepe, F. Eisenbeiß, G. Weber, R. Hergenröder, Sensors and Actuators B: Chemical 72 (2001) 249.
[25] X.-J. Huang, A.M. O'Mahony, R.G. Compton, Small 5 (2009) 776.
[26] H. Becker, C. Gärtner, Analytical and Bioanalytical Chemistry 390 (2008) 89.
[27] S.H. Cho, S.H. Kim, J.G. Lee, N.E. Lee, Microelectronic Engineering 77 (2005) 116.
[28] S. Metz, R. Holzer, P. Renaud, Lab on a Chip 1 (2001) 29.
[29] Y.-C. Lin, C.-M. Jen, M.-Y. Huang, C.-Y. Wu, X.-Z. Lin, Sensors and Actuators B: Chemical 79 (2001) 137.
[30] J. Liu, H. Qiao, C. Liu, Z. Xu, Y. Li, L. Wang, Sensors and Actuators B: Chemical 141 (2009) 646.
[31] H. Shadpour, M.L. Hupert, D. Patterson, C. Liu, M. Galloway, W. Stryjewski, J. Goettert, S.A. Soper, Analytical Chemistry 79 (2007) 870.
[32] Topas Advanced Polymers, http://www.topas.com/productstopas_coc.
[33] Zeon Chemicals, http://www.zeonex.com/default.asp.
[34] Y. Yang, J. Kameoka, T. Wachs, J.D. Henion, H.G. Craighead, Analytical Chemistry 76 (2004) 2568.
[35] T. Nielsen, D. Nilsson, F. Bundgaard, P. Shi, P. Szabo, O. Geschke, A. Kristensen, Journal of Vacuum Science & Technology B: Microelectronics and Nanometer Structures 22 (2004) 1770.
[36] L. Yi, X.D. Wang, Y. Fan, Journal of Materials Processing Technology 208 (2008) 63.
[37] X. Illa, W. De Malsche, J. Bomer, H. Gardeniers, J. Eijkel, J.R. Morante, A. Romano-Rodriguez, G. Desmet, Lab on a Chip 9 (2009) 1511.
[38] K.W. Ro, J. Liu, D.R. Knapp, Journal of Chromatography A 1111 (2006) 40.
[39] C. Das, J. Zhang, N.D. Denslow, Z.H. Fan, Lab on a Chip 7 (2007) 1806.
[40] J. Zhang, C. Das, Z.H. Fan, Microfluidics and Nanofluidics 5 (2008) 327.

[41] M. Grumann, J. Steigert, L. Riegger, I. Moser, B. Enderle, K. Riebeseel, G. Urban, R. Zengerle, J. Ducree, Biomedical Microdevices 8 (2006) 209.

[42] W. Ick Jang, K.H. Chung, H. Bong Pyo, S.H. Park, Proceedings of SPIE 6415 (2006) 641512.

[43] A. Gulliksen, L.A. Solli, K.S. Drese, O. Sorensen, F. Karlsen, H. Rogne, E. Hovig, R. Sirevag, Lab on a Chip 5 (2005) 416.

[44] A.V. Larsen, L. Poulsen, H. Birgens, M. Dufva, A. Kristensen, Lab on a Chip 8 (2008) 818.

[45] M. Castano-Alvarez, M. Fernandez-Abedul, A. Costa-Garcia, Electrophoresis 28 (2007) 4679.

[46] M. Hansen, D. Nilsson, D.M. Johansen, S. Balslev, A. Kristensen, in Advancements in Polymer Optics Design, Fabrication and Materials, SPIE Symposium on Optics & Photonics, San Diego, USA, 2005.

[47] J. Kameoka, H.G. Craighead, H. Zhang, J. Henion, Analytical Chemistry 73 (2001) 1935.

[48] H. Shinohara, T. Suzuki, F. Kitagawa, J. Mizuno, K. Otsuka, S. Shoji, Sensors and Actuators B: Chemical 132 (2008) 368.

[49] D.S. Lee, H. Yang, K.H. Chung, H.B. Pyo, Analytical Chemistry 77 (2005) 5414.

[50] Z. Zou, J. Kai, M.J. Rust, J. Han, C.H. Ahn, Sensors and Actuators A: Physical 136 (2007) 518.

[51] J.S. Shim, M.J. Rust, C.H. Ahn, in 2008 8th IEEE Conference on Nanotechnology, IEEE-NANO, 2008, p. 851.

[52] S.M. MacDonald, J.D. Watkins, S.D. Bull, I.R. Davies, Y. Gu, K. Yunus, A.C. Fisher, P.C.B. Page, Y. Chan, C. Elliott, F. Marken, Journal of Physical Organic Chemistry 22 (2009) 52.

[53] S.M. MacDonald, J.D. Watkins, Y. Gu, K. Yunus, A.C. Fisher, G. Shul, M. Opallo, F. Marken, Electrochemistry Communications 9 (2007) 2105.

[54] J.A. Alden, M.A. Feldman, E. Hill, F. Prieto, M. Oyama, B.A. Coles, R.G. Compton, P.J. Dobson, P.A. Leigh, Analytical Chemistry 70 (1998) 1707.

[55] F. Prieto, J.A. Alden, M. Feldman, B.A. Coles, R.G. Compton, M. Oyama, S. Okazaki, Electroanalysis 11 (1999) 541.

[56] V.G. Levich, Physicochemical Hydrodynamics, Prentice Hall, Englewood Cliffs, N. J., 1962.

[57] AZ5214E, http://www.first.ethz.ch/infrastructure/Chemicals/Photolithography/Data_AZ5214E.pdf.

[58] P.N. Bartlett, S.L. Taylor, Journal of Electroanalytical Chemistry 453 (1998) 49.

[59] O. Gustafsson, K.B. Mogensen, J.P. Kutter, Electrophoresis 29 (2008) 3145.

[60] M.B. Esch, S. Kapur, G. Irizarry, V. Genova, Lab on a Chip 3 (2003) 121.

[61] J. Wang, Analytical Electrochemistry, Wiley-VCH, New York, 2001.

[62] R.G. Compton, P.R. Unwin, Journal of Electroanalytical Chemistry 206 (1986) 57.
[63] A.C. Fisher, R.G. Compton, Journal of Applied Electrochemistry 22 (1992) 38.
[64] A.J. Bard, L.R. Faulkner, Electrochemical methods: Fundamentals and Applications, Wiley, Chichester, 2001.
[65] J.A. Alden, R.G. Compton, Journal of Electroanalytical Chemistry 404 (1996) 27.
[66] M. Sharp, Electrochimica Acta 28 (1983) 301.

CHAPTER 7

Conclusions & Future perspectives

7.1 Conclusions

In this PhD dissertation, the design, fabrication and successful analysis of a reversed-phase liquid chromatography column containing an array of ordered pillars entirely made on unmodified cyclo olefin polymer (COP) has been presented. This is the first time that such analytical system is fabricated in this material. The efficiency and separation power of this column have been investigated, showing very good results that pave the way to further development of low-cost batch-fabricated liquid chromatography columns and analytical devices fabricated on this material. Particular conclusions are listed in the following:

1) The fabrication process of the COP pillar array liquid chromatographic separation column has been developed and optimized, starting from the material in the form of sheets. The process involves the design and fabrication of a silicon master *via* Deep Reactive Ion Etching, embossing of the column in a COP sheet and subsequent pressure-assisted thermal bonding to a blank COP lid.

2) The chromatographic properties of the fabricated columns have been analyzed in a home-made injection setup. Fluorescence detection of coumarins using a CCD camera coupled to an inverted microscope has been employed to study both the efficiency and the separation power of the column.

3) The efficiency of the column has been evaluated by analyzing the band broadening effect. For that, van Deemter plots containing the plate heights at different velocities under different retention conditions have been deduced for different pillar height columns. Better column efficiencies have been obtained for the COP column in comparison to silicon pillar array columns and the best packed-bed columns, as it is shown in Fig. 1. The influence of the pillar height in the band broadening effect has analyzed, being observed and understood that better results are for the shallower columns. For that, one could expect to achieve better efficiencies in the silicon case if shallower channels were fabricated.

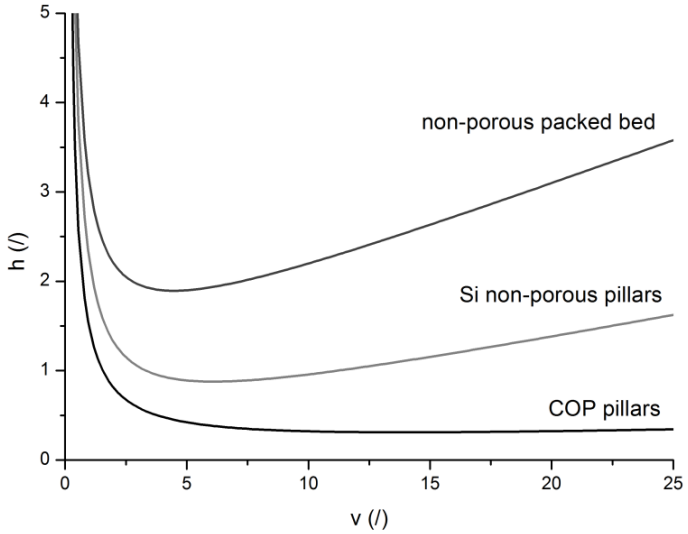

Fig. 1 Comparison between the COP pillar array column under retentive conditions (k = 1.2) extracted from chapter 4, non-porous silicon pillar array columns (k = 1.2) [1] and a very good packed bed of non-porous particles in reduced coordinates. The external porosities are in all cases of the order of 0.4

4) Retention factors up to k = 2.5 have been obtained for the shallowest COP fabricated column under the most retentive conditions, a larger value than the one obtained for the non-porous silicon pillar array column. Moreover, the relation between the retention factor and both the surface-to-volume ratio and the ratio of organic modifier have been monitored and verified with the theoretical predictions.

5) The use of unmodified COP sheets to perform the separation experiments is an excellent result as no modification of the surface is needed. This is in opposition to the silicon case where a hydrophobic layer is coated over the pillar surface. In our case, the high hydrophobic nature of the COP surface is enough to achieve even better retention factors than in the silicon case. Thus, in addition, simplifies even more the fabrication process of such columns.

6) The integration of metallic microbands in the COP has been successfully addressed. The fabrication of gold electrodes on COP by using standard photolithography, electron-beam assisted deposition and lift-off processes without the need of an adhesion layer has been developed and optimized.

7) With the aim of removing the complex optical detection system and substitute it, when possible, by an electrochemical detection system, the fabricated microelectrodes have been integrated in a microfluidic channel and successfully tested under aqueous and organic conditions for the first time to the best of our knowledge. This represents a large step in the direction of fabricating an entirely polymeric lab-on-a-chip system for on-chip LC.

Concerning the pillar array column fabricated in COP, and despite the excellent results achieved, there are some issues that need to be further studied. Firstly, in the fabrication process, the demoulding of the embossed COP has observed to be a critical step; it is an entire manual process with the used equipment, which can affect the possibility of mass-production. However, this can be overcome if an automated equipment can be used. And secondly, albeit the bonding of the columns is good enough to perform pressure-driven separations, extreme care has to be taken when manipulating the chip in order to avoid damage. In addition, applying too high pressures, that may be required to remove air bubbles from the channel or simply, when using columns with smaller structures or longer channels, might result in the detachment of the bonded parts, destroying the chip. For that, other bonding methodologies should be studied to overcome this minor drawback.

Furthermore, and as it has been analyzed in chapter 5, retention factors using the COP pillar array column are smaller than the case of porous silicon pillar arrays. For that, this novel column format presented in this PhD dissertation is not intended to be compared with any porous columns, be it the pillar array format or the porous particle packed bed. Despite that almost all the applications where HPLC is used a high retention power is required, there are a few applications like protein and nucleic-acid separation where non-porous columns play a major role [2,3]. For the separation of these large molecules the inherently small diffusion coefficient has a dramatic impact on dispersion. When the pore size is of the same order as an analyte, the internal surface can become inaccessible or, when accessible, give rise to a small intra-particle diffusion coefficient and hence, a dramatic increase of the C-term. It is in this direction where it is believed that this here presented technology must be evaluated for real-world applications.

7.2 Future work

Many directions can be followed in order to continue the work described in this PhD dissertation. As it has been just mentioned, the integration of the fabricated COP pillar array column with the microelectrodes described in the chapter 6 it is an obvious step to take, and first results in this direction are presented below. In addition to the portability that can be achieved when using electrochemical detection, its combination with the fluorescence detection will expand the number of possible applications of the chip.

Revisiting the comparison between the reduced plate heights shown in Fig. 1, it can be stated that if the absolute plate heights are taken into account, the COP pillars present larger plate heights than the non-porous silicon pillars due to the different pillar diameter used, as we have fabricated pillars three times bigger than the ones reported by De Malsche *et al.* [1]. Then, large improvements in the performance of the COP columns can be obtained by decreasing the pillar diameter and by reducing the pillar depth even more. The former issue is discussed in the following section, while

the latter, despite the fact that it would reduce both the top and bottom plate contribution to the band broadening effect and the problems related to the pillar non-uniformities, seems difficult to achieve as we are near to the fabrication limit when using pressure-assisted thermal bonding. Another possible strategy to improve both the efficiency and the mass transfer is by increasing the length of the separation column by connecting several channel tracks using low dispersion turns and inlet/outlet distributors.

7.2.1. Integration of gold microelectrodes in the pillar array column for electrochemical detection

Nowadays, fluorescence continues to be the most popular detection method for μTAS due to its high sensitivity and ease of application, while electrochemical detection, although being ideally suited for the microchip format, has encountered many drawbacks. The fact that most of the μTAS devices have been focused to electro-driven separations, decoupling of the separation voltage from the electrochemical detector has been a major issue [4]. In pressure-driven on-chip LC, although there are no problems with electrical signal coupling, electrochemical detection is hence still a topic to explore. Only a couple of studies in this direction have been presented [5,6]. Electrochemical detection is very well-suited for the microchip format for mainly two reasons; firstly, it is independent of the path length, therefore the microelectrodes can be miniaturized without loss of sensitivity. And secondly, the microelectrodes can be fabricated onto the chip, leading to a fully integrated system which can simplify the detection setup, as a complex and expensive optical device could be replaced (or complemented) by a simple electronic detection.

Both fabrications, the pillar array column and the gold microelectrodes, have been described in Chapter 3 and 6, respectively. The integration of both parts, as it is shown in Fig. 2, has been done using the same conditions that were developed for the bonding of the pillar array column described in Chapter 3. In particular, a 8.0 μm deep COP column was bonded to a COP sheet containing the electrodes in a NanoImprint Lithography apparatus at 123 ◦C and 40 bar for 600 s. A detail of the

end of the column where the pillars and the microelectrodes can be observed is shown in Fig. 3.

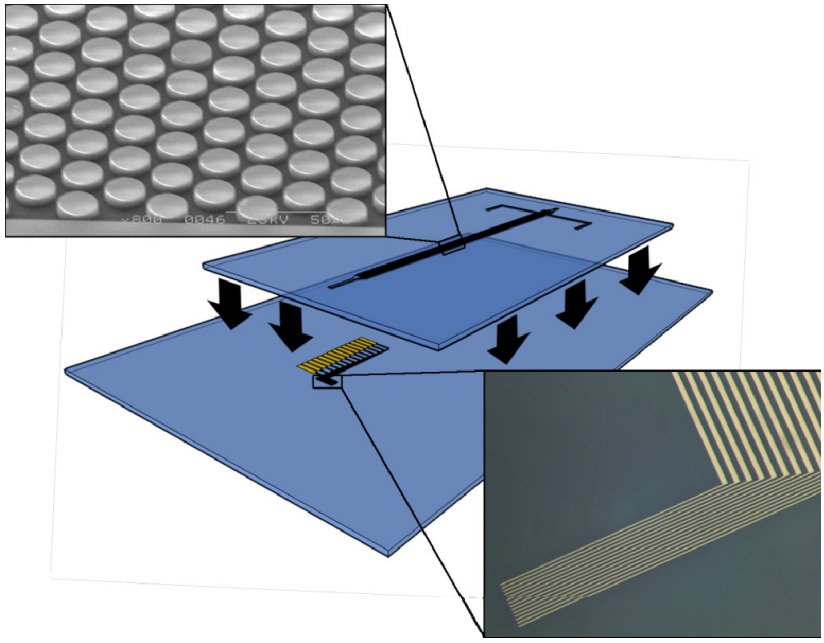

Fig. 2 Sketch of the different layers comprising the COP chip. Above, the sheet containing the pillar array column with a detailed SEM image of the pillars (top). Below, the sheet containing the deposited microband gold electrodes with an optical microscope image of the microelectrodes (bottom).

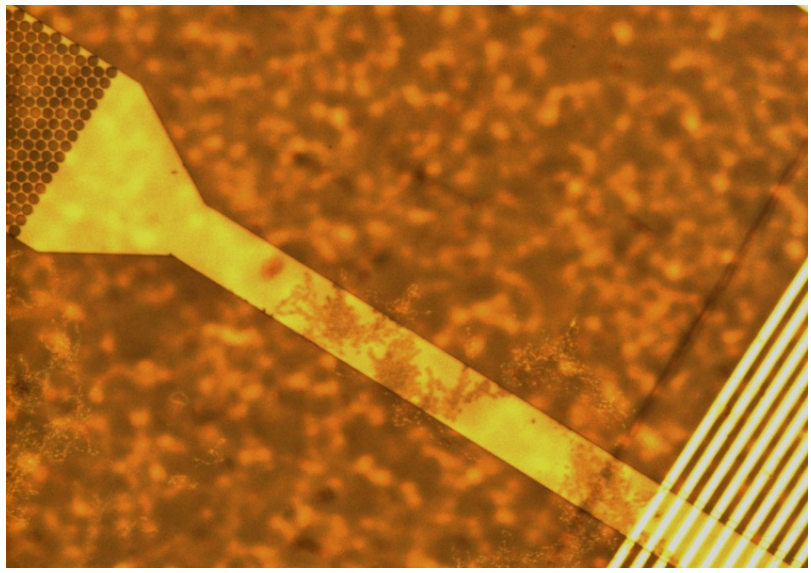

Fig. 3 Optical microscope image of the bonded chip showing the end of the pillar array

To perform a preliminary study of the potential of the microfabricated device, and to explore its possible application in the proteomics world, simultaneous fluorescence and impedance measurements of proteins have been performed. Proteins can be a good indicator to assess the performance of the microchip as they can be easy labelled with a fluorescent marker and are electroactive. Moreover, reversed-phase liquid chromatography has been shown to be the favoured mode for the separation of proteins due to its excellent resolving power and versatility [7]. In particular, avidin (labelled by means of Alexa Fluor® 488 conjugate) was dissolved in a phosphate buffered saline solution (PBS) in a concentration of 0.2 mg/ml and injected into the fabricated microchannel. Fluorescence measurements were obtained with the same setup described in the previous chapters while impedance measurements were obtained by connecting two gold band electrodes from the electrode array to an impedance analyzer and monitoring the resistance of the system using an RC parallel mode. The results of a detected protein plug have been compared, showing perfect agreement as there is no substantial difference in the peak width, as it is shown in Fig. 4.

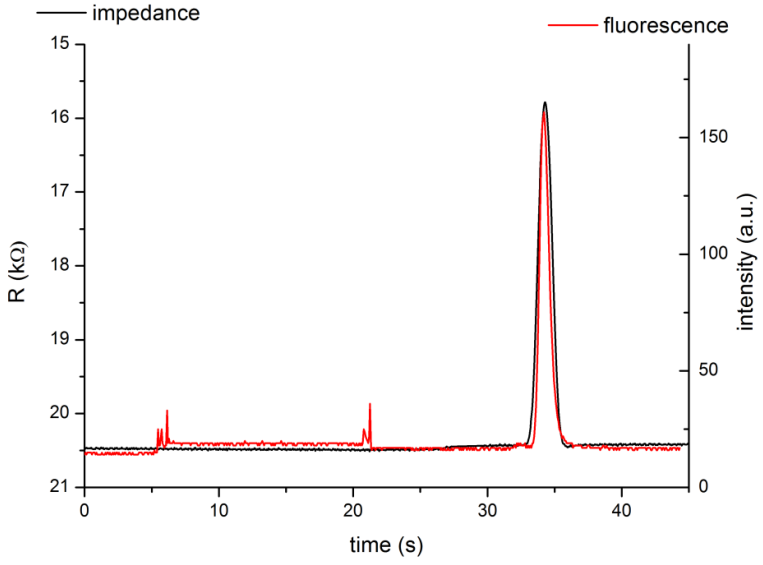

Fig. 4 Impedance (black) and fluorescence (red) response of an injected avidin plug detected by an impedance analyzer and a CCD camera, respectively.

Reversed-phase LC separation experiments is the next step to follow, but although it has already been demonstrated that is possible to separate proteins in a microchip under isocratic conditions [8], the partition range available for efficient protein separation is very narrow so, gradient elution conditions are required unless the conditions for an isocratic elution separation are completely optimized [9]. Then, since the expertise of our group in the proteomics field is very limited and the equipment to perform a gradient elution is not available in our lab, we are establishing a collaboration with the Department of Chemical Engineering of the Vrije Universiteit Brussel to couple the columns with a commercial capillary flow HPLC instrument.

7.2.2. Geometry improvements

As it has been discussed before, a way to improve the mass transfer and the efficiency of the fabricated column an easy strategy would be to decrease the pillar diameter size. With this, all the dimensions would have to be recalculated according to the Vervoort *et al.* [10] in order to diminish the band broadening contribution arising from the sidewall region. For that, distances smaller than 2 μm should be patterned, leading to the use of deep-UV lithography, which would increase the fabrication cost.

Another interesting strategy to increase the number of theoretical plates is by using longer columns. For that, and due to the geometric restrictions of the chip area, the introduction of turns may be desirable. However, the turns in the separation column generally cause tremendous skewing of the flat solute bands because of the locally non-uniform fluid velocity and, thus, deteriorate the separation performance. Strategies to fabricate low-dispersion turns in pillar array columns have been already reported [11]. In our case, we have designed different parallel columns that are connected by narrow channels to avoid extra band broadening contributions. Then, optimized flow distributors [12] have been placed at the entrance and exit of each column. The first results of the fabrication of these columns are show in Fig. 5. It can be observed that the embossing of the diamonds that form the distributor is not as

good as desired, as the edges of the structures seem to be too thin to be successfully replicated. In addition, the pressure applied during the bonding process damages these structures even more, so, more experiments in order to optimize the process are required.

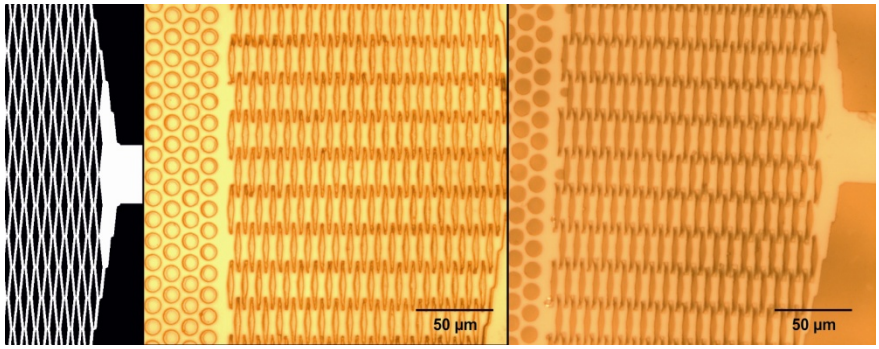

Fig. 5 Sketch of the design (left) and optical microscope images of the embossed (middle) and bonded (right) column containing a flow distributor.

7.3 References

[1] W. De Malsche, H. Eghbali, D. Clicq, J. Vangelooven, H. Gardeniers, G. Desmet, Analytical Chemistry 79 (2007) 5915.

[2] G. Jilge, K.K. Unger, U. Esser, H.J. Schafer, G. Rathgeber, W. Muller, Journal of Chromatography 476 (1989) 37.

[3] P.J. Oefner, C.G. Huber, Journal of Chromatography B 782 (2002) 27.

[4] J.P. Kutter, Y. Fintschenko, Separation Methods In Microanalytical Systems, CRC Press, Boca Raton, 2006.

[5] A. Ishida, M. Natsume, T. Kamidate, Journal of Chromatography A 1213 (2008) 209.

[6] J.-H. Seo, P.L. Leow, S.-H. Cho, H.-W. Lim, J.-Y. Kim, B.A. Patel, J.-G. Park, D. O'Hare, Lab on a Chip 9 (2009) 2238.

[7] M.-I. Aguilar, HPLC of Peptides and Proteins. Methods and Protocols, Humana Press Inc., Totowa, 2004.

[8] D.S. Reichmuth, T.J. Shepodd, B.J. Kirby, Analytical Chemistry 77 (2005) 2997.

[9] C.T. Mant, R.S. Hodges, High-Performance Liquid Chromatography of Peptides and Proteins: Separation, Analysis and Conformation, CRC Press, Boca Raton, 1991.

[10] N. Vervoort, J. Billen, P. Gzil, G.V. Baron, G. Desmet, Analytical Chemistry 76 (2004) 4501.

[11] C. Aoyama, A. Saeki, M. Noguchi, Y. Shirasaki, S. Shoji, T. Funatsu, J. Mizuno, M. Tsunoda, Analytical Chemistry 82 (2010) 1420.

[12] J. Vangelooven, W. De Malsche, J. Op De Beeck, H. Eghbali, H. Gardeniers, G. Desmet, Lab on a Chip 10 (2010) 349.

RESUM EN CATALÀ

Introducció

Durant els últims anys i gràcies a l'evolució que han experimentat les tècniques de microfabricació emprades en la indústria microelectrònica, s'ha generat un creixent interès per a la miniaturització dels sistemes analítics que es poden trobar en un laboratori, per tal d'integrar totes les seves funcions en un sol microxip. Aquests dispositius són coneguts com a *lab-on-a-chip*, és a dir, laboratori en un xip, o més concretament, quan ens referim a sistemes analítics hom parla de *μ-TAS* (acrònim de la traducció anglesa de MicroSistemes d'Anàlisi Total). En aquest àmbit, les tècniques de separació han estat una de les disciplines més actives, contribuint al desenvolupament d'aquests microsistemes d'una manera molt important. Entre les diferents tècniques de separació, la cromatografia de líquids (LC) és possiblement la més estesa, ja que s'usa en una gran varietat d'àmbits, tals com el control mediambiental, la recerca farmacèutica, la diagnosi clínica, l'anàlisi químic i/o biològic, els controls de qualitat en la indústria alimentària, etc.

Aquesta tesi està inspirada en el treball previ endegat pel grup de recerca d'en Fred Regnier i que posteriorment ha prosseguit el grup encapçalat per en Gert Desmet de la *Vrije Universiteit Brussel*. El grup d'en Regnier va tenir la idea revolucionària de substituir les tradicionals columnes cromatogràfiques amb rebliment polimèric o particulat per un nou concepte basat en la fabricació d'estructures de suport col·locades monolíticament dins la mateixa columna cromatogràfica. Amb aquesta idea l'homogeneïtat de l'empaquetament per al suport de la fase estacionària pot ésser perfectament controlat, fet íntimament relacionat amb la millora de l'eficiència d'un sistema cromatogràfic i possible d'ésser realitzat gràcies a les tècniques de microfabricació desenvolupades fins al moment. Seguint aquesta idea, el grup d'en Gert Desmet ha presentat estudis teòrics que demostren i quantifiquen els avantatges i les limitacions d'aquest nou suport cromatogràfic. A més a més, en un dels seus

treballs experimentals s'han presentat les primeres separacions cromatogràfiques en un xip de silici que integra una columna amb una xarxa de pilars ordenats.

Aquesta tesi doctoral pren com a punt de partida les idees d'aquests treballs previs per a la possible fabricació i desenvolupament d'aquest nou format de columna cromatogràfica amb un material termoplàstic, concretament polímer de cicloolefina (de l'anglès, COP). El treball realitzat s'ha estructurat per a l'assoliment dels següents objectius:

1) Implementar els protocols adequats per a (i) l'òptima reproducció de microestructures en COP mitjançant tècniques de replicació i (ii) l'òptima soldadura entre dues làmines de COP.

2) Avaluar la viabilitat de la columna fabricada en COP que conté una matriu de pilars ordenats per a l'obtenció de separacions mitjançant cromatografia de líquids en fase invertida.

3) Desenvolupar i optimitzar el mètode per a la fabricació de microelèctrodes d'or sobre el COP. Integrar-los en un dispositiu microfluídic i caracteritzar-ne la seva resposta en medi aquós i orgànic.

4) Explorar la possibilitat d'utilitzar els microelèctrodes d'or fabricats en COP com a unitat de detecció per a la columna cromatogràfica fabricada també en COP i que conté la matriu de pilars ordenats.

Aquesta tesi inclou un capítol inicial en què es fa un repàs de les diferents tècniques de fabricació que s'han emprat en el transcurs de la mateixa. En aquest capítol inicial també es fa una petita introducció a la cromatografia de líquids, presentant-ne els diferents modes d'operació i explicant-ne els principis teòrics més bàsics. Finalment es presenta un extens resum de la situació actual del procés d'integració en xips dels diferents tipus de columna existents, fent especial èmfasi en els sistemes fabricats amb material termoplàstic.

A continuació es mostra el resum dels capítols en què es descriu el treball realitzat durant el transcurs d'aquest últims anys i que ha donat lloc a aquesta tesi.

Una matriu ordenada de pilars per a cromatografia de líquids fabricada directament en polímer de cicloolefina

La fabricació d'un xip de COP amb una columna cromatogràfica que conté una matriu ordenada de pilars s'ha realitzat mitjançant un equip de litografia per estampació en calent (HEL). Per això s'han fet servir els motlles fabricats prèviament en silici mitjançant tècniques estàndard de fotolitografia i un sistema de gravat iònic reactiu profund (DRIE). Finalment el xip de COP s'ha soldat a través d'una termosoldadura assistida per pressió realitzada en un equip de nanolitografia per impressió (NIL). La columna cromatogràfica té 5 cm de llargada i 318 μm d'amplada; el diàmetre dels pilars fabricats és de 15,3 μm i la distància entre pilars 4,1 μm, cosa que dóna lloc a una porositat externa de 0,43.

Per tal injectar diferents tipus de cumarines i detectar-ne la seva fluorescència, s'ha fet servir un sistema d'injecció dissenyat per parts i un sistema de detecció òptica, respectivament. A partir d'aquestes cumarines s'han realitzat els primers estudis sobre l'eficiència de la columna, analitzant l'eixamplament de les seves bandes. En condicions no retentives s'han assolit valors per a l'altura de plat semblants als resultats anteriorment publicats per a columnes amb matrius de pilars fabricades en silici. A més a més, en condicions retentives també s'han assolit valors sorprenentment baixos tenint en compte el diàmetre relativament gran del pilars fabricats. Aquests bons resultats confirmen la qualitat de la columna fabricada en COP. Finalment, també s'ha dut a terme la separació d'una barreja de 4 cumarines diferents, fet que mostra les propietats retentives de la columna fabricada. Amb això i tenint en compte el fet que no ha estat necessària la funcionalització de la superfície de la columna (cosa que sí és necessària en les columnes fabricades en silici) s'han presentat les possibilitats d'aquest nou format de columna cromatogràfica.

Estudi experimental de l'efecte d'eixamplament de les bandes

Fent servir els processos descrits en el capítol anterior s'han fabricat xips de COP que contenen columnes amb matrius de pilars de tres altures diferents per tal de fer un estudi acurat de l'eficiència d'aquest nou format de columna. Amb aquesta voluntat, s'ha estudiat l'efecte de l'eixamplament de les bandes en condicions no retentives en les diferents columnes fabricades. Concretament, s'ha analitzat la contribució extra a aquest efecte provocada per les cobertes inferior i superior dels canals i per l'altura dels pilars. Per això, s'ha mesurat l'altura dels plats, h (variable indicadora del grau d'eixamplament de les bandes) en funció de la velocitat de la fase mòbil, v, per a les diferents columnes.

Els resultats obtinguts s'han comparat amb els valors simulats obtinguts pel cas bidimensional en què l'altura dels pilars, així com les cobertes del canal són negligibles. Els tres termes de l'equació que relaciona aquestes dues variables es poden tractar independentment, ja que depenen de fenòmens diferents tals com l'homogeneïtat del sistema, la difusió longitudinal i la resistència a la transferència de massa de la fase mòbil. Així doncs, els valors obtinguts experimentalment per a cada terme s'han analitzat i comparat amb els valors resultants de les simulacions. Les diferències existents poden explicar-se tenint en compte el mètode de fabricació i gràcies a l'aproximació feta en què es tracta l'espai entre els pilars com un canal capil·lar, podent així validar teòricament els resultats obtinguts. Finalment, també s'ha demostrat que en aquest tipus de columnes, les millors eficiències s'aconsegueixen amb els pilars més baixos.

Estudi experimental de les propietats retentives en fase invertida

Fent ús dels mateixos xips fabricats per a l'estudi descrit en el capítol anterior, s'ha fet una anàlisi exhaustiva de les propietats retentives de la columna fabricada en COP. Per fer-ho, s'ha validat la relació lineal definida teòricament entre el coeficient de retenció i la superfície de la fase estacionària (en el cas de no ser una superfície

porosa, com és el cas del COP). A més a més, també s'ha analitzat la relació entre el mateix coeficient de retenció i la proporció d'agent orgànic usat en la fase mòbil, típica de les separacions cromatogràfiques realitzades en fase invertida.

Per acabar, s'ha mostrat un exemple del comportament de l'efecte d'eixamplament de les bandes en condicions retentives on els valors que s'assoleixen són molt baixos en comparació amb el cas dels pilars fabricats en silici. Això, sumat als excel·lents valors obtinguts per a la retenció en la columna fabricada en COP, en comparació, també, al cas de la columna amb pilars no porosos fabricada en silici, fan que aquest nou format de columna pugui ser especialment útil per a aplicacions com la separació de proteïnes, on les columnes no poroses són les més emprades.

Microelèctrodes d'or integrats en un xip microfluídic fabricat en polímer de cicloolefina

La implementació i resposta de microelèctrodes sobre el COP per tal de poder efectuar detecció electroquímica en una cel·la microfluídica ha estat desenvolupada i comprovada, respectivament, en aquest capítol. La fabricació de microbandes d'or sobre el COP s'ha realitzat mitjançant tècniques de litografia estàndards fent ús de la resistència del COP als agents químics usats durant tot el procés. A més a més, els microelèctrodes d'or s'han dipositat sense la necessitat d'una capa adhesiva, evitant la necessitat d'haver de passivar-los, fet que facilita enormement el procés de fabricació.

Per validar el comportament dels microelèctrodes, aquests han estat integrats satisfactòriament en un xip microfluídic. S'ha fabricat un microcanal en una làmina de COP a través de litografia per estampació en calent i soldat a una làmina de COP on s'han fabricat els microelèctrodes gràcies a una termosoldadura assistida per pressió. S'ha caracteritzat la resposta elèctrica dels microelèctrodes, primer en medi aquós i després en medi orgànic, tot comparant els corrents límits mesurats en els experiments de voltametria cíclica realitzats durant el pas de diferents solucions per la cel·la microfluídica. En ambdós casos els resultats han estat comparats amb els

valors predits teòricament tenint en compte la geometria del sistema, donant lloc a una discrepància inferior al 5 %. Val a dir que els resultats assolits en medi orgànic són especialment interessants, atès que per primer cop i gràcies a l'estabilitat química que presenta el COP vers diversos agents orgànics, s'han pogut realitzar experiments electroquímics en medi orgànic dins una cel·la microfluídica fabricada completament amb un material polimèric.

Conclusions

Les conclusions finals d'aquesta tesi doctoral es poden resumir en els següents punts:

1) El procés de fabricació en COP d'un xip amb una columna cromatogràfica que conté una matriu de pilars ha estat desenvolupat i optimitzat.

2) S'ha desenvolupat un sistema d'injecció i detecció òptica per fluorescència per a poder estudiar les propietats cromatogràfiques de les columnes fabricades fent ús de diferents tipus de cumarines.

3) L'eficiència de la columna s'ha avaluat a través de l'anàlisi de l'efecte d'eixamplament de les bandes, assolint millors resultats que en el cas de columnes reblertes o amb pilars fabricades amb silici. A més a més, s'ha analitzat la influència de l'altura dels pilars en l'eficiència de la columna, explicant-se el perquè dels millors resultats per als pilars més baixos.

4) El poder de retenció de les columnes fabricades en COP ha demostrat ser més alt que en el cas de la columna amb pilars fabricada amb silici no porós. Així mateix, s'han analitzat i validat les relacions teòriques típiques de les separacions cromatogràfiques en fase invertida.

5) S'ha demostrat que la superfície del COP és prou hidrofòbica per actuar directament com a fase estacionària sense necessitat d'ésser funcionalitzada (fet que no passa en el cas del silici), simplificant encara més el procés de fabricació.

6) S'ha demostrat la possibilitat d'integrar microelèctrodes sobre el COP a través de la fabricació de microbandes d'or mitjançant tècniques de litografia estàndard i sense la necessitat de dipositar una capa adhesiva.

7) Amb l'objectiu de substituir el sistema de detecció òptica, que és força complex, per un sistema més simple de detecció electroquímica, s'han integrat els microelèctrodes dins una cel·la microfluídica fabricada en COP. La seva resposta elèctrica ha estat validada primer en medi aquós i després, i per primer cop, en medi orgànic.

Com a treball futur en aquesta tesi es proposa la integració dels microelèctrodes fabricats sobre el COP a la sortida de la columna que conté la matriu de pilars, també fabricada en COP. En aquesta direcció es presenten les primeres mesures sobre la detecció de proteïnes, una de les aplicacions proposades per al tipus de columna fabricat. Finalment, també es proposen diferents estratègies basades en canvis en la geometria de la columna per tal de millorar-ne el seu comportament.

PUBLICATIONS

Selected publications in indexed journals

1. X. Illa, W. De Malsche, J. Bomer, H. Gardeniers, J. Eijkel, J.R. Morante, A. Romano-Rodríguez, G. Desmet, *"An array of ordered pillars with retentive properties for pressure-driven liquid chromatography fabricated directly from an unmodified cyclo olefin polymer"*, Lab on a Chip **9** (2009) 1511-1519. ***Hot & cover article*** *(Fig. 1).*

2. X. Illa, O. Ordeig, D. Snakenborg, A. Romano-Rodríguez, R.G. Compton, J. Kutter, *"A cyclo olefin polymer microfluidic chip with integrated gold microelectrodes for aqueous and non-aqueous electrochemistry"*, Lab on a Chip **10** (2010) 1254-1261.

3. X. Illa, W. De Malsche, H. Gardeniers, G. Desmet, A. Romano-Rodríguez, *"Experimental study of the depth influence on the band broadening effect in a cyclo olefin polymer column containing an array of ordered pillars"*, Journal of Chromatography A, accepted for publication, DOI: 10.1016/j.chroma.2010.07.057.

4. X. Illa, W. De Malsche, H. Gardeniers, G. Desmet, A. Romano-Rodríguez, *"Experimental study of the retention properties of a cyclo olefin polymer pillar array column in reversed phase mode"*, Journal of Separation Science, under review.

Other publications in indexed journals

1. C. Zamani, X. Illa, S. Abdollahzadeh-Ghom, J.R. Morante, A. Romano-Rodríguez, *"Mesoporous Silica: A Suitable Adsorbent for Amines"*, Nanoscale Research Letters **4** (2009) 1303-1308.

2. R. Triantafyllopoulou, X. Illa, O. Casals, S. Chatzandroulis, C. Tsamis, A. Romano-Rodriguez, J.R. Morante, *"Nanostructured oxides on porous silicon microhotplates for NH_3 sensing"*, Microelectronic Engineering **85** (2008) 1116-1119.

3. A.M. Ruiz, X. Illa, R. Díaz, A. Romano-Rodríguez, J.R. Morante, *"Analyses of the ammonia response of integrated gas sensors working in pulsed mode"*, Sensors and Actuators B: Chemical **118** (2006) 318-322

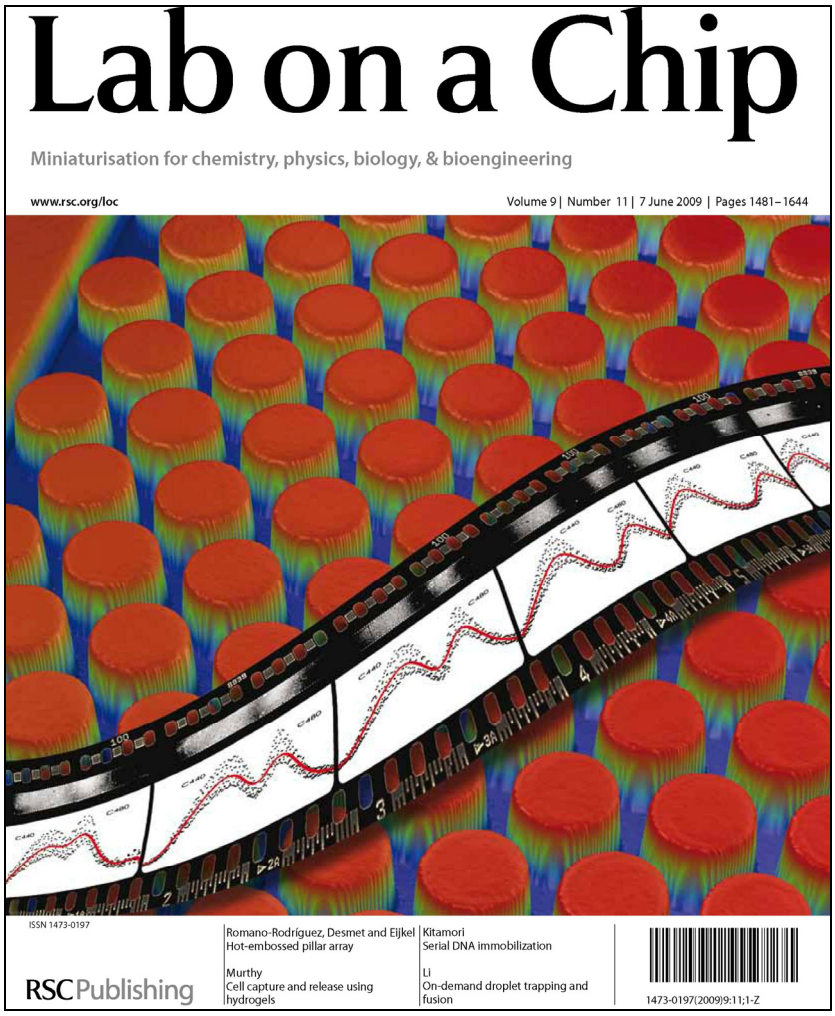

Fig.1 Cover of the volume of Lab on a Chip with the artwork referred to the article "*An array of ordered pillars with retentive properties for pressure-driven liquid chromatography fabricated directly from an unmodified cyclo olefin polymer"* published by the author of the PhD dissertation.

Selected contributions in conferences

- Conference: *35th International Conference on Micro- and Nano-Engineering (MNE 2009)*
  Location: Ghent (BELGIUM) Year: 2009
  Type of Contribution: **Oral**
  Authors: X. Illa, W. De Malsche, H. Gardeniers, G. Desmet, J. Eijkel, A. Romano-Rodríguez
  Title: *A cyclo-olefin polymer chip containing a column with an array of ordered pillars for pressure-driven liquid chromatography*

- Conference: *Third Spanish Workshop on Nanolithography (Nanolitho 2009)*
  Location: Madrid (SPAIN) Year: 2009
  Type of Contribution: **Oral**
  Authors: X. Illa, W. De Malsche, H. Gardeniers, G. Desmet, J. Eijkel, A. Romano-Rodríguez
  Title: *A cyclo-olefin polymer chip containing a column with an array of ordered pillars for pressure-driven liquid chromatography*

- Conference: *Reunión de la Iber Red en Micro y Nanotecnologías (IBERNAM 2008)*
  Location: Tarragona (SPAIN) Year: 2008
  Type of Contribution: **Oral**
  Authors: X. Illa, J.R: Morante, A. Romano-Rodriguez, J. Bomer, J. Eijkel, W. De Malsche, G. Desmet
  Title: *A polymer microchip for pressur-dirven liquid chromatography*

- Conference: *II International Workshop on Analytical Miniaturization (WAM 2010)*
  Location: Oviedo (SPAIN) Year: 2010
  Type of Contribution: **Flash Communication + Poster**
  Authors: X. Illa, W. De Malsche, H. Gardeniers, G. Desmet, A. Romano-Rodríguez
  Title: *A cyclo olefin polymer chip containing a pillar array column for pressure-driven liquid chromatography*

- Conference: *14th International Conference on Miniaturized Systems for Chemistry and Life Sciences (μTAS 2010)*
  Location: Groningen (The NETHERLANDS) Year: 2010
  Type of Contribution: **Poster**
  Authors: X. Illa, R. Rodriguez-Trujillo, O. Ordeig, W. De Malsche, A. Homs-Corbera, H. Gardeniers, G. Desmet, J.P. Kutter, J. Samitier and A. Romano-Rodríguez
  Title: *Simultaneous impedance and fluorescence detection of proteins in a cyclo olefin polymer chip containing a column with an ordered pillar array with integrated gold microelectrodes*

- Conference: *34th International Symposium on High-Performance Liquid Phase Separations and Related Techniques (HPLC 2009)*
  Location: Dresden (GERMANY) Year: 2009
  Type of Contribution: **Poster**
  Authors: X. Illa, W. De Malsche, J. Bomer, H. Gardeniers, J. Eijkel, J.R. Morante, A. Romano-Rodríguez, G. Desmet
  Title: *A polymer microchip for pressure-driven liquid chromatography separations*

- Conference: *34th International Conference on Micro- and Nano-Engineering (MNE 2008)*
  Location: Athens (GREECE) Year: 2008
  Type of Contribution: **Poster**
  Authors: X. Illa, W. De Malsche, J. Bomer, H. Gardeniers, J. Eijkel, J.R. Morante, A. Romano-Rodríguez, G. Desmet
  Title: *Fabrication of a plastic column for pressure-driven LC with an ordered pillar array*

- Conference: *Second Spanish Workshop on Nanolithography (Nanolitho 2008)*
  Location: Bellaterra (SPAIN) Year: 2008
  Type of Contribution: **Poster**
  Authors: X. Illa, W. De Malsche, J. Bomer, J. R. Morante, A. Romano-Rodríguez, G. Desmet, H. Gardeniers, J. Eijkel
  Title: *Embossing an array of perfectly ordered pillars in cyclo olefin copolymer for liquid chromatography applications*

- Conference: *Microtechnologies for the New Millenium 2007*
  Location: Maspalomas (SPAIN) Year: 2007
  Type of Contribution: **Poster**
  Authors: O.Casals, A. Romano-Rodríguez, X. Illa, C. Zamani, A.Vilà, J.R. Morante, I. Gràcia, P. Ivanov, N. Sabaté, L. Fonseca, J. Santander, E. Figueras, C. Cané
  Title: *Micro and nanotechnologies for the development of an integrated chromatographic system*

Other contributions in conferences

- Conference: *Materials Science and Engineering (MSE) 2008*
  Location: Nürnberg (GERMANY) Year: 2008
  Type of Contribution: **Invited**
  Authors: A. Romano-Rodriguez, J.D. Prades, R. Jimenez-Diaz, A. Cirera, O. Casals, J.R. Morante, X. Illa, T. Andreu, S. Barth, S. Mathur, F.Hernandez-Ramirez
  Title: *Individual Zinc Oxide Nanowires as UV Photodetectors*

- Conference: *Eurosensors XXII*
  Location: Dresden (GERMANY) Year: 2008
  Type of Contribution: **Oral**
  Authors: C. Zamani, X. Illa, T. Andreu, S. Abdollahzadeh Ghom, A. Romano-Rodriguez, J.R. Morante
  Title: *Pre-concentration of amines with KIT-6 mesoporous silica*

- Conference: *Eurosensors XXII*
  Location: Dresden (GERMANY) Year: 2008
  Type of Contribution: **Oral**
  Authors: J.D. Prades, R. Jimenez-Diaz, F. Hernandez-Ramirez, X. Illa, T. Andreu, A. Cirera, A. Romano-Rodriguez, A. Cornet, J.R. Morante, S. Barth, S. Mathur
  Title: *Platform And Electronic Interface For Photo Sensor Devices Based On Individual Nanowires*

- Conference: *Eurosensors XX*
  Location: Göteborg (SWEDEN) Year: 2006
  Type of Contribution: **Oral**
  Authors: X. Illa, O. Casals, C. Durand, A. Prim, E. Rossinyol, A. Vilà, F. Peiró, A. Romano-Rodríguez, J.R. Morante, S. Capone, L. Francioso, P. Siciliano
  Title: *Sensing of ammonia, dimetyl- and trimetylamine using WO_3 nanomaterials deposited on microhotplates*

- Conference: *International Meeting on Chemical Sensors (IMCS) 2006*
  Location: Brescia (ITALY) Year: 2006
  Type of Contribution: **Oral**
  Authors: X. Illa, A. Prim, E. Rossinyol, A. Vilà, A. Romano-Rodríguez, F. Peiró, J.R. Morante
  Title: *NH_3 sensing using WO_3 nanostructures obtained from different hard nanotemplates*

- Conference: *Materials Research Society (MRS) - Spring Meeting 2006*
  Location: San Francisco (USA) Year: 2006
  Type of Contribution: **Oral**
  Authors: A. Prim, X. Illa, A. Romano-Rodríguez, J.R. Morante
  Title: *Gas sensors based on nano-WO_3 and nano-WO_3:Cr obtained from different hard template routes*

- Conference: *Eurosensors XXII*
  Location: Dresden (GERMANY) Year: 2008
  Type of Contribution: **Poster**
  Authors: C. Zamani, O. Casals, X. Illa, T. Andreu, S. Abdollahzadeh Ghom, A. Romano-Rodriguez, J.R. Morante
  Title: *Mesoporous WO3-based sensors for detection of amines in integrated chromatographic systems*

- Conference: *12th International Meeting on Chemical Sensors (IMCS) 2008*
  Location: Columbus (USA) Year: 2008
  Type of Contribution: **Poster**
  Authors: C. Zamani, X. Illa, T. Andreu, S. Abdollahzadeh Ghom, A. Romano-Rodriguez, J.R. Morante
  Title: *Mesoporous silica: a suitable trap for amines*

- Conference: *33rd International Conference on Micro- and Nano-Engineering (MNE 2007)*
  Location: Copenhagen (DENMARK) Year: 2007
  Type of Contribution: **Poster**
  Authors: R. Triantafyllopoulou, X. Illa, O. Casals, C. Tsamis, A. Romano-Rodriguez, J.R. Morante
  Title: *Nanostructured oxides on porous silicon microhotplates for NH_3 sensing*

- Conference: *Eurosensors XIX*
  Location: Barcelona (SPAIN) Year: 2005
  Type of Contribution: **Poster**
  Authors: A.M. Ruiz, X. Illa, R. Díaz, A. Romano-Rodríguez, J.R. Morante
  Title: *Analyses of the ammonia response of integrated gas sensors working in pulsed mode.*